Analysis of Cooperative Communication and Link Layer Performance under Imperfectly Known Fading Channel Gains

by

Ali Zarei Ghanavati

M.Sc., Sharif University of Technology, 2009

B.Sc., University of Tehran, 2006

A Thesis submitted in partial fulfillment
of the requirements for the degree of

Doctor of Philosophy

in the
School of Engineering Science
Faculty of Applied Sciences

SIMON FRASER UNIVERSITY
Fall 2015

APPROVAL

Name: Ali Zarei Ghanavati

Degree: Doctor of Philosophy

Title of Thesis: Analysis of Cooperative Communication and Link Layer Performance under Imperfectly Known Fading Channel Gains

Examining Committee:

Dr. Ivan Bajic
Chair

Dr. Daniel C. Lee
Professor, Engineering Science
Simon Fraser University, Senior Supervisor

Dr. Paul Ho
Professor, Engineering Science
Simon Fraser University, Supervisor

Dr. Rodney Vaughan
Professor, Engineering Science
Simon Fraser University, Internal Examiner

Dr. Lutz Lampe
Professor, Electrical and Computer Engineering
University of British Columbia, External Examiner

Date Approved: September 4th, 2015

Abstract

One of the main issues of wireless communication systems is to cope with random variation of their channel conditions. In many wireless communication systems, the receiver estimates the channel for symbol detection. It is usually assumed that channel estimation is perfect, but in practice, channel estimation error (CEE) can become significant and can degrade the performance of wireless communication systems. This thesis addresses the effects of channel estimation error in two contexts: CEE in cooperative communication systems and CEE in link layer performance.

Cooperative diversity, which has been recently presented as an effective way of mitigating the effect of deep fades in wireless channels and improving spectral and power efficiency of the wireless networks, is considered in the first part of this dissertation. Taking into consideration the presence of CEE, part I of this thesis analyzes a few cooperative communication system models, which display different levels of practicality and represent large classes of cooperative systems in the literature. This thesis spells out delineating aspects of these models and rigorously compares their error probabilities. Furthermore, a novel signal detection scheme in the presence of CEE is presented for large classes of cooperative communication systems.

Part II of this dissertation focuses on cross layer issues between the physical and link layers of wireless communication systems. In particular, the frame error probability (FEP) is derived for a wireless communication system over fading channels in the presence of CEE. Part II also explores the issue of optimizing bit transmission power for minimizing the expected energy required to reliably deliver a frame to the destination node through an ARQ mechanism over a fading channel. Also, an optimization algorithm is designed to minimize the expected energy for reliable delivery of a frame for the systems under consideration.

Acknowledgments

I am pleased to have the privilege of arriving at this notable moment in my life; however, I could not have partaken on this journey alone. That is to say, without the love, compassion and wisdom of many people important in my life, this journey would not have been probable.

I thank God most solemnly and sincerely for giving me the will to endure during the rough times, and endowing upon me the proper attitude to stay upright during difficult times.

The most notable inspiration is of course my senior supervisor, Dr. Daniel Lee. His wisdom, care and attention to detail inspired me to better myself in both my academic career and personal life. I would like to express my special appreciation and thanks to Dr. Lee. He was a tremendous mentor for me, and I would like to thank him for encouraging my research and for allowing me to grow as a research scientist.

Additionally, I would like to thank my parents for their support during my academic career. They continued to express their love and compassion for me during my study, and I could feel their love even though we were physically far apart.

I would also like to thank my committee members, Professors Paul Ho, Rodney Vaughan, Ivan Bajic and Lutz Lampe for serving as my committee members.

Lastly, I would like to thank my amazing friends for their support during my PhD study.

Contents

List of Tables

List of Figures

List of Symbols

X	Random variable X.
$\mathbf{x}$	A boldface lowercase letter denotes a vector.
$\mathbf{X}$	A boldface uppercase letter denotes a matrix.
$\hat{X}$	Estimation of random variable X.
S	Source node.
R	Relay node.
D	Destination node.
$\mathcal{CN}(0, \sigma^2)$	Complex Gaussian random variable with zero mean and variance σ^2.
$f_X(\cdot)$	PDF of random variable X.
$F_X(\cdot)$	CDF of random variable X.
h_{ij}	Communication channel between node i and node j.
$\det(\mathbf{X})$	The determinant of $\mathbf{X}$.
$\mathrm{E}(X)$	The expected value of random variable X.
$(\cdot)^{\mathrm{T}}$	Transpose operation.
$(\cdot)^{\mathrm{H}}$	Hermitian transpose operation.
$(\cdot)^{-1}$	Inverse operation.
x^*	Complex conjugate of x.
$\mathrm{Re}(x)$	Real part of x.
$\mathrm{Im}(x)$	Imaginary part of x.
$\angle x$	Angle of x.
$\lvert \cdot \rvert$	Absolute value.
$[\cdot]_{k,l}$	$(k,l)^{th}$ entry of a matrix.
$[\cdot]_k$	k^{th} entry of a vector.
$\mathbf{I}_M$	Identity matrix of size M.
$\lVert \cdot \rVert$	Euclidean norm of a vector.
$C(n, r)$	Number of all combinations of r objects, selected from n objects.

List of Acronyms

AF	Amplify-and-Forward
ARQ	Automatic Repeat Request
AWGN	Additive White Gaussian Noise
BEP	Bit Error Probability
BPSK	Binary Phase Shift Keying
BTP	Bit Transmission Power
CDF	Cumulative Density Function
CEE	Channel Estimation Error
CRC	Cyclic Redundancy Codes
DAA	Design and Analysis
DF	Decode-and-Forward
FEP	Frame Error Probability
LB	Lower Bound
LLEE	Link Layer Energy Efficiency
MAP	Maximum a Posteriori
MIMO	Multi-Input-Multi-Output
MMSE	Minimum Mean Square Error
MPSK	M-ary Phase Shift Keying
MRC	Maximum Ratio Combining
ML	Maximum Likelihood
OFDM	Orthogonal Frequency-Division Multiplexing
PDF	Probability Density Function
PDU	Protocol Data Unit
PSAM	Pilot Symbol-Assisted Modulation
PSK	Phase Shift Keying
SDF	Selective Decode-and-Forward
SDS	Symbol Detection Schemes
SEP	Symbol Error Probability
SISO	Single-Input-Single-Output
SNR	Signal-to-Noise Ratio

Chapter 1

Introduction

1.1 Background

Cooperative communication systems received much attention in the recent past due to its ability to achieve diversity gain [1] [2] and its potential for power efficiency [3]. The main idea behind cooperative diversity is that in a wireless environment, the signal transmitted by the source is retransmitted by other nodes, which can be termed as "relays," so that source and relay nodes can effectively share their antennas in a manner that creates a "virtual antenna array" [4] [5] (see Fig. 1.1). In comparison to the point-to-point communication system, the cooperative system may appear to need more communication resources such as power or bandwidth than the point-to-point communication system for the same performance because the cooperative communication system has more transmitting nodes and the signals transmitted from the source and the relays are often separated in time or in frequency band. Nevertheless, studies show that the Shannon capacity of the system in fact increases due to the cooperation diversity [6]-[10].

Cooperative communication can be applied to many wireless communication systems to extend their coverage area [7]. In many wireless applications, the distance between the source node and the destination node can be more than the distance that the source node can cover, and increasing the source's transmission power is not desired. For example, in sensor networks, transmitters and receivers use low-power signals to communicate; if the distance between the transmitter and receiver is more than several meters, they cannot have a reliable communication [11]. In this example, by multiple sensors playing the role of relays for one another, the distance between the source and destination can be extended.

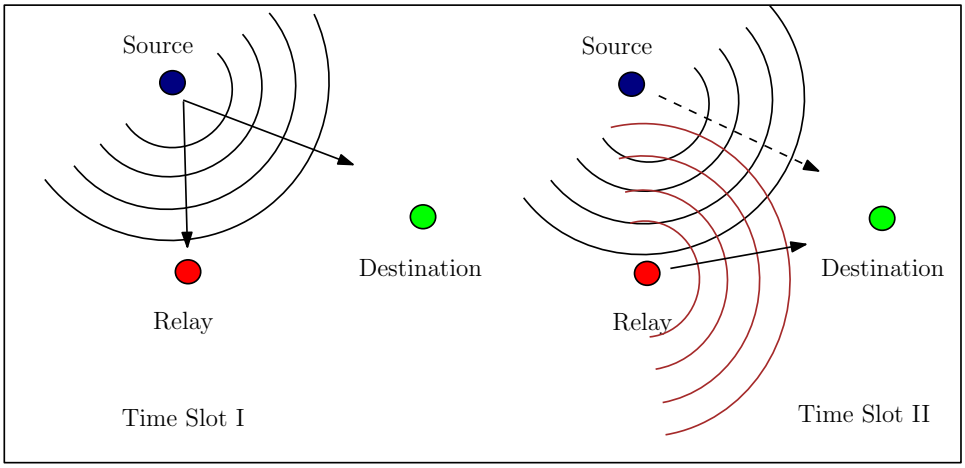

Figure 1.1: Cooperative diversity

Based on the way in which the information is transmitted from the source terminal to relay terminals and the way it is processed at the relay terminals, typical cooperative protocols can generally be divided into two types: amplify-and-forward (AF) protocols and decode-and-forward (DF) protocols, where DF protocols can be further categorized into conventional DF and selective decode-and-forward (SDF) protocols [1] [2] [12] (Fig. 1.2). In AF protocols, the relay terminal simply forwards a scaled version of the signal that it receives from the source terminal to the destination terminal. In the conventional DF protocol, the relay terminal detects the received signal, and regenerates signal to transmit to the destination terminal. Error propagation from the relay to the destination is the main drawback of this protocol, and a complex demodulation scheme is needed to achieve the full diversity gain [12] [13]. A third option is to use a selective decode-and-forward protocol. In the SDF protocol, the relay terminal detects the received signal and forwards it to the destination only if the relay has high confidence that the symbol has been detected correctly, and remains silent otherwise to avoid error propagation. In this dissertation, we focus on the decode-and-forward relay communication systems. The scope of this dissertation's interest includes both the conventional DF and SDF protocols. (In fact, the conventional DF protocol can be viewed as a special case of SDF protocol in which the relay nodes always forward the detected signal to the destination.)

One of the simplifying assumption we often find in modelling an SDF system in the literature is that the relay node perfectly knows whether a symbol has been detected correctly or

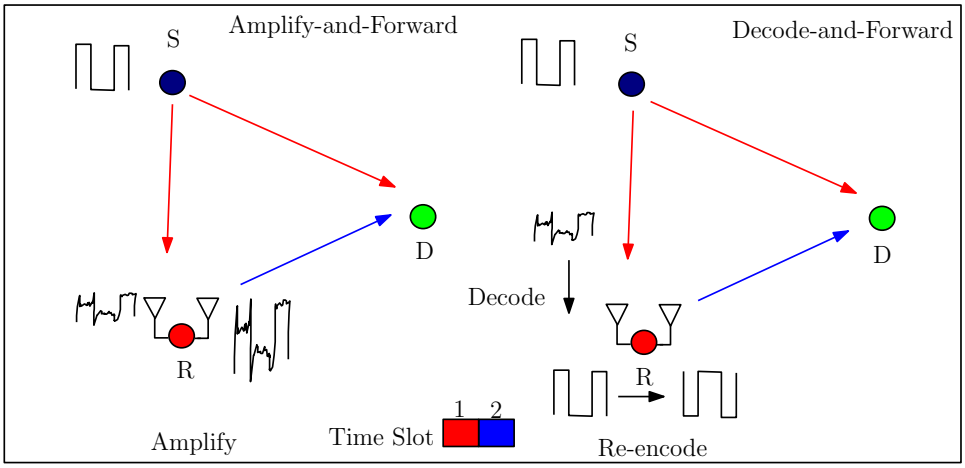

Figure 1.2: AF and DF cooperative protocols

not; if the detected symbol is erroneous, the relay node remains silent to avoid propagation of errors [14] [15] [16]. However, this assumption is quite idealistic, and in reality the relay node must make the forwarding decision with the uncertainty about the correctness of the detected symbol [18]. In the literature, we find three major kinds of strategies for making the forwarding decision under the uncertainty of the relay's correctness in detecting the symbol. In one kind, the relay node monitors the source-relay instantaneous SNR. If the received signal SNR is above some threshold, the relay node has high confidence of correct detection and sends the detected symbol to the destination [17] [19] [20]. In another kind, the system employs a block error detection (e.g., cyclic redundancy check) [21] [22] [23]. If the relay concludes that a symbol in a frame has been detected with error, the whole frame received from the source is kept from being forwarded to the destination. Another kind of forwarding strategy defines an erasure region for the relay, where the erasure region is a region in the signal space in which the received signal is declared unclear (e.g., the erasure region can be a set of signals that are sufficiently far from constellation signal points) [18]. The relay does not forward symbols corresponding to received signals that fall into the erasure region [18].

There is yet another issue to be addressed in modelling of selective decode-and-forward systems. In most of the existing work on the SDF protocols, it has been assumed that the destination node perfectly knows whether the relay has forwarded a particular symbol or not [15]-[20]. However, in reality the destination node must detect the incoming information symbols while being uncertain about whether the received signal contains the relay

node's transmitted signal [30]. From the destination node's vantage point, the forwarding decision made by the relay can only be guessed. Traditionally, three methods can be used to detect the presence of a signal at the destination: energy detector, matched filter, and cyclostationary feature detection [31]. Energy detection, which is the most popular method, is suboptimal and non-coherent and can be simply implemented [32]. Matched filter is a coherent detection that maximizes the signal to noise ratio. Cyclostationary feature detection exploits the inherent periodicity of the received signal. Besides all of the methods mentioned above for detecting the presence of the signal, flag-based methods are also of interest [33]. However, sending a flag signal has the drawback of consuming additional energy and bandwidth. In [30], a novel signal detection scheme in the presence of channel estimation error for SDF protocols has been presented.

Part I of this dissertation addresses the simplifying assumptions aforementioned (both the assumptions on the relay and destination nodes). Chapter 2 explores system models that relax these simplifying assumptions. In this chapter, based on the relay's forwarding policy and destination's level of knowledge about the relay's forwarding decision, we will classify SDF communication system models and then we will rigorously compare their error probability performances under the presence of channel estimation error. In chapter 3, we will pursue novel signal detection schemes in the presence of channel estimation error for the SDF communication system with the uncertainty at the destination node about the relay's forwarding policy. It will be shown that our signal detection schemes result in an excellent performance.

Part II of this dissertation studies cross-layer issues between the physical layer and the link layer in the point-to-point wireless communication systems. While the bit error probability (BEP) and symbol error probability (SEP) are important measures for physical layer performance, the link layer with automatic repeat request (ARQ) intends to provide a reliable packet pipe to its upper layers. As such, the combination of throughput and delay for reliable packet (frame) delivery has been much used as a performance measure for the link layer in communication networks. There is an interesting body of work on the link layer performance of wireless networks (e.g., [42]-[53]). These papers consider various combinations of error correction, error detection, ARQ, and buffer management schemes and analyze the link layer performance in wireless networks. Furthermore, some presentations of such analysis show the relation between the physical-layer performance and the link-layer performance. However, most existing works, to our knowledge, focus on the throughput

(or goodput) and delay as the link layer performance measure. In this research, instead of throughput or goodput, we will focus on the energy efficiency and delay for analyzing the link layer performance in wireless networks.

Focusing on energy efficiency instead of throughput or goodput indeed changes the design decision. For a simple example, Stop-and-Wait ARQ [59] will be preferred to Go-Back-N ARQ scheme [59] if the energy efficiency is the primary concern, and Go-Back-N ARQ scheme will be preferred if the throughput is the primary concern. For the purpose of obtaining simple insight, under simple wireless channel models and ARQ model, this dissertation will discuss the problem of optimizing the physical layer's transmission power to minimize the expected total transmission energy including energy for retransmissions required for successful delivery of a link layer protocol data unit (PDU). A PDU will be referred to as a frame or a packet interchangeably in the present dissertation.

1.2 Outline

The objectives of the first part of this dissertation are to analyze the effects of channel estimation errors, relay's forwarding policy and destination's signal detection scheme in the SDF cooperative communication system. In the second part of this dissertation, we analyze link layer performances in the point-to-point wireless communication system. In particular, we study the frame error probability and minimization of energy required to successfully deliver a frame in the point-to-point wireless communication system in the presence of channel estimation errors. In each topic, we will perform theoretical analysis and use simulations to complement the theoretical results. The following is a summary of the main topics and contributions in this thesis:

1.2.1 Performance of wireless communication systems under channel estimation errors

Most of the existing work on cooperative communications and point-to-point wireless communication systems has assumed perfect knowledge of the fading channel coefficients at the receiver side [14]-[28], [42]-[46] which is an overly optimistic assumption. Although research results based on these assumptions provide valuable insights, in practical systems these coefficients are estimated and then used in the detection process. Especially, in mobile applications, the assumption of perfect channel knowledge is unwarranted as randomly varying

channel conditions are learned by the receivers imperfectly. In recent work (e.g., [29][16]), the effects of the channel estimation error on the bit error rate (BER) performance of cooperative communication systems have been studied with a simple model for the channel estimation error, where the variance of the channel estimation error is assumed to be fixed for all values of the signal-to-noise ratio (SNR).

One technique employed in practical systems to estimate the time-varying channels is to send training (pilot) signals. The transmitter periodically inserts known symbols, from which the receiver estimates the channel based on the received pilot symbols [24] [25]. In this research, we consider pilot symbol-assisted modulation (PSAM) scheme with a channel estimation scheme based on minimum mean square error (MMSE) channel estimation in two contexts: PSAM in cooperative communication systems and PSAM in link layer performance.

1.2.2 Classifying Decode-and-Forward system models and performance bounds

In this research, based on the relay's forwarding policy and destination's knowledge of symbol forwarding decisions, we classify general DF systems into three systems. We then compare the BEP performance of those three systems. Regardless of relay's forwarding policy and also the destination's knowledge of symbol forwarding decisions, we derive a lower bound on the BEP performance for implementable SDF and DF relay communication systems. The derived lower bound is very computationally efficient and in some cases results in an excellent approximation for the BEP performance of an implementable DF communication system. We apply the lower bound expression of BEP as the performance metric of the system, and solve a power allocation problem to allocate power optimally to training and data sequences.

1.2.3 Signal detection schemes for SDF systems

In this research, we relax the simplifying assumption of the destination node's knowledge of the relay's forwarding decision to make our SDF system model more realistic. In SDF protocols, the relay forwards a symbol only if the relay has high confidence that the symbol has been detected correctly, and remains silent otherwise. The destination node has to detect data symbols with the uncertainty about the relay's forwarding decision. However,

one of the simplifying assumption we often find in modelling an SDF system in the literature is that the destination node perfectly knows whether the relay has forwarded a particular symbol or not. In chapter 2, we include system models that relax this assumption and discuss the issue of imperfection of the destination's knowledge of the signal presence in the SDF relay networks. We compare the BEP performance of an SDF system in which the destination node has perfect knowledge of the relay's forwarding policy with a system in which the destination node does not have such perfect knowledge. In chapter 3, we will assume that the destination must detect the incoming information symbols with the uncertainty about whether the received signal contains the relay nodes transmitted signal. We then explore the issues related to optimally detecting data symbols in the SDF relay communication system under this assumption. We design novel schemes that can be used by the destination for detecting whether the relay has forwarded a particular symbol or not. We then use those schemes for signal detection at the destination node.

1.2.4 Frame error probability of a point-to-point wireless link

While bit error probability (BEP) and symbol error probability (SEP) are the most commonly used performance criteria at the physical layer, at the link layer, the frame error probability (FEP) is often a more relevant criterion than the BEP or SEP for the system performance. Even in a circuit-switching networks such as the modern cellular system, a frame structure is often imposed on the system, and the frame error probability is used for the purpose of resources allocation and control decisions such as the transmit power control. In a packetized network, the packet error probability, which is conceptually identical to the frame error probability, is a factor that is more directly related to the performance of link layer functions such as the ARQ schemes.

In recent work (e.g., [49] [50] [51]), the effects of channel estimation error on frame error probability were studied. L. Cao *et al.* [49] [50] investigated effects of channel estimation error on the FEP performance using chernoff bound. M. Wu *et al.* [51] assumed that the power is allocated between pilot and data equally. Moreover, authors considered chernoff bound and some other lower and upper bounds instead of the exact Q-function to derive the FEP expression. In chapter 4, we will use a more accurate approximation for the Q-function and derive a closed-form approximation for the FEP expression in the presence of channel estimation error. We will later show that our approximation is more accurate than the Chernoff bound. We also discuss the issue of allocating the transmit energy between pilot

and data symbols optimally in a frame for the goal of minimizing the frame error probability in a wireless communication system.

1.2.5 Optimizing bit transmission power for link layer energy efficiency

Every wireless communication network has a frame (packet) structure in the data link layer. In wireless networks, the relationship between the physical layer performance and the link layer performance becomes important from the standpoint of optimizing the application-layer performance resulting from the composite system. In this research, we analyze the issue of optimizing transmission power (energy per symbol) for minimizing the expected energy required to reliably deliver a frame to the destination node in a point-to-point wireless link over a fading channel. We start with a simple model in chapter 5 in which the wireless channel is perfectly known by the destination node. Next in chapter 6, we relax this known channel assumption and consider a more complex case in which the wireless channel coefficient must be estimated by the destination. At the end, we come up with a simple algorithm for minimizing the expected energy required for a reliable frame transmission for two different models: 1) Wireless channel is known by the destination, and 2) A more complex case in which the wireless channel must be estimated by the destination node. For the case 2, not only we optimize the bit transmission power for the purpose of minimizing expected energy required for reliable frame delivery but also optimize the allocated power to pilot symbols (which are required in each frame for channel estimation) and the power which is allocated to the data symbols.

1.3 Thesis layout

This thesis has six chapters. **Part I** contains the introduction and two other chapters and studies performance analysis of decode-and-forward relay communication systems under imperfectly known fading channels. **Part II** contains three chapters and studies the cross layer issues between physical layer and link layer in wireless communication systems in the presence of CEE. Chapter 2 classifies DF relay communication systems and compares their BEPs. Chapter 3 studies design and analysis of symbol detection schemes for SDF relay networks. Chapter 4 studies frame error probability for a point to point wireless communication system in the presence of CEE. Chapter 5 and 6 study optimizing the bit transmission power for link layer energy efficiency.

1.4 Scholarly publications

The research efforts during my Ph.D. program have resulted in the following scholarly publications. The materials in this thesis present only a portion of the works that have been done during this period. Classifying the decode-and-forward relay communication systems and clarifying their performances are introduced for the first time to the literature via the works that are presented in this dissertation.

1. A. Zarei Ghanavati and D. C. Lee, "Tight Bound on the Error Probability of Rotation Code in Rayleigh Fading Channels," in *Proc. 80th IEEE Veh. Technol. Conf. (VTC 2014 Fall)*, Sep. 2010, pp. 1-5, Sep. 2014, Vancouver, Canada.

2. A. Zarei Ghanavati, and D. C. Lee, "Design and Analysis of Symbol Detection Schemes with Imperfect CSI for SDF-Relay Networks," in *Proc. 28th IEEE Int. Conf. on Adv. Inf. Net. and Applicat. (AINA)*, May 2014, pp. 884-891.

3. A. Zarei Ghanavati, and D. C. Lee, "Optimizing Bit Transmission Power for Link Layer Energy Efficiency," in *Proc. 28th IEEE Int. Conf. Adv. Inf. Net. and Applicat. Workshops (WAINA)*, May 2014, pp. 714-718.

4. A. Zarei Ghanavati and D. C. Lee, "Optimal Energy Allocation between Pilot and Data Symbols for Minimizing Frame Error Probability under Imperfect Fading Channel Information," *IEEE Wireless Commun. Net. Conf. (WCNC)*, Apr. 2014, pp. 1990-1995.

5. A. Zarei Ghanavati, and D. C. Lee, "On the Performance of Selective Decode-and-Forward Relaying over Imperfectly Known Fading Relay Channels," in *Proc. Int. Conf. on Wireless and Mobile Commun. (ICWMC)*, Jul. 2013, pp. 173-178.

6. A. Z. Ghanavati, U. Pareek, S.Muhaidat, D. Lee, "On the Performance of Imperfect Channel Estimation for Vehicular Ad-Hoc Network," in *Proc. 72nd IEEE Veh. Technol. Conf. (VTC 2010 Fall)*, Sep. 2010, pp. 1-5.

Papers 2 and 3 are the basis of chapters 3 and 5, respectively. Paper 4 is the basis of chapter 4 and paper 5 is the basis of section 2.4 of chapter 2. Papers 1 and 6 do not have any contribution in this thesis.

Part I

Performance Analysis of Selective Decode-and-Forward Relay Systems under Imperfectly Known Fading Channels

Chapter 2

Lower bound on the Performance of Decode and Forward Relaying

2.1 Objective

In this chapter, we analyze three decode-and-forward relay-assisted communication system models. We spell out delineating aspects of the three different classes of system models and show inequalities among their BEPs. All three system models assume imperfect knowledge of the channel gain at the receivers. Our results also include a closed-form expression of a lower bound on the BEP performance for a large class of decode-and-forward systems in the presence of channel estimation error. The derived lower bound expression is computationally efficient and can be a good approximation for the BEP. Finally, we will provide power-allocation that optimally assigns power constraint to training and data transmission phases to minimize the lower bound expression.

2.2 Related work and contribution

Most of the the existing work on cooperative communications assumes perfect knowledge of the fading channel coefficients at the receiver side [14]-[28], which is an overly optimistic assumption. Another simplifying assumption we often find in modelling an SDF system in the literature is that the relay node perfectly knows whether a symbol has been detected correctly or not in making the decision whether to forward a symbol or not [14] [15] [16]. Again, this assumption is quite idealistic, and in reality the relay node must make the

forwarding decision with the uncertainty about the correctness of the detected symbol. Furthermore, in most of the existing work on the SDF protocols, it is assumed that the destination node has perfect knowledge of whether the relay has forwarded a particular symbol or not [17]-[18]. However, in reality the destination node must detect the incoming information symbols while being uncertain about whether the received signal contains the relay node's transmitted signal [30]. The present chapter's analysis includes a model that relaxes these simplifying assumptions.

In this chapter, based on the relay's forwarding policy and the destination node's level of knowledge about the relay's symbol forwarding decisions, we classify the general DF systems into three systems, both under the assumption of imperfect channel information: 1) the system in which the relay has perfect knowledge about correctness of its symbol detection, and the destination has perfect knowledge of the relay's forwarding decision, 2) the system in which the relay has perfect knowledge about correctness of its symbol detection, and the destination does not have perfect knowledge of the relay's forwarding decision and 3) the system in which the relay and destination do not have such perfect knowledge. We then compare the BEP performance of these three systems. Although it is intuitively compelling at first glance that the BEP associated with the former system model should be a lower bound of the BEP associated with the latter systems, we need to be cautious in making such a general statement because these system models do not specify the modulation schemes, the relay's forwarding policy, the destination's symbol detection schemes, etc.

We first introduce our system model in Sec. 2.3. In Section 2.4, the lower bound expression is derived for the systems under consideration. In Sections 2.5-2.8, we compare the BEP performance between all the systems under consideration. Simulation results are presented in Section 2.9, followed by summary and discussions in Section 2.10.

2.3 System Model

We consider the three-node relay network, which consists of the source, relay, and destination nodes. This relay network model is depicted in Figure 2.1. We assume BPSK[1] transmission over flat fading channels. Let h_{sd}, h_{sr} and h_{rd} denote the source-destination,

[1]Note that this assumption is imposed only for the convenience of notation. The analysis in this chapter can also be applied, after some minor modifications, to the case wherein the source employs any binary IQ modulation.

source-relay, and relay-destination channel gains, respectively. Each node-to-node channel gain is modelled by a zero-mean complex Gaussian random variable with variance $\sigma^2_{h_{ij}}$. The system conveys transmitted information as a sequence of frames, and each frame accommodates m symbols. Each channel is assumed to be constant during the frame transmission and only one pilot symbol is transmitted in each frame in order to estimate the channel gains. We assume that nodes cannot transmit and receive signals at the same time in the same frequency band, as is the case for most simple and cost-effective nodes.

As in [1], the transmission protocol can be described as follows. Two time slots are allocated to each symbol; in the first time slot, the source transmits data with power $\mathcal{P}_s$. The data signals received at the relay and the destination in the first time slot can be written as:

$$y^i_{sr} = \sqrt{\mathcal{P}_s} h_{sr} x_i + n^i_{sr},\ i = 1, 2, ..., m-1, \tag{2.1}$$

$$y^i_{sd} = \sqrt{\mathcal{P}_s} h_{sd} x_i + n^i_{sd},\ i = 1, 2, ..., m-1, \tag{2.2}$$

where n^i_{sr} and n^i_{sd} represent the additive noise terms, x_i represents the transmitted symbol with unit average energy, i.e., $\mathrm{E}\{|x_i|^2\} = 1$ and $\mathcal{P}_s$ is the source power (energy per symbol time) for data transmission. The relay first tries to detect the symbol received from the source using the optimal detection and decides whether to forward the detected symbol or not. For the present chapter's purpose, we define and name the following three systems based on the relay's forwarding policy and destination's knowledge of symbol forwarding decisions:

1)*Ideal System*: In this system, we assume that the relay perfectly knows whether a particular symbol has been detected correctly or not. If the relay correctly detects the received symbol, then the relay will forward it to the destination in the second time slot; otherwise, the relay will remain silent [14] [15]. Also, the destination node perfectly knows whether the relay has forwarded a particular symbol or not and uses its optimal signal detection.

2) *Relay-Agnostic System*: In this system, we assume that the relay does not necessarily know whether the symbol has been detected correctly or not and uses some policy for making the forwarding decision. The destination node perfectly knows whether the relay has forwarded the detected symbol or not and performs optimal signal detection. To illustrate the meaning of the forwarding decision policy, we provide the following examples:

Example 1: An example of the forwarding policy would be to forward all symbols–thus, a forwarded symbol may be erroneous.

Example 2: In another example of the forwarding policy, the relay uses the source-relay link's SNR to evaluate the reliability of the signal received from the source. The relay forwards a detected symbol to the destination only if the received SNR at the relay is above some pre-assigned threshold value. Otherwise, the relay remains silent in the second time slot to avoid propagating errors [17] [19] [20].

Example 3: As a forwarding policy, the relay may use an error detection scheme (e.g., cyclic redundancy check). If the relay concludes that there is a symbol that is detected wrong in the frame, at the second time slot the relay remains silent and the whole frame is kept from being forwarded to the destination.

3) *Agnostic System*: In this system, as in the *Relay-Agnostic System*, we assume that the relay node does not necessarily know whether the symbol has been detected correctly or not and uses some policy for making the forwarding decision in the second time slot. However, the destination node does not know whether the relay has forwarded the detected symbol or not.

Throughout this chapter, we will use superscript Id, RA and A to distinguish between these system models; for example, we denote by $P^{\mathrm{Id}}(e)$, $P^{\mathrm{RA}}(e)$ and $P^{\mathrm{A}}(e)$, the BEP performance of the *Ideal System*, *Relay-Agnostic System*, and *Agnostic System*, respectively.[2] In this chapter, we consider uncoded (no error correction code) systems in our analysis, and in all three systems (*Ideal*, *Relay-Agnostic* and *Agnostic Systems*), the signals received by the relay and the destination in the first time slot are modelled as (2.1) and (2.2). In the second time slot, in the *Ideal System*, the data signals received by the destination is in the following form:

$$y_{rd}^{i} = \theta_i \sqrt{\mathcal{P}_r} h_{rd} x_i + n_{rd}^{i},\ i = 1, 2, ..., m-1, \tag{2.3}$$

where θ_i can be either 0 or 1 indicating whether the relay was silent or not, n_{rd}^{i} is additive noise term, and $\mathcal{P}_r$ is the relay power (energy per symbol time) for data transmission. At the end of the second time slot, the destination will combine the desired signals from the source and the relay, if any, and attempt to detect the symbol.

[2] In addition to these three system models, one can imagine another model that may be termed as *Destination-Agnostic System*: the system in which the relay perfectly knows whether its detection of a symbol is correct or not and the destination does not know whether the relay has forwarded the symbol or not. We defer discussion of such a system beyond the present dissertation.

In the *Agnostic* and *Relay-Agnostic Systems*, the data signals received by the destination in the second time slot can be expressed as:

$$y_{rd}^{i} = \theta_i{}' \sqrt{\mathcal{P}_r} h_{rd} \tilde{x}_i + n_{rd}^{i},\ i = 1, 2, ..., m-1, \tag{2.4}$$

where θ_i' can be either 0 or 1 indicating whether the relay was silent or not and $\tilde{x}_i$ can be either x_i or $-x_i$ indicating whether the relay detected the symbol without error or not.

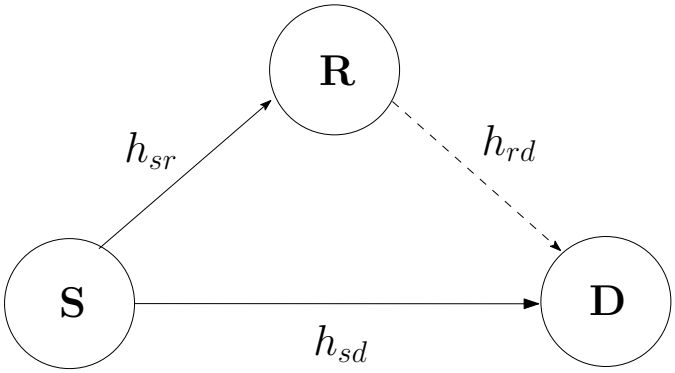

Figure 2.1: Three-node relay network model

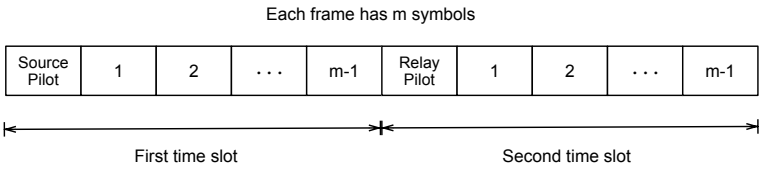

Figure 2.2: Transmission structure in a block of m symbols

The transmission block in all systems, consists of two phases−training phase and data transmission phase. Over these phases the source and the relay are subject to the following power constraint [34]:

$$|x_{s,t}|^2 + (m-1)\,\mathcal{P}_s \leq m\mathcal{P}_1,\ \ |x_{r,t}|^2 + (m-1)\,\mathcal{P}_r \leq m\mathcal{P}_2, \tag{2.5}$$

where $x_{s,t}$, $\mathcal{P}_s$, $x_{r,t}$, $\mathcal{P}_r$ and m are the source training symbol, source power for data transmission, relay training symbol, relay power for data transmission and frame length, respectively. Also $\mathcal{P}_1$ and $\mathcal{P}_2$ refer to the source average symbol energy and the relay average symbol energy, respectively. We consider a method in which the symbols are detected individually (i.e., in a symbol-by-symbol fashion); the symbol-by-symbol detection requires much less computation than the block detection.

2.3.1 Training Phase

Each frame transmission starts with the training phase. As in [36] [37] [38], we assume that only one pilot symbol is used to estimate the channel coefficient (It was shown in [36] [37] that one pilot symbol can achieve the same channel estimation performance by using the same power). At the beginning of the frame during the first time slot, the source sends a pilot symbol, which we denote as $x_{s,t}$, to the relay and destination (Figure 2.2). The received pilot signals can be expressed as:

$$y_{sr}^t = h_{sr}x_{s,t} + n_{sr},\ y_{sd}^t = h_{sd}x_{s,t} + n_{sd}, \tag{2.6}$$

where y_{sr}^t and y_{sd}^t are the received pilot signals at the relay and at the destination, respectively. Then, the relay sends pilot symbol $x_{r,t}$ to the destination in the second time slot (Figure 2.2). The received pilot signal at the destination can be expressed as:

$$y_{rd}^t = h_{rd}x_{r,t} + n_{rd}. \tag{2.7}$$

The noise terms n_{sd}, n_{sr} in (2.6) and n_{rd} in (2.7) are modelled as zero mean complex Gaussian random variables with equal variance N_0 ($N_0/2$ per real dimension). We assume that in the considered schemes, the source and the relay can allocate power to the pilot phase and the data phase in different proportions. Accordingly, we express $|x_{s,t}|^2$ and $|x_{r,t}|^2$ (the transmit energies for the training phase) as $\alpha\, m\mathcal{P}_1$ (for transmission by the source) and $\beta\, m\mathcal{P}_2$ (for transmission by the relay), respectively. Parameters α and β are the fraction of pilot transmission energy of the source and the relay frame, respectively, where $0 < \alpha, \beta < 1$. The relay communication systems considered in the present chapter assume that the relay and the destination both estimate the wireless channel gain from the received pilot signal by using the MMSE channel estimation method. MMSE estimate of the channel is obtained at the relay and destination by using $\hat{h}_{sr} = \mathrm{E}\{h_{sr}{y_{sr}^t}^*\}\left(\mathrm{E}\{y_{sr}^t{y_{sr}^t}^*\}\right)^{-1} y_{sr}^t$, $\hat{h}_{sd} = \mathrm{E}\{h_{sd}{y_{sd}^t}^*\}\left(\mathrm{E}\{y_{sd}^t{y_{sd}^t}^*\}\right)^{-1} y_{sd}^t$ and $\hat{h}_{rd} = \mathrm{E}\{h_{rd}{y_{rd}^t}^*\}\left(\mathrm{E}\{y_{rd}^t{y_{rd}^t}^*\}\right)^{-1} y_{rd}^t$ [34]. Based on [37], we can write:

$$h_{ij} = \hat{h}_{ij} + e_{ij}, \tag{2.8}$$

where e_{ij} is the channel estimation error modelled as a zero mean complex Gaussian random variable with variance $\sigma^2_{e_{ij}}$ and we have [37]:

$$\begin{aligned}
\hat{h}_{sd} &\sim \mathcal{CN}\left(0, \frac{\sigma^4_{h_{sd}}|x_{s,t}|^2}{\sigma^2_{h_{sd}}|x_{s,t}|^2 + N_0}\right), \; e_{sd} \sim \mathcal{CN}\left(0, \frac{\sigma^2_{h_{sd}} N_0}{\sigma^2_{h_{sd}}|x_{s,t}|^2 + N_0}\right), \\
\hat{h}_{sr} &\sim \mathcal{CN}\left(0, \frac{\sigma^4_{h_{sr}}|x_{s,t}|^2}{\sigma^2_{h_{sr}}|x_{s,t}|^2 + N_0}\right), \; e_{sr} \sim \mathcal{CN}\left(0, \frac{\sigma^2_{h_{sr}} N_0}{\sigma^2_{h_{sr}}|x_{s,t}|^2 + N_0}\right), \\
\hat{h}_{rd} &\sim \mathcal{CN}\left(0, \frac{\sigma^4_{h_{rd}}|x_{r,t}|^2}{\sigma^2_{h_{rd}}|x_{r,t}|^2 + N_0}\right), \; e_{rd} \sim \mathcal{CN}\left(0, \frac{\sigma^2_{h_{rd}} N_0}{\sigma^2_{h_{rd}}|x_{r,t}|^2 + N_0}\right),
\end{aligned} \tag{2.9}$$

where $\mathcal{CN}(\cdot, \cdot)$ denotes complex Gaussian distribution. It can be easily shown that e_{ij} and $\hat{h}_{ij}$ are statistically independent.

2.3.2 Data Transmission Phase

During the block of m symbols, the first symbol is allocated for channel estimation. In the remaining duration of $m-1$ symbols, data transmission takes place. In all three systems, the source transmits $m-1$ data symbols x_1, x_2, ..., x_{m-1} with power $\mathcal{P}_s$ during the first time slot subject to the following power constraint:

$$\mathcal{P}_s = \frac{(1-\alpha)m\mathcal{P}_1}{(m-1)}. \tag{2.10}$$

In the second time slot, the relay transmits $m-1$ data symbols x_i (in the *Ideal System*) or $\tilde{x}_i$ (in the *Relay-Agnostic* and *Agnostic Systems*) with power $\mathcal{P}_r$ to the destination subject to the following power constraint:

$$\mathcal{P}_r = \frac{(1-\beta)m\mathcal{P}_2}{(m-1)}. \tag{2.11}$$

2.4 Closed Form Expression of the BEP Performance of the Ideal System

In this section, we derive a closed-form expression for the BEP performance of the *Ideal System*. In accordance with (2.2), (2.3) and (2.8), the signals received at the destination in

the *Ideal System* can be written as:

$$\begin{aligned} y_{sd}^i &= \sqrt{\mathcal{P}_s}\hat{h}_{sd}x_i + \underbrace{\sqrt{\mathcal{P}_s}e_{sd}x_i + n_{sd}^i}_{\tilde{n}_{sd}^i}, \\ y_{rd}^i &= \theta_i\sqrt{\mathcal{P}_r}\hat{h}_{rd}x_i + \theta_i\underbrace{\sqrt{\mathcal{P}_r}e_{rd}x_i + n_{rd}^i}_{\tilde{n}_{rd}^i}, \end{aligned} \tag{2.12}$$

where $i = 1, 2, ..., m-1$ and $\theta_i \in \{0, 1\}$. With θ_i known by the destination, optimal detection rule to be used by the destination can be written as:

$$\hat{x} = \arg \max_{x\in\{-1,+1\}} p(y_{sd}, y_{rd} \mid x, \hat{h}_{sd}, \hat{h}_{rd}, \theta). \tag{2.13}$$

Conditioned on the transmitted symbol (x), estimated channel gains ($\hat{h}_{sd}$ and $\hat{h}_{rd}$) and θ, it can be easily seen that y_{sd} and y_{rd} are two independent complex Gaussian random variables with means $\sqrt{\mathcal{P}_s}\hat{h}_{sd}x$, $\theta\sqrt{\mathcal{P}_r}\hat{h}_{rd}x$ and variances $\mathcal{P}_s\sigma_{e_{sd}}^2 + N_0$, $\theta\mathcal{P}_r\sigma_{e_{rd}}^2 + N_0$, respectively. The decision rule is given by:

$$\hat{x} = \arg\max_{x\in\{-1,+1\}} \left\{ \frac{\exp\left(\frac{-|y_{sd}-\sqrt{\mathcal{P}_s}\hat{h}_{sd}x|^2}{\mathcal{P}_s\sigma_{e_{sd}}^2+N_0}\right)}{\pi(\mathcal{P}_s\sigma_{e_{sd}}^2 + N_0)} \cdot \frac{\exp\left(\frac{-|y_{rd}-\theta\sqrt{\mathcal{P}_r}\hat{h}_{rd}x|^2}{\theta\mathcal{P}_r\sigma_{e_{rd}}^2+N_0}\right)}{\pi(\theta\mathcal{P}_r\sigma_{e_{rd}}^2 + N_0)} \right\}. \tag{2.14}$$

Due to the symmetry, BEP is the same for sending 1 or -1 from the source. We can therefore write for each symbol, omitting the subscript for simple notation:

$$\begin{aligned} P^{\mathrm{Id}}(e) &= P^{\mathrm{Id}}(e|x=1) \\ &= P^{\mathrm{Id}}(e|x=1,\theta=0)P(\theta=0|x=1) + P^{\mathrm{Id}}(e|x=1,\theta=1)P(\theta=1|x=1) \\ &= P^{\mathrm{Id}}(e|x=1,\theta=0)P(\theta=0) + P^{\mathrm{Id}}(e|x=1,\theta=1)P(\theta=1). \end{aligned} \tag{2.15}$$

where the last equality in (2.15) is due to the fact that the transmitted symbol (x) and θ are independent.

If $x = 1$ is sent and the relay makes detection error, that symbol is not forwarded to the destination (i.e., $\theta = 0$) and the conditional BEP is given by:

$$P^{\mathrm{Id}}(e|x=1,\theta=0) = P\left\{ \exp\left(-\frac{|\tilde{n}_{sd}|^2}{\sigma_1^2}\right) < \exp\left(-\frac{|2\sqrt{\mathcal{P}_s}\hat{h}_{sd} + \tilde{n}_{sd}|^2}{\sigma_1^2}\right) \right\}, \tag{2.16}$$

where

$$\tilde{n}_{sd} = \sqrt{\mathcal{P}_s}e_{sd} + n_{sd}^i, \;\; \sigma_1^2 = \mathcal{P}_s\sigma_{e_{sd}}^2 + N_0. \tag{2.17}$$

If $x = 1$ is sent and the relay detects the symbol without error, that symbol is forwarded to the destination (i.e., $\theta = 1$) and the conditional BEP is given by:

$$P^{\mathrm{Id}}(e|x=1,\theta=1) = P\Bigg\{ \exp\left(-\frac{|\tilde{n}_{sd}|^2}{\sigma_1^2}\right)\exp\left(-\frac{|\tilde{n}_{rd}|^2}{\sigma_2^2}\right) < \exp\left(-\frac{|2\sqrt{\mathcal{P}_s}\hat{h}_{sd}+\tilde{n}_{sd}|^2}{\sigma_1^2}\right)\exp\left(-\frac{|2\sqrt{\mathcal{P}_r}\hat{h}_{rd}+\tilde{n}_{rd}|^2}{\sigma_2^2}\right)\Bigg\}, \quad (2.18)$$

where

$$\tilde{n}_{rd} = \sqrt{\mathcal{P}_r}e_{rd} + n_{rd}^i, \;\; \sigma_2^2 = \mathcal{P}_r\sigma_{e_{rd}}^2 + N_0. \quad (2.19)$$

We can simplify (2.16) and (2.18) as in the following:

$$P^{\mathrm{Id}}(e|x=1,\theta=0) = P\left(|\tilde{n}_{sd}|^2 > |2\sqrt{\mathcal{P}_s}\hat{h}_{sd}+\tilde{n}_{sd}|^2\right),$$
$$P^{\mathrm{Id}}(e|x=1,\theta=1) = P\left(\frac{|\tilde{n}_{sd}|^2}{\sigma_1^2}+\frac{|\tilde{n}_{rd}|^2}{\sigma_2^2} > \frac{|2\sqrt{\mathcal{P}_s}\hat{h}_{sd}+\tilde{n}_{sd}|^2}{\sigma_1^2}+\frac{|2\sqrt{\mathcal{P}_r}\hat{h}_{rd}+\tilde{n}_{rd}|^2}{\sigma_2^2}\right). \quad (2.20)$$

From (2.20) follows that:

$$P^{\mathrm{Id}}(e|x=1,\theta=0) = P\left(\mathcal{P}_s|\hat{h}_{sd}|^2 + \sqrt{\mathcal{P}_s}\mathrm{Re}\{\hat{h}_{sd}^*\tilde{n}_{sd}\} < 0\right),$$
$$P^{\mathrm{Id}}(e|x=1,\theta=1) = P\left(\frac{\mathcal{P}_s|\hat{h}_{sd}|^2}{\sigma_1^2}+\frac{\mathcal{P}_r|\hat{h}_{rd}|^2}{\sigma_2^2}+\frac{\sqrt{\mathcal{P}_s}\mathrm{Re}\{\hat{h}_{sd}^*\tilde{n}_{sd}\}}{\sigma_1^2}+\frac{\sqrt{\mathcal{P}_r}\mathrm{Re}\{\hat{h}_{rd}^*\tilde{n}_{rd}\}}{\sigma_2^2} < 0\right). \quad (2.21)$$

Conditioned on $\hat{h}_{sd}$ and $\hat{h}_{rd}$, we have:

$$\frac{\sqrt{\mathcal{P}_s}\mathrm{Re}\{\hat{h}_{sd}^*\tilde{n}_{sd}\}}{\sigma_1^2}+\frac{\sqrt{\mathcal{P}_r}\mathrm{Re}\{\hat{h}_{rd}^*\tilde{n}_{rd}\}}{\sigma_2^2} \sim \mathcal{N}\left(0, \frac{\mathcal{P}_s|\hat{h}_{sd}|^2}{\sigma_1^2}+\frac{\mathcal{P}_r|\hat{h}_{rd}|^2}{\sigma_2^2}\right), \quad (2.22)$$

where $\mathcal{N}(\cdot,\cdot)$ denotes real Gaussian distribution. We denote $|\hat{h}_{sd}|^2$ and $|\hat{h}_{rd}|^2$ by Z_1 and Z_2, respectively. Conditioned on $\hat{h}_{sd}$, $\hat{h}_{rd}$, and θ, the conditional BEP can be written as:

$$\begin{aligned} P^{\mathrm{Id}}\left(e|x=1,\hat{h}_{sd},\hat{h}_{rd},\theta\right) &= Q\left(\sqrt{2\left(A_{sd}|\hat{h}_{sd}|^2+\theta A_{rd}|\hat{h}_{rd}|^2\right)}\right) \\ &= Q\left(\sqrt{2\left(A_{sd}Z_1+\theta A_{rd}Z_2\right)}\right), \end{aligned} \quad (2.23)$$

where

$$A_{sd} = \frac{\mathcal{P}_s}{\mathcal{P}_s\sigma_{e_{sd}}^2+N_0}, \; A_{rd} = \frac{\mathcal{P}_r}{\mathcal{P}_r\sigma_{e_{rd}}^2+N_0}. \quad (2.24)$$

In accordance with the complex Gaussian channel model, Z_1 and Z_2 are exponentially distributed; we can therefore write:

$$f_{Z_1}(z_1) = \lambda_{sd} e^{-\lambda_{sd} z_1},\ z_1 \geq 0, \quad f_{Z_2}(z_2) \ = \ \lambda_{rd} e^{-\lambda_{rd} z_2},\ z_2 \geq 0, \tag{2.25}$$

where

$$\lambda_{sd} = \frac{1}{\sigma^2_{\hat{h}_{sd}}} = \frac{\alpha m \mathcal{P}_s \sigma^2_{h_{sd}} + N_0}{\alpha m \mathcal{P}_s \sigma^4_{h_{sd}}}, \quad \lambda_{rd} = \frac{1}{\sigma^2_{\hat{h}_{rd}}} = \frac{\beta m \mathcal{P}_r \sigma^2_{h_{rd}} + N_0}{\beta m \mathcal{P}_r \sigma^4_{h_{rd}}}. \tag{2.26}$$

Conditioned on θ, by using (2.23), (2.25), and $Q(x) = \frac{1}{\pi}\int_0^{\frac{\pi}{2}} \exp\left(-\frac{x^2}{2\sin^2\varphi}\right) d\varphi$ [40], BEP can be expressed as:

$$P^{\mathrm{Id}}(e|\theta) = \frac{1}{\pi}\int_0^{\frac{\pi}{2}} \int_0^{\infty} \int_0^{\infty} \exp\left(-\frac{A_{sd} z_1 + \theta A_{rd} z_2}{\sin^2\varphi}\right) f_{Z_1}(z_1) f_{Z_2}(z_2) dz_1 dz_2 d\varphi. \tag{2.27}$$

By using the moment generating function approach [40], we can rewrite (2.27) as:

$$P^{\mathrm{Id}}(e|\theta) = \frac{1}{\pi}\int_0^{\frac{\pi}{2}} \frac{\lambda_{sd}\sin^2\varphi}{\lambda_{sd}\sin^2\varphi + A_{sd}} \cdot \frac{\lambda_{rd}\sin^2\varphi}{\lambda_{rd}\sin^2\varphi + A_{rd}\theta} d\varphi. \tag{2.28}$$

Then, by using (5A.42) of [40] we obtain:

$$\begin{aligned} P^{\mathrm{Id}}(e) = {} & \frac{1}{4}\left[1+\sqrt{\frac{A_{sr}}{A_{sr}+\lambda_{sr}}}\right]\left[1+\frac{\lambda_{sd}\lambda_{rd}}{A_{rd}\lambda_{sd}-A_{sd}\lambda_{rd}}\left(\frac{A_{sd}}{\lambda_{sd}}\sqrt{\frac{A_{sd}}{A_{sd}+\lambda_{sd}}}-\frac{A_{rd}}{\lambda_{rd}}\sqrt{\frac{A_{rd}}{A_{rd}+\lambda_{rd}}}\right)\right] \\ & +\frac{1}{4}\left[1-\sqrt{\frac{A_{sr}}{A_{sr}+\lambda_{sr}}}\right]\left[1-\sqrt{\frac{A_{sd}}{A_{sd}+\lambda_{sd}}}\right]. \end{aligned} \tag{2.29}$$

where

$$A_{sr} = \frac{\mathcal{P}_s}{\mathcal{P}_s \sigma^2_{e_{sr}} + N_0}, \quad \lambda_{sr} = \frac{1}{\sigma^2_{\hat{h}_{sr}}} = \frac{\alpha m \mathcal{P}_s \sigma^2_{h_{sr}} + N_0}{\alpha m \mathcal{P}_s \sigma^4_{h_{sr}}}. \tag{2.30}$$

Because (2.29) is the BEP of the *Ideal System* (the most idealized system model), it is intuitively compelling that this should serve as a lower bound of the BEPs associated with the other two system models. However, proving that is quite challenging, and the next sections will prove it.

2.5 On the BEP inequalities among three systems

We assumed that in the *Ideal System*, the relay perfectly knows whether a symbol has been detected correctly or not. Furthermore, we assumed that the destination node in the *Ideal*

System perfectly knows whether the relay has forwarded a particular symbol or not. In the *Relay-Agnostic* and *Agnostic Systems*, we assumed that the relay node does not know whether a particular symbol has been detected correctly or not and uses some policy for making the forwarding decision. Also, the destination node in the *Agnostic System* does not know whether the relay has forwarded the detected symbol or not. The relay node may use any policy for making the forwarding decisions both in *Relay-Agnostic* and *Agnostic Systems*; these systems represent a large class of SDF systems. For the rest of the present chapter, we study the relation among the BEPs of the "*Ideal System*," the "*Relay-Agnostic System*," and the "*Agnostic System*." We will compare the BEPs of these three systems for an arbitrary forwarding policy employed by both the *Relay-Agnostic* and the *Agnostic Systems*. We will prove that the following inequality holds:

$$P^{\mathrm{Id}}(e) \leq P^{\mathrm{RA}}(e) \leq P^{\mathrm{A}}(e), \tag{2.31}$$

for any forwarding policy employed by the relay in the *Relay-Agnostic* and the *Agnostic Systems*. For the rest of this section, we provide a simple proof of the second inequality in (2.31), and we will prove the first inequality in sections 2.6 and 2.7. What is shown in this section is that the BEP performance of the *Relay-Agnostic System* is a lower bound on the BEP performance of the *Agnostic System* for any given forwarding policy of the relay. The optimal symbol detection (maximum likelihood) rules at destination in the *Agnostic System* and the *Relay-Agnostic System* are, respectively,

$$\text{Optimal detection rule in } \textit{Agnostic System} : \hat{x} = \arg\max_{x\in\{-1,+1\}} p(y_{sd}, y_{rd}|x, \hat{h}_{sd}, \hat{h}_{rd}), \tag{2.32}$$

$$\text{Optimal detection rule in } \textit{Relay}-\textit{Agnostic System} : \hat{x} = \arg\max_{x\in\{-1,+1\}} p(y_{sd}, y_{rd}|x, \hat{h}_{sd}, \hat{h}_{rd}, \theta') \tag{2.33}$$

Theorem 2.5.1. *For any given forwarding policy employed by both Relay-Agnostic and Agnostic Systems, optimal signal detection at the destination in (2.33) using* $(\hat{h}_{sd}, \hat{h}_{rd}, \theta')$ *information results in no worse BEP performance than the optimal signal detection in (2.32) using* $(\hat{h}_{sd}, \hat{h}_{rd})$ *information.*

Proof. Detection rule in (2.32) can be viewed as a detection rule that does not utilize information (θ') in the *Relay-Agnostic System*. Because the maximum likelihood rule of the *Relay-Agnostic System* in (2.33) is optimal, it cannot perform worse than rule (2.32). □

Theorem 2.5.1 says that the detection rule in (2.33) results in a better BEP performance than the detection rule in (2.32). We therefore proved that the BEP performance of the *Relay-Agnostic System* is a lower bound on the BEP performance of the *Agnostic System*, even if the destination node in the *Agnostic System* uses optimal signal detection. Obviously, if the destination node in the *Agnostic System* does not use the optimal detection, it results in a poorer detection in comparison with an *Agnostic System* in which the destination uses the optimal detection rule in (2.32).

2.6 Performance Comparison between the *Ideal System* and the *Relay-Agnostic System*: a Special Case

In this section, we discuss the first inequality of (2.31). Proving this inequality for the general case appears to be difficult. However, for a special case of $P(\theta = 1) \geq P(\theta' = 1)$, we can provide a simple and insightful proof. This special case represents a *Relay-Agnostic System* in which the relay node has a conservative forwarding policy in comparison with the idealized system. We present a simple proof for this special case in this section and defer the proof for the general case to the next section.

The probability of error in the *Ideal System* and the *Relay-Agnostic System*, can be respectively written as the following:

$$P^{\mathrm{Id}}(e) = P^{\mathrm{Id}}(e|\theta = 0)P(\theta = 0) + P^{\mathrm{Id}}(e|\theta = 1)P(\theta = 1), \tag{2.34}$$

$$P^{\mathrm{RA}}(e) = P^{\mathrm{RA}}(e|\theta' = 0)P(\theta' = 0) + P^{\mathrm{RA}}(e|\theta' = 1)P(\theta' = 1). \tag{2.35}$$

The signal received from the source at the destination (y_{sd}) is the same in both *Ideal* and *Relay-Agnostic Systems*. In accordance with (2.3) and (2.4), given that the relay transmitted the symbol, the signals received from the relay at the destination in the *Ideal System* and the *Relay-Agnostic System* are, respectively,

$$\textit{Ideal}\ (\text{given}\ \theta = 1): \quad y_{rd} = \sqrt{\mathcal{P}_r} h_{rd} x + n_{rd}, \tag{2.36}$$

$$\textit{Relay}-\textit{Agnostic}\ (\text{given}\ \theta' = 1): \quad y_{rd} = \sqrt{\mathcal{P}_r} h_{rd} \tilde{x} + n_{rd}, \tag{2.37}$$

where x is the correct symbol value and $\tilde{x}$ in (2.37) can be either x or $-x$. In the *Relay-Agnostic System*, we denote the probability that the relay sends $-x$ instead of x by δ:

$$\delta = P(\tilde{x} = -x|\theta' = 1). \tag{2.38}$$

Therefore, in the *Relay-Agnostic System*, given $\theta' = 1$ we have:

$$\text{with probability } 1-\delta,\ y_{rd} = \sqrt{\mathcal{P}_r} h_{rd} x + n_{rd}, \tag{2.39}$$

$$\text{with probability } \delta,\ y_{rd} = \sqrt{\mathcal{P}_r} h_{rd}(-x) + n_{rd} = -\left(\sqrt{\mathcal{P}_r} h_{rd} x - n_{rd}\right). \tag{2.40}$$

We point out that n_{rd} in (2.40) is circular symmetric Gaussian random variable and both n_{rd} and $-n_{rd}$ are statistically indistinguishable.

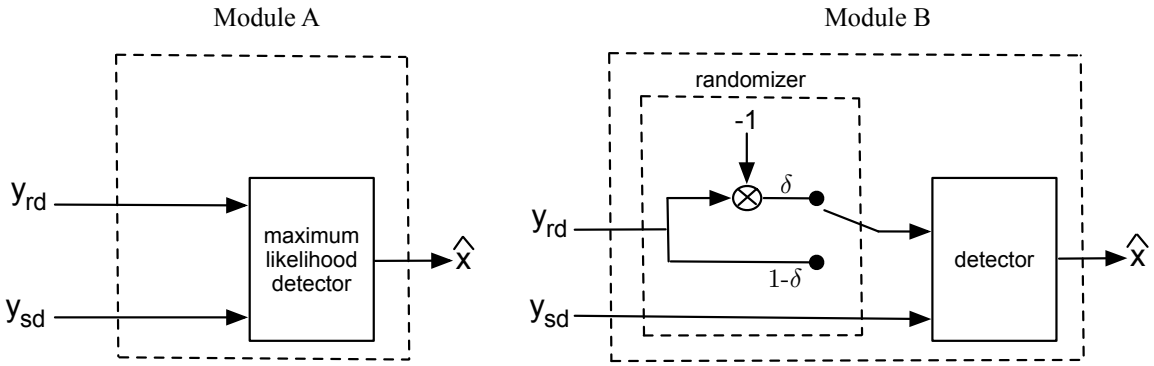

(a) *Ideal System* (b) *Relay-Agnostic System*

Figure 2.3: Signal detection at the destination in the: *Ideal System* conditioned on $\theta = 1$ (a) and in the *Relay-Agnostic System* conditioned on $\theta' = 1$ (b)

In the *Ideal System*, given $\theta = 1$, the destination tries to detect the transmitted symbol (x), based on both y_{sd} and y_{rd} and using maximum likelihood (ML) detection. In the *Relay-Agnostic System*, given $\theta' = 1$, the relay might send to the destination either the correct symbol (x), the probability of which is $1-\delta$, or the wrong symbol ($-x$), the probability of which is δ. Then the destination tries to detect the transmitted symbol based on y_{sd} and y_{rd} and using ML detection. Given the event that $\theta = \theta' = 1$, for comparing conditional error probabilities, $P^{\text{Id}}(e|\theta = 1)$ and $P^{\text{RA}}(e|\theta' = 1)$, the operations of the *Ideal System* and the *Relay-Agnostic System* can be both viewed as a mapping from (y_{rd}, y_{sd}) to decision $\hat{x}$, as illustrated in Fig. 2.3 a) and b). The *Relay-Agnostic System*'s operation (Module B) can be viewed as the cascade of the "randomizer" system and the "detector" system, wherein the randomizer multiplies y_{rd} by -1 with probability δ and leaves y_{rd} alone with probability $1-\delta$. Module B is thus a rule for detection $\hat{x}$ based on (y_{rd}, y_{sd}). The *Ideal System*'s

operation (Module A) is the maximum likelihood (optimal) rule for detection $\hat{x}$ based on (y_{rd}, y_{sd}). The optimal detection rule (Module A) cannot perform worse than Module B, and thus the following Lemma has been proved.

Lemma 2.6.1. $P^{\mathrm{Id}}(e|\theta = 1) \leq P^{\mathrm{RA}}(e|\theta' = 1)$.

The next lemma is intuitively compelling, and the proof is straightforward.

Lemma 2.6.2. $P^{\mathrm{Id}}(e|\theta = 1) \leq P^{\mathrm{Id}}(e|\theta = 0)$.

Proof. By using (2.23) we have:

$$P^{\mathrm{Id}}\left(e|x=1,\hat{h}_{sd},\hat{h}_{rd},\theta=1\right) = Q\left(\sqrt{2\left(A_{sd}|\hat{h}_{sd}|^2+A_{rd}|\hat{h}_{rd}|^2\right)}\right) \leq Q\left(\sqrt{2\left(A_{sd}|\hat{h}_{sd}|^2\right)}\right)$$
$$= P^{\mathrm{Id}}\left(e|x=1,\hat{h}_{sd},\hat{h}_{rd},\theta=0\right), \tag{2.41}$$

where the inequality in (2.41) is due to the fact that $Q()$ is a monotonically decreasing function and $A_{rd}|\hat{h}_{rd}|^2 \geq 0$. For each realization of $\hat{h}_{sd}, \hat{h}_{rd}$, the inequality in (2.41) holds. By averaging over all the realizations of $\hat{h}_{sd}, \hat{h}_{rd}$, we can simply conclude the following inequality:

$$P^{\mathrm{Id}}(e|\theta = 1) \leq P^{\mathrm{Id}}(e|\theta = 0). \tag{2.42}$$

□

Theorem 2.6.1. *Assume that* $P(\theta = 1) \geq P(\theta' = 1)$*, then we have:* $P^{\mathrm{Id}}(e) \leq P^{\mathrm{RA}}(e)$.

Proof. By using (2.35) and Lemma 2.6.1, we can write:

$$\begin{aligned} P^{\mathrm{RA}}(e) &= P^{\mathrm{RA}}(e|\theta'=0)P(\theta'=0) + P^{\mathrm{RA}}(e|\theta'=1)P(\theta'=1) \\ &\geq P^{\mathrm{RA}}(e|\theta'=0)P(\theta'=0) + P^{\mathrm{Id}}(e|\theta=1)P(\theta'=1). \end{aligned} \tag{2.43}$$

We also have:

$$P^{\mathrm{RA}}(e|\theta' = 0) = P^{\mathrm{Id}}(e|\theta = 0) \tag{2.44}$$

because given $\theta = 0$ and $\theta' = 0$, in both *Ideal* and *Relay-Agnostic Systems*, the symbol is optimally detected based on the received signal in the first time slot (y_{sd}) in (2.2), which is

identical in both systems and result in the same performance. From (2.43) and (2.44), we have:

$$\begin{aligned} P^{\mathrm{RA}}(e) &\geq P^{\mathrm{Id}}(e|\theta=0)P(\theta'=0)+P^{\mathrm{Id}}(e|\theta=1)P(\theta'=1) \\ &= P^{\mathrm{Id}}(e|\theta=0)\left[1-P(\theta'=1)\right]+P^{\mathrm{Id}}(e|\theta=1)P(\theta'=1) \\ &= P^{\mathrm{Id}}(e|\theta=0)+\left[\underbrace{P^{\mathrm{Id}}(e|\theta=1)-P^{\mathrm{Id}}(e|\theta=0)}_{\leq 0 \text{ from Lemma 2.6.2}}\right]P(\theta'=1), \end{aligned} \tag{2.45}$$

Then from (2.45) follows:

$$\begin{aligned} P^{\mathrm{RA}}(e) &\geq P^{\mathrm{Id}}(e|\theta=0)+\left[P^{\mathrm{Id}}(e|\theta=1)-P^{\mathrm{Id}}(e|\theta=0)\right]P(\theta=1) \\ &= P^{\mathrm{Id}}(e|\theta=0)-P^{\mathrm{Id}}(e|\theta=0)P(\theta=1)+P^{\mathrm{Id}}(e|\theta=1)P(\theta=1) \\ &= P^{\mathrm{Id}}(e|\theta=0)P(\theta=0)+P^{\mathrm{Id}}(e|\theta=1)P(\theta=1)=P^{\mathrm{Id}}(e), \end{aligned} \tag{2.46}$$

where the first inequality in (2.46) is due to the assumption $P(\theta=1)\geq P(\theta'=1)$. □

We proved that the first inequality in (2.31) holds for the special case in which we assume that $P(\theta=1)\geq P(\theta'=1)$. In the next section, we will relax this assumption and prove that the BEP performance of the *Ideal System* is a lower bound on the BEP performance of the *Relay-Agnostic System* for the general case.

2.7 Performance Comparison between the *Ideal System* and *Relay-Agnostic System*: General Case

2.7.1 A natural approach to the first inequality of (2.31) and its challenge

In this subsection, we will set the course of proving the first inequality of (2.31), and also show the challenging aspects of proving it. In accordance with (2.2), (2.4) and (2.8), the signals received by the destination in the *Relay-Agnostic System* can be written as:

$$\begin{aligned} y_{sd}^i &= \sqrt{\mathcal{P}_s}\hat{h}_{sd}x_i+\underbrace{\sqrt{\mathcal{P}_s}e_{sd}x_i+n_{sd}^i}_{\tilde{n}_{sd}^i}, \\ y_{rd}^i &= \theta_i'\sqrt{\mathcal{P}_r}\hat{h}_{rd}\tilde{x}_i+\theta_i'\underbrace{\sqrt{\mathcal{P}_r}e_{rd}\tilde{x}_i+n_{rd}^i}_{\tilde{n}_{rd}^i}, \end{aligned} \tag{2.47}$$

where $i = 1, 2, ..., m-1$, $\theta'_i \in \{0, 1\}$; $\tilde{x}_i$ can be either $-x_i$ or x_i, depending on whether the relay detected the symbol with error or not. The optimal detection rule at the destination is given by:

$$\hat{x} = \arg \max_{x \in \{-1,+1\}} p(y_{sd}, y_{rd} | x, \hat{h}_{sd}, \hat{h}_{rd}, \theta'). \tag{2.48}$$

Conditioned on the transmitted symbol (x), estimated channel gains ($\hat{h}_{sd}$ and $\hat{h}_{rd}$), and θ', it can be easily seen that y_{sd} and y_{rd} are statistically independent and the optimal decision rule can be written as the following:

$$\hat{x} = \arg \max_{x \in \{-1,+1\}} \Big\{ p(y_{sd} | x, \hat{h}_{sd})\, p(y_{rd} | x, \hat{h}_{rd}, \theta') \Big\}. \tag{2.49}$$

The probability density function (PDF) of y_{rd}, given $x, \hat{h}_{rd}$ and θ', can be written as follows:

$$\begin{aligned} p(y_{rd} | x, \hat{h}_{rd}, \theta') \;=\; & p(y_{rd} | x, \hat{h}_{rd}, \theta', \tilde{x} = x) P(\tilde{x} = x | x, \hat{h}_{rd}, \theta') \\ & + p(y_{rd} | x, \hat{h}_{rd}, \theta', \tilde{x} = -x) P(\tilde{x} = -x | x, \hat{h}_{rd}, \theta'). \end{aligned} \tag{2.50}$$

Obviously, the events $\tilde{x} = x$ and $\tilde{x} = -x$ are independent of x and $\hat{h}_{rd}$. Thus, in accordance with (2.49) and (2.50), the decision rule can be written as:

$$\begin{aligned} \hat{x} = \arg \max_{x \in \{-1,+1\}} \Big\{ p(y_{sd} | x, \hat{h}_{sd}) \Big[& p(y_{rd} | x, \hat{h}_{rd}, \theta', \tilde{x} = x) P(\tilde{x} = x | \theta') \\ & + p(y_{rd} | x, \hat{h}_{rd}, \theta', \tilde{x} = -x) P(\tilde{x} = -x | \theta') \Big] \Big\}. \end{aligned} \tag{2.51}$$

Hence, we have:

$$\begin{aligned} \hat{x} = \arg \max_{x \in \{-1,+1\}} \Bigg\{ & \frac{1}{\pi(\mathcal{P}_s \sigma^2_{e_{sd}} + N_0)} \exp\left(- \frac{|y_{sd} - \sqrt{\mathcal{P}_s} \hat{h}_{sd} x|^2}{\mathcal{P}_s \sigma^2_{e_{sd}} + N_0} \right) \\ & \times \Bigg[\frac{1}{\pi(\theta' \mathcal{P}_r \sigma^2_{e_{rd}} + N_0)} \exp\left(- \frac{|y_{rd} - \theta' \sqrt{\mathcal{P}_r} \hat{h}_{rd} x|^2}{\theta' \mathcal{P}_r \sigma^2_{e_{rd}} + N_0} \right) P(\tilde{x} = x | \theta') \\ & + \frac{1}{\pi(\theta' \mathcal{P}_r \sigma^2_{e_{rd}} + N_0)} \exp\left(- \frac{|y_{rd} + \theta' \sqrt{\mathcal{P}_r} \hat{h}_{rd} x|^2}{\theta' \mathcal{P}_r \sigma^2_{e_{rd}} + N_0} \right) P(\tilde{x} = -x | \theta') \Bigg] \Bigg\} \end{aligned} \tag{2.52}$$

Due to the symmetric nature of the system, we have $P^{\mathrm{RA}}(e|x = 1) = P^{\mathrm{RA}}(e|x = -1)$, so we have:

$$\begin{aligned} P^{\mathrm{RA}}(e) = P^{\mathrm{RA}}(e|x = 1) \;=\; & P^{\mathrm{RA}}(e|x = 1, \tilde{x} = -1) P(\tilde{x} = -1 | x = 1) \\ & + P^{\mathrm{RA}}(e|x = 1, \tilde{x} = 1) P(\tilde{x} = 1 | x = 1). \end{aligned} \tag{2.53}$$

From (2.53) follows that:

$$P^{\mathrm{RA}}(e)=\Big[P^{\mathrm{RA}}(e|x=1,\tilde{x}=-1,\theta'=1)P(\theta'=1|x=1,\tilde{x}=-1)$$
$$+P^{\mathrm{RA}}(e|x=1,\tilde{x}=-1,\theta'=0)P(\theta'=0|x=1,\tilde{x}=-1)\Big]\times P(\tilde{x}=-1|x=1)$$
$$+\Big[P^{\mathrm{RA}}(e|x=1,\tilde{x}=1,\theta'=1)P(\theta'=1|x=1,\tilde{x}=1)$$
$$+P^{\mathrm{RA}}(e|x=1,\tilde{x}=1,\theta'=0)P(\theta'=0|x=1,\tilde{x}=1)\Big]\times P(\tilde{x}=1|x=1). \quad (2.54)$$

In accordance with (2.38) and (2.52), we have:

$$P^{\mathrm{RA}}(e|x=1,\tilde{x}=-1,\theta'=1) \quad (2.55)$$
$$=P\Bigg\{\exp\left(-\frac{|\tilde{n}_{sd}|^2}{\sigma_1^2}\right)\left[(1-\delta)\exp\left(-\frac{|2\sqrt{\mathcal{P}_r}\hat{h}_{rd}-\tilde{n}_{rd}|^2}{\sigma_2^2}\right)+\delta\exp\left(-\frac{|\tilde{n}_{rd}|^2}{\sigma_2^2}\right)\right]<$$
$$\exp\left(-\frac{|2\sqrt{\mathcal{P}_s}\hat{h}_{sd}+\tilde{n}_{sd}|^2}{\sigma_1^2}\right)\left[(1-\delta)\exp\left(-\frac{|\tilde{n}_{rd}|^2}{\sigma_2^2}\right)+\delta\exp\left(-\frac{|2\sqrt{\mathcal{P}_r}\hat{h}_{rd}-\tilde{n}_{rd}|^2}{\sigma_2^2}\right)\right]\Bigg\},$$

$$P^{\mathrm{RA}}(e|x=1,\tilde{x}=-1,\theta'=0)=P\left\{\exp\left(-\frac{|\tilde{n}_{sd}|^2}{\sigma_1^2}\right)<\exp\left(-\frac{|2\sqrt{\mathcal{P}_s}\hat{h}_{sd}+\tilde{n}_{sd}|^2}{\sigma_1^2}\right)\right\}, \quad (2.56)$$

$$P^{\mathrm{RA}}(e|x=1,\tilde{x}=1,\theta'=1) \quad (2.57)$$
$$=P\Bigg\{\exp\left(-\frac{|\tilde{n}_{sd}|^2}{\sigma_1^2}\right)\left[\delta\exp\left(-\frac{|2\sqrt{\mathcal{P}_r}\hat{h}_{rd}-\tilde{n}_{rd}|^2}{\sigma_2^2}\right)+(1-\delta)\exp\left(-\frac{|\tilde{n}_{rd}|^2}{\sigma_2^2}\right)\right]<$$
$$\exp\left(-\frac{|2\sqrt{\mathcal{P}_s}\hat{h}_{sd}+\tilde{n}_{sd}|^2}{\sigma_1^2}\right)\left[\delta\exp\left(-\frac{|\tilde{n}_{rd}|^2}{\sigma_2^2}\right)+(1-\delta)\exp\left(-\frac{|2\sqrt{\mathcal{P}_r}\hat{h}_{rd}-\tilde{n}_{rd}|^2}{\sigma_2^2}\right)\right]\Bigg\},$$

$$P^{\mathrm{RA}}(e|x=1,\tilde{x}=1,\theta'=0)=P\left\{\exp\left(-\frac{|\tilde{n}_{sd}|^2}{\sigma_1^2}\right)<\exp\left(-\frac{|2\sqrt{\mathcal{P}_s}\hat{h}_{sd}+\tilde{n}_{sd}|^2}{\sigma_1^2}\right)\right\}, \quad (2.58)$$

where $\tilde{n}_{sd}$, σ_1^2, $\tilde{n}_{rd}$, and σ_2^2 are defined in (2.17) and (2.19). Analyzing (2.55) and (2.57) indicates that a closed-form BEP of the *Relay-Agnostic System* will not be available. For the purpose of comparing $P^{\mathrm{Id}}(e)$ and $P^{\mathrm{RA}}(e)$, we point out that $P^{\mathrm{Id}}(e)$ as shown in (2.15) can be expressed as a convex combination of (2.16) and (2.18) and $P^{\mathrm{RA}}(e)$ as shown in (2.54) can be expressed as a convex combination of (2.55)-(2.58). A natural approach to establish

the first inequality of (2.31) would be to compare the two convex combinations individual terms. However, comparing the individual terms of the two convex combinations does not offer an obvious way of establishing the first inequality of (2.31). In the next subsections, we present a clever way of comparing these individual terms to prove $P^{\mathrm{Id}}(e) \leq P^{\mathrm{RA}}(e)$.

2.7.2 A specially designed function

In view of equations (2.16), (2.18), and (2.55)-(2.58), for facilitating the comparison of BEP performances of the *Ideal System* and *Relay-Agnostic System*, we define a function $P^{+}(\xi)$ over $\xi \in [0,1]$ as follows:

$$\begin{aligned} &P^{+}(\xi) \\ &= P\Bigg\{ \exp\left(-\frac{|\tilde{n}_{sd}|^2}{\sigma_1^2}\right)\left[(1-\xi)\exp\left(-\frac{|2\sqrt{\mathcal{P}_r}\hat{h}_{rd}-\tilde{n}_{rd}|^2}{\sigma_2^2}\right)+\xi\exp\left(-\frac{|\tilde{n}_{rd}|^2}{\sigma_2^2}\right)\right] < \\ &\qquad \exp\left(-\frac{|2\sqrt{\mathcal{P}_s}\hat{h}_{sd}+\tilde{n}_{sd}|^2}{\sigma_1^2}\right)\left[(1-\xi)\exp\left(-\frac{|\tilde{n}_{rd}|^2}{\sigma_2^2}\right)+\xi\exp\left(-\frac{|2\sqrt{\mathcal{P}_r}\hat{h}_{rd}-\tilde{n}_{rd}|^2}{\sigma_2^2}\right)\right]\Bigg\} \end{aligned} \tag{2.59}$$

We note that both $P^{\mathrm{Id}}(e)$ and $P^{\mathrm{RA}}(e)$ can be expressed rather simply by using this function, $P^{+}()$; for example, in accordance with (2.15), (2.16) and (2.18), the BEP of the *Ideal System* can be written in terms of $P^{+}(\xi)$ as the following:

$$P^{\mathrm{Id}}(e) = P^{+}\left(\frac{1}{2}\right)P(\theta=0) + P^{+}(1)P(\theta=1). \tag{2.60}$$

Expressing both $P^{\mathrm{Id}}(e)$ and $P^{\mathrm{RA}}(e)$ in terms of a common monotonic function $P^{+}()$ is our main strategy of proving $P^{\mathrm{Id}}(e) \leq P^{\mathrm{RA}}(e)$ in subsection 2.7.3. For now, we are to overcome a major hurdle of proving function $P^{+}()$'s monotonicity.

Lemma 2.7.1. *$P^{+}(\xi)$ is a monotonically non-increasing function of ξ in [0,1].*

Proof. By multiplying both sides of the inequality among random variables in (2.59) by $\exp\left(\frac{|\tilde{n}_{sd}|^2}{\sigma_1^2}+\frac{|\tilde{n}_{rd}|^2}{\sigma_2^2}\right)$, we have:

$$P^{+}(\xi) = P\Big\{(1-\xi)X + \xi < (1-\xi)Y + \xi XY\Big\} \tag{2.61}$$

where

$$X = \exp\left(\frac{|\tilde{n}_{rd}|^2-|2\sqrt{\mathcal{P}_r}\hat{h}_{rd}-\tilde{n}_{rd}|^2}{\sigma_2^2}\right), Y = \exp\left(\frac{|\tilde{n}_{sd}|^2-|2\sqrt{\mathcal{P}_s}\hat{h}_{sd}+\tilde{n}_{sd}|^2}{\sigma_1^2}\right). \tag{2.62}$$

From (2.61) follows that:

$$P^{+}(\xi) = P\left\{Y > g(X,\xi)\right\} = \int_0^{\infty}\int_{g(x,\xi)}^{\infty} f_{XY}(x,y)dydx, \tag{2.63}$$

where

$$g(x,\xi) = \frac{(1-\xi)x+\xi}{1-\xi+\xi x}, \tag{2.64}$$

and $f_{XY}(x,y)$ is the joint PDF of X and Y. We point out that $\hat{h}_{rd}$, $\tilde{n}_{rd}$, $\hat{h}_{sd}$ and $\tilde{n}_{sd}$ are statistically independent; therefore, X and Y as seen in (2.62) are two positive independent random variables and their joint pdf can be written as $f_{XY}(x,y) = f_X(x)f_Y(y)$. In accordance with (2.63) we have:

$$\begin{aligned} P^{+}(\xi) &= \int_0^{\infty}\int_{g(x,\xi)}^{\infty} f_X(x)f_Y(y)dydx \\ &= \int_0^{\infty} f_X(x)\int_{g(x,\xi)}^{\infty} f_Y(y)dydx = \int_0^{\infty} f_X(x)\left[1-F_Y\left(g(x,\xi)\right)\right]dx. \end{aligned} \tag{2.65}$$

where $F_Y()$ is the cumulative distribution function (CDF) of random variable Y. Taking the derivative, we have:

$$\begin{aligned} \frac{\partial P^{+}(\xi)}{\partial \xi} &= \frac{\partial}{\partial \xi}\int_0^{\infty} f_X(x)\left[1-F_Y\left(g(x,\xi)\right)\right]dx = \int_0^{\infty} f_X(x)\frac{\partial}{\partial \xi}\left[1-F_Y\left(g(x,\xi)\right)\right]dx \\ &= -\int_0^{\infty} f_X(x)f_Y\left[g(x,\xi)\right]D_2 g(x,\xi)dx. \end{aligned} \tag{2.66}$$

where

$$D_2 g(x,\xi) = \frac{\partial g(x,\xi)}{\partial \xi} = \frac{1-x^2}{(1-\xi+\xi x)^2}. \tag{2.67}$$

We denoted $|\hat{h}_{sd}|^2$ and $|\hat{h}_{rd}|^2$ by Z_1 and Z_2, respectively. We can write (2.66) as the following:

$$\frac{\partial P^{+}(\xi)}{\partial \xi} = -\int_0^{\infty}\int_0^{\infty}\int_0^{\infty} f_{X|Z_2}(x|z_2)f_{Y|Z_1}\left[g(x,\xi)|z_1\right]D_2 g(x,\xi)f_{Z_1}(z_1)f_{Z_2}(z_2)dxdz_1dz_2 \tag{2.68}$$

We note that $D_2 g(x,\xi)$ is non-negative if $x \in (0,1]$ and negative if $x \in (1,\infty)$. We then write (2.68) as:

$$\begin{aligned} \frac{\partial P^{+}(\xi)}{\partial \xi} = &-\int_0^{\infty}\int_0^{\infty}\int_0^{1} f_{X|Z_2}(x|z_2)f_{Y|Z_1}\left[g(x,\xi)|z_1\right]D_2 g(x,\xi)f_{Z_1}(z_1)f_{Z_2}(z_2)dxdz_1dz_2 \\ &-\int_0^{\infty}\int_0^{\infty}\int_1^{\infty} f_{X|Z_2}(x|z_2)f_{Y|Z_1}\left[g(x,\xi)|z_1\right]D_2 g(x,\xi)f_{Z_1}(z_1)f_{Z_2}(z_2)dxdz_1dz_2 \end{aligned} \tag{2.69}$$

By using variable $\tau = 1/x$ in the second integral in (2.69), we have:

$$\frac{\partial P^+(\xi)}{\partial \xi} = -\int_0^\infty\int_0^\infty\int_0^1 f_{X|Z_2}(x|z_2) f_{Y|Z_1}\left[g(x,\xi)|z_1\right] D_2 g(x,\xi) f_{Z_1}(z_1) f_{Z_2}(z_2) dz_1 dz_2 \tag{2.70}$$
$$+\int_0^\infty\int_0^\infty\int_1^0 f_{X|Z_2}\left(\frac{1}{\tau}\middle| z_2\right) f_{Y|Z_1}\left[g\left(\frac{1}{\tau},\xi\right)\middle| z_1\right] D_2 g\left(\frac{1}{\tau},\xi\right) f_{Z_1}(z_1) f_{Z_2}(z_2)\frac{d\tau}{\tau^2} dz_1 dz_2$$

It is straightforward to show that:

$$g\left(\frac{1}{x},\xi\right) = \frac{1}{g(x,\xi)}. \tag{2.71}$$

We also have (See Appendix for derivation):

$$f_{X|Z_2}\left(\frac{1}{x}\middle| z_2\right) = x^3 f_{X|Z_2}(x|z_2), \;\; f_{Y|Z_1}\left(\frac{1}{y}\middle| z_1\right) = y^3 f_{Y|Z_1}(y|z_1). \tag{2.72}$$

In accordance with (2.70), (2.71) and (2.72) we have:

$$\begin{aligned}\frac{\partial P^+(\xi)}{\partial \xi} =& -\int_0^\infty\int_0^\infty\int_0^1 f_{X|Z_2}(x|z_2) f_{Y|Z_1}\left[g(x,\xi)|z_1\right] D_2 g(x,\xi) f_{Z_1}(z_1) f_{Z_2}(z_2) dx dz_1 dz_2 \\ &-\int_0^\infty\int_0^\infty\int_0^1 x^3 f_{X|Z_2}(x|z_2)\left[g(x,\xi)\right]^3 f_{Y|Z_1}\left[g(x,\xi)|z_1\right] D_2 g\left(\frac{1}{x},\xi\right) f_{Z_1}(z_1) f_{Z_2}(z_2)\frac{dx}{x^2} dz_1 dz_2 \\ =& -\int_0^\infty\int_0^\infty\int_0^1 f_{X|Z_2}(x|z_2) f_{Y|Z_1}\left[g(x,\xi)|z_1\right] f_{Z_1}(z_1) f_{Z_2}(z_2)\left[D_2 g(x,\xi) + x\left[g(x,\xi)\right]^3 D_2 g\left(\frac{1}{x},\xi\right)\right] \\ & dx dz_1 dz_2 \end{aligned} \tag{2.73}$$

In order to simplify the notations, we define $A(x,\xi)$ as in the following:

$$A(x,\xi) = D_2 g(x,\xi) + x\left[g(x,\xi)\right]^3 D_2 g\left(\frac{1}{x},\xi\right). \tag{2.74}$$

In accordance with (2.64), (2.67) and (2.74) we have:

$$A(x,\xi) = \frac{1-x^2}{(1-\xi+\xi x)^2} + \frac{x\left[(1-\xi)x+\xi\right]^3}{(1-\xi+\xi x)^3}\cdot\frac{\left(1-\frac{1}{x^2}\right)}{\left(1-\xi+\frac{\xi}{x}\right)^2} = \frac{(1-\xi)\left(1-x^2\right)^2}{(1-\xi+\xi x)^3}. \tag{2.75}$$

From (2.75) we deduce that $A(x,\xi)$ is non-negative if $\xi \in [0,1]$ and $x > 0$; thus we can conclude that:

$$\frac{\partial P^+(\xi)}{\partial \xi} = -\int_0^\infty\int_0^\infty\int_0^1 \underbrace{f_{X|Z_2}(x|z_2)}_{>0}\underbrace{f_{Y|Z_1}\left[g(x,\xi)|z_1\right]}_{>0}\underbrace{f_{Z_1}(z_1)}_{>0}\underbrace{f_{Z_2}(z_2)}_{>0}\underbrace{A(x,\xi)}_{\geq 0} dx dz_1 dz_2 \leq 0, \tag{2.76}$$

and Lemma 2.7.1 is proved. □

2.7.3 Proving the first inequality of (2.31)

In this subsection, we prove the first inequality of (2.31).

Theorem 2.7.1. $P^{\mathrm{Id}}(e) \leq P^{\mathrm{RA}}(e)$.

Proof. As mentioned in (2.60), $P^{\mathrm{Id}}(e)$ can be written in terms of $P^{+}()$ as the following:

$$P^{\mathrm{Id}}(e) = P^{+}\left(\frac{1}{2}\right) P(\theta = 0) + P^{+}(1)P(\theta = 1). \tag{2.77}$$

In both *Ideal* and *Relay-Agnostic Systems*, the relay employs the same signal detection scheme and the difference between both systems is only in their forwarding policies. Therefore, probability that a particular symbol is detected with error at the relay is the same for both systems; we can therefore write:

$$\begin{aligned} P(\theta = 0) &= P(\tilde{x} \neq x) = P(\tilde{x} = -1, x = +1) + P(\tilde{x} = +1, x = -1) \\ &= \frac{1}{2}\Big[P(\tilde{x} = -1|x = +1) + P(\tilde{x} = +1|x = -1)\Big] = P(\tilde{x} = -1|x = +1), \end{aligned} \tag{2.78}$$

where the last equality in (2.78) is due to the symmetric nature of the system. Thus we can rewrite (2.54) as:

$$\begin{aligned} P^{\mathrm{RA}}(e) = \Big[& P^{\mathrm{RA}}(e|x = 1, \tilde{x} = -1, \theta' = 1)P(\theta' = 1|x = 1, \tilde{x} = -1) \\ & + P^{\mathrm{RA}}(e|x = 1, \tilde{x} = -1, \theta' = 0)P(\theta' = 0|x = 1, \tilde{x} = -1)\Big] P(\theta = 0) \\ & + \Big[P^{\mathrm{RA}}(e|x = 1, \tilde{x} = 1, \theta' = 1)P(\theta' = 1|x = 1, \tilde{x} = 1) \\ & + P^{\mathrm{RA}}(e|x = 1, \tilde{x} = 1, \theta' = 0)P(\theta' = 0|x = 1, \tilde{x} = 1)\Big] P(\theta = 1). \end{aligned} \tag{2.79}$$

In accordance with (2.55)-(2.58), and (2.79), the BEP of the *Relay-Agnostic System* can be written in terms of $P^{+}()$ as the following:

$$\begin{aligned} P^{\mathrm{RA}}(e) = & \left[P^{+}(\delta)\, P(\theta' = 1|x = 1, \tilde{x} = -1) + P^{+}\left(\frac{1}{2}\right) P(\theta' = 0|x = 1, \tilde{x} = -1)\right] P(\theta = 0) \\ & + \left[P^{+}(1-\delta)\, P(\theta' = 1|x = 1, \tilde{x} = 1) + P^{+}\left(\frac{1}{2}\right) P(\theta' = 0|x = 1, \tilde{x} = 1)\right] P(\theta = 1) \end{aligned} \tag{2.80}$$

We consider the two following cases:

case I: $\delta < \frac{1}{2}$. In this case, from Lemma 2.7.1 we have: $P^+(\delta) \geq P^+\left(\frac{1}{2}\right)$. Since $1-\delta < 1$, we also have $P^+(1-\delta) \geq P^+(1)$. Thus, (2.80) can be lower bounded as:

$$\begin{aligned} P^{\mathrm{RA}}(e) = & \Bigg[\underbrace{P^+(\delta)}_{\geq P^+\left(\frac{1}{2}\right)} P(\theta'=1|x=1,\tilde{x}=-1) + P^+\left(\frac{1}{2}\right) P(\theta'=0|x=1,\tilde{x}=-1) \Bigg] P(\theta=0) \\ & + \Bigg[\underbrace{P^+(1-\delta)}_{\geq P^+(1)} P(\theta'=1|x=1,\tilde{x}=1) + \underbrace{P^+\left(\frac{1}{2}\right)}_{\geq P^+(1)} P(\theta'=0|x=1,\tilde{x}=1) \Bigg] P(\theta=1) \\ \geq & \; P^+\left(\frac{1}{2}\right) P(\theta=0) + P^+(1) P(\theta=1) = P^{\mathrm{Id}}(e). \end{aligned} \tag{2.81}$$

case II: $\delta \geq \frac{1}{2}$. In this case, from Lemma 2.7.1 we have: $P^+(\delta) \geq P^+(1)$. Since $1-\delta \leq \frac{1}{2}$, we also have $P^+(1-\delta) \geq P^+\left(\frac{1}{2}\right)$. Thus, (2.80) can be lower bounded as:

$$\begin{aligned} P^{\mathrm{RA}}(e) = & \Bigg[\underbrace{P^+(\delta)}_{\geq P^+(1)} P(\theta'=1|x=1,\tilde{x}=-1) + \underbrace{P^+\left(\frac{1}{2}\right)}_{\geq P^+(1)} P(\theta'=0|x=1,\tilde{x}=-1) \Bigg] P(\theta=0) \\ & + \Bigg[\underbrace{P^+(1-\delta)}_{\geq P^+\left(\frac{1}{2}\right)} P(\theta'=1|x=1,\tilde{x}=1) + P^+\left(\frac{1}{2}\right) P(\theta'=0|x=1,\tilde{x}=1) \Bigg] P(\theta=1) \\ \geq & \; P^+(1) P(\theta=0) + P^+\left(\frac{1}{2}\right) P(\theta=1) \\ = & \; P^+(1) \Big[1 - P(\theta=1) \Big] + P^+\left(\frac{1}{2}\right) P(\theta=1) \\ = & \; P^+(1) + \underbrace{\left[P^+\left(\frac{1}{2}\right) - P^+(1) \right]}_{\geq 0} \underbrace{P(\theta=1)}_{\geq P(\theta=0)}, \end{aligned} \tag{2.82}$$

From Lemma 2.7.1 we have $P^+\left(\frac{1}{2}\right) - P^+(1) \geq 0$. We point out that $P(\theta=0)$ is the probability that the relay in the *Ideal System* detects the symbol with error; thus, we have $P(\theta=1) \geq P(\theta=0)$ because in the case of binary signalling and using optimal symbol detection, it is less likely that a detection error occurs. Therefore, in accordance with (2.82) we have:

$$\begin{aligned} P^{\mathrm{RA}}(e) & \geq P^+(1) + \left[P^+\left(\frac{1}{2}\right) - P^+(1) \right] P(\theta=0) \\ & = P^+\left(\frac{1}{2}\right) P(\theta=0) + P^+(1) - P^+(1) P(\theta=0) \\ & = P^+\left(\frac{1}{2}\right) P(\theta=0) + P^+(1) P(\theta=1) = P^{\mathrm{Id}}(e). \end{aligned} \tag{2.83}$$

Thus, Theorem 2.7.1 is proved. □

We proved that the BEP of the *Ideal System* is a lower bound on the BEP of the *Relay-Agnostic System*. Thus, we proved that the BEP of the *Ideal System* is a lower bound on the BEP performance of the *Agnostic System*.

2.8 Performance Comparison for an MRC Receiver

In this section, by using a simple argument, we prove that the SEP performance of the ideal system is a lower bound on the SEP performance of the agnostic system in which the destination node employs MRC receiver. We assume that in both ideal and agnostic systems, destination uses MRC as the following [35] [39]:

$$y_{\text{MRC}}^{\text{Id}} = \frac{\sqrt{\mathcal{P}_s}}{\mathcal{P}_s\sigma_{e_{sd}}^2 + N_0}\hat{h}_{sd}^* y_{sd} + \frac{\theta\sqrt{\mathcal{P}_r}}{\mathcal{P}_r\sigma_{e_{rd}}^2 + N_0}\hat{h}_{rd}^* y_{rd}, \tag{2.84}$$

$$y_{\text{MRC}}^{\text{A}} = \frac{\sqrt{\mathcal{P}_s}}{\mathcal{P}_s\sigma_{e_{sd}}^2 + N_0}\hat{h}_{sd}^* y_{sd} + \frac{\hat{\theta}'\sqrt{\mathcal{P}_r}}{\mathcal{P}_r\sigma_{e_{rd}}^2 + N_0}\hat{h}_{rd}^* y_{rd}, \tag{2.85}$$

where $\hat{\theta}'$ is the destination's estimation of θ' in the agnostic system.

The contribution of this section is to articulate a sufficient condition under which the "ideal system's" SEP is a lower bound on the "agnostic system's" through a simple argument. We consider the following four events:

I) $\tilde{x} = x$ and $\theta' = 0$: In this event, at the second time slot, the relay in the agnostic system remains silent and the symbol is kept from being forwarded (i.e., $\theta' = 0$). However, in the ideal system the symbol is forwarded to the destination node (i.e., $\theta = 1$) in accordance with the ideal system's knowledge of the correct detection and its forwarding rule. In the agnostic system, if $\hat{\theta}' = 0$, the final symbol detection at the destination is made only based on the received signal at the first time slot. If $\hat{\theta}' = 1$, the destination combines the received signal at the first time slot from the source with noise. In both events, the conditional SEP in the agnostic system has no less SEP than that in the ideal system. Therefore, we have $P_s^{\text{Id}}(e|\tilde{x} = x, \theta' = 0) \leq P_s^{\text{A}}(e|\tilde{x} = x, \theta' = 0)$ where $P_s^{\text{Id}}(e)$ and $P_s^{\text{A}}(e)$ are SEPs of the ideal and agnostic systems, respectively.

II) $\tilde{x} = x$ and $\theta' = 1$: In the ideal system, the symbol is forwarded to the destination (i.e., $\theta = 1$) because the relay correctly detects the symbol. In the agnostic system, if $\hat{\theta}' = 1$,

both systems have the same SEP performance. However, if $\hat{\theta}' = 0$, the destination node in the agnostic system uses only the received signal at the first time slot, and this results in a poorer conditional SEP than the ideal system. We can therefore write $P_s^{\mathrm{Id}}(e|\tilde{x} = x, \theta' = 1) \leq P_s^{\mathrm{A}}(e|\tilde{x} = x, \theta' = 1)$.

III) $\tilde{x} \neq x$ and $\theta' = 0$: In this event, the destination in the ideal system detects the symbol based only on the received signal in the first time slot. In the agnostic system, if $\hat{\theta}' = 0$, the destination detects the symbol based only on the signal received in the first time slot and thus has the same SEP performance as the ideal system. In the agnostic system, if $\hat{\theta}' = 1$, the destination combines the received signal at the first time slot from the source with noise which results in a poorer detection than the ideal system. Therefore, the ideal system will have less likelihood of making a symbol error and we have $P_s^{\mathrm{Id}}(e|\tilde{x} \neq x, \theta' = 0) \leq P_s^{\mathrm{A}}(e|\tilde{x} \neq x, \theta' = 0)$.

IV) $\tilde{x} \neq x$ and $\theta' = 1$: In this event, in the ideal system, the symbol is kept from being forwarded by the relay (i.e., $\theta = 0$) and the destination will detect the transmitted symbol only based on the received signal form the source during the first time slot. If $\hat{\theta}' = 0$, the agnostic system's destination will also detect the transmitted symbol only based on the received signal form the source during the first time slot, so we have:

$$P_s^{\mathrm{A}}(e|\tilde{x} \neq x, \theta' = 1, \hat{\theta}' = 0) = P_s^{\mathrm{Id}}(e|\tilde{x} \neq x, \theta' = 1, \hat{\theta}' = 0). \tag{2.86}$$

We note that

$$P_s^{\mathrm{Id}}(e|\tilde{x} \neq x, \theta' = 1, \hat{\theta}' = 0) = P_s^{\mathrm{Id}}(e|\tilde{x} \neq x), \tag{2.87}$$

as the symbol error event in the ideal system is independent of the agnostic system's decisions θ' and $\hat{\theta}'$. Thus, from (2.86) and (2.87) we have:

$$\begin{aligned} &P_s^{\mathrm{A}}(e|\tilde{x} \neq x, \theta' = 1) = P(\hat{\theta}' = 1|\tilde{x} \neq x, \theta' = 1) P_s^{\mathrm{A}}(e|\tilde{x} \neq x, \theta' = 1, \hat{\theta}' = 1) \\ &+ P(\hat{\theta}' = 0|\tilde{x} \neq x, \theta' = 1) P_s^{\mathrm{A}}(e|\tilde{x} \neq x, \theta' = 1, \hat{\theta}' = 0) \\ &= P(\hat{\theta}' = 1|\tilde{x} \neq x, \theta' = 1) P_s^{\mathrm{A}}(e|\tilde{x} \neq x, \theta' = 1, \hat{\theta}' = 1) + P(\hat{\theta}' = 0|\tilde{x} \neq x, \theta' = 1) P_s^{\mathrm{Id}}(e|\tilde{x} \neq x). \end{aligned} \tag{2.88}$$

From (2.88) we can state that if $P_s^{\mathrm{Id}}(e|\tilde{x} \neq x) \leq P_s^{\mathrm{A}}(e|\tilde{x} \neq x, \theta' = 1, \hat{\theta}' = 1)$, then we have: $P_s^{\mathrm{Id}}(e|\tilde{x} \neq x, \theta' = 1) \leq P_s^{\mathrm{A}}(e|\tilde{x} \neq x, \theta' = 1)$. Thus, by averaging probabilities under the conditioning events *I*, *II*, *III*, and *IV*, the following Theorem is proved.

Theorem 2.8.1. *For any modulation scheme, any forwarding policy at the relay in the agnostic system, and any method of deciding whether to combine the signal at the second time slot in the agnostic system, if* $P_s^{\mathrm{Id}}(e|\tilde{x}\neq x)\leq P_s^{\mathrm{A}}(e|\tilde{x}\neq x,\theta'=1,\hat{\theta}'=1)$*, then we have we have* $P_s^{\mathrm{Id}}(e)\leq P_s^{\mathrm{A}}(e)$.

2.8.1 Example use of Theorem 2.8.1

In this section, we will provide an example use of Theorem 2.8.1. For the ideal and the agnostic systems employing QPSK modulation, we will show that the antecedent of Theorem 2.8.1, $P_s^{\mathrm{Id}}(e|\tilde{x}\neq x)\leq P_s^{\mathrm{A}}(e|\tilde{x}\neq x,\theta'=1,\hat{\theta}'=1)$ is true; that is, for QPSK modulation, MRC combining a wrong symbol with the correct symbol at the destination, results in a higher SEP than the case in which the wrong symbol is not combined at the destination node. In light the equivalence (2.87), we will prove that

$$P_s^{\mathrm{Id}}(e|\tilde{x}\neq x,\theta'=1,\hat{\theta}'=1)\leq P_s^{\mathrm{A}}(e|\tilde{x}\neq x,\theta'=1,\hat{\theta}'=1). \tag{2.89}$$

Since QPSK modulation is considered, the transmitted symbol, x, can be represented by one of $\{+1,+j,-1,-j\}$. Without loss of generality, we will assume $x=+1$ and prove that

$$P_s^{\mathrm{Id}}(e|x=1,\tilde{x}\neq x,\theta'=1,\hat{\theta}'=1)\leq P_s^{\mathrm{A}}(e|x=1,\tilde{x}\neq x,\theta'=1,\hat{\theta}'=1). \tag{2.90}$$

Then, this inequality will be also proven for $x=j,-j,-1$ by symmetrical arguments, and as a result, inequality (2.89) will be proven. To this end, for the rest of this section, our discussion will be under the condition $x=1$, $\tilde{x}\neq x$, $\theta'=1$, and $\hat{\theta}'=1$. By definition of the ideal system, $\tilde{x}\neq+1$ implies that $\theta=0$, so the destination node in the ideal system detects the transmitted symbol based on y^{Id} in (2.84) with $\theta=0$. In accordance with (2.12) and (2.84) we have:

$$y^{\mathrm{Id}} \;=\; \frac{\mathcal{P}_s}{\mathcal{P}_s\sigma_{e_{sd}}^2+N_0}|\hat{h}_{sd}|^2+\frac{\sqrt{\mathcal{P}_s}}{\mathcal{P}_s\sigma_{e_{sd}}^2+N_0}\hat{h}_{sd}^*\tilde{n}_{sd}=S^I+n_{sd}^I+jn_{sd}^Q, \tag{2.91}$$

where $\tilde{n}_{sd}=\sqrt{\mathcal{P}_s}e_{sd}+n_{sd}$, $S^I=\frac{\mathcal{P}_s}{\mathcal{P}_s\sigma_{e_{sd}}^2+N_0}|\hat{h}_{sd}|^2$, and

$$n_{sd}^I=\mathrm{Re}\left(\frac{\sqrt{\mathcal{P}_s}\hat{h}_{sd}^*\tilde{n}_{sd}}{\mathcal{P}_s\sigma_{e_{sd}}^2+N_0}\right),\, n_{sd}^Q=\mathrm{Im}\left(\frac{\sqrt{\mathcal{P}_s}\hat{h}_{sd}^*\tilde{n}_{sd}}{\mathcal{P}_s\sigma_{e_{sd}}^2+N_0}\right). \tag{2.92}$$

Therefore in the ideal system, the received signal vector in I-Q plane can be written as $\mathbf{r}^{\mathrm{Id}}=[S^I+n_{sd}^I\,,n_{sd}^Q]$.

In the agnostic system, we will consider sub-events $\tilde{x}=j,-j,-1$ and prove that

$$P_s^{\mathrm{Id}}(e|x=1,\tilde{x}=z,\theta'=1,\hat{\theta}'=1)\leq P_s^{\mathrm{A}}(e|x=1,\tilde{x}=z,\theta'=1,\hat{\theta}'=1), \tag{2.93}$$

for each case $z=j,-j,-1$. This will then prove (2.90).

Sub-event $\tilde{x}=j$: In the agnostic system, the signal detection is made based on y^{A} in (2.85). If $\tilde{x}=j$, by using (2.47) and (2.85) we can write

$$\begin{aligned} y^{\mathrm{A}} &= \frac{\mathcal{P}_s}{\mathcal{P}_s\sigma_{e_{sd}}^2+N_0}|\hat{h}_{sd}|^2+\frac{\sqrt{\mathcal{P}_s}}{\mathcal{P}_s\sigma_{e_{sd}}^2+N_0}\hat{h}_{sd}^*\tilde{n}_{sd}+j\frac{\mathcal{P}_r}{\mathcal{P}_r\sigma_{e_{rd}}^2+N_0}|\hat{h}_{rd}|^2+\frac{\sqrt{\mathcal{P}_r}}{\mathcal{P}_r\sigma_{e_{rd}}^2+N_0}\hat{h}_{rd}^*\tilde{n}_{rd} \\ &= S^I+jS^{\mathrm{Er}}+n_{sd}^I+jn_{sd}^Q+n_{rd}^I+jn_{rd}^Q, \end{aligned} \tag{2.94}$$

where $\tilde{n}_{rd}=j\sqrt{\mathcal{P}_r}e_{rd}+n_{rd}$, $S^{\mathrm{Er}}=\frac{\mathcal{P}_r}{\mathcal{P}_r\sigma_{e_{rd}}^2+N_0}|\hat{h}_{rd}|^2$, and

$$n_{rd}^I=\mathrm{Re}\left(\frac{\sqrt{\mathcal{P}_r}\hat{h}_{rd}^*\tilde{n}_{rd}}{\mathcal{P}_r\sigma_{e_{rd}}^2+N_0}\right), n_{rd}^Q=\mathrm{Im}\left(\frac{\sqrt{\mathcal{P}_r}\hat{h}_{rd}^*\tilde{n}_{rd}}{\mathcal{P}_r\sigma_{e_{rd}}^2+N_0}\right). \tag{2.95}$$

Therefore, the received signal vector in I-Q plane is $\mathbf{r}^{\mathrm{A}}=[S^I+n_{sd}^I+n_{rd}^I\,,S^{\mathrm{Er}}+n_{sd}^Q+n_{rd}^Q]$. In order to compare the result of signal detection in the ideal system (which is made based on $\mathbf{r}^{\mathrm{Id}}$) and the agnostic system (which is made based on $\mathbf{r}^{\mathrm{A}}$), we first normalize the noise variances in both $\mathbf{r}^{\mathrm{Id}}$ and $\mathbf{r}^{\mathrm{A}}$. Obviously, signal detection based on $\mathbf{r}^{\mathrm{Id}}$ and $\mathbf{r}^{\mathrm{A}}$ results in the same performance as signal detection based on $\tilde{\mathbf{r}}^{\mathrm{Id}}=\mathbf{r}^{\mathrm{Id}}/\sigma_1$ and $\tilde{\mathbf{r}}^{\mathrm{A}}=\mathbf{r}^{\mathrm{A}}/\sigma_2$ where $\sigma_1^2=\mathrm{Var}(n_{sd}^I)=\mathrm{Var}(n_{sd}^Q)$ and $\sigma_2^2=\mathrm{Var}(n_{sd}^I+n_{rd}^I)=\mathrm{Var}(n_{sd}^Q+n_{rd}^Q)$. The received normalized signal vectors in the ideal and agnostic systems are respectively $\tilde{\mathbf{r}}^{\mathrm{Id}}=[S_1+n_1,n_2]$ and $\tilde{\mathbf{r}}^{\mathrm{A}}=[S_1'+n_1\,,S_2+n_2]$, where n_1 and n_2 are normalized noise components, $S_1=S^I/\sigma_1$, $S_1'=S^I/\sigma_2$ and $S_2=S^{\mathrm{Er}}/\sigma_2$. The probability that the destination in the ideal system makes the correct decision is as follows:

$$P_s^{\mathrm{Id}}(c|x=1,\tilde{x}=j,\theta'=1,\hat{\theta}'=1)=P\left(-S_1-n_1<n_2<S_1+n_1,S_1+n_1>0\right). \tag{2.96}$$

Since n_1 and n_2 are zero mean, independent and identically distributed Gaussian random variable with unit variance, conditioned on $\hat{h}_{sd}$ and $\hat{h}_{rd}$, we can write (2.96) as the following:

$$\begin{aligned} P_s^{\mathrm{Id}}(c|\hat{h}_{sd},\hat{h}_{rd},x=1,\tilde{x}=j,\theta'=1,\hat{\theta}'=1) &= \int_{-S_1}^{+\infty}\int_{-\nu_1-S_1}^{\nu_1+S_1}\frac{e^{-\frac{{\nu_2}^2}{2}}}{\sqrt{2\pi}}\cdot\frac{e^{-\frac{{\nu_1}^2}{2}}}{\sqrt{2\pi}}d\nu_2 d\nu_1 \\ &= \int_{-S_1}^{+\infty}\frac{e^{-\frac{{\nu_1}^2}{2}}}{\sqrt{2\pi}}\left[Q\left(-\nu_1-S_1\right)-Q\left(\nu_1+S_1\right)\right]d\nu_1 = \int_{-S_1}^{+\infty}\frac{e^{-\frac{{\nu_1}^2}{2}}}{\sqrt{2\pi}}h\left(\nu_1,S_1,0\right)d\nu_1, \end{aligned} \tag{2.97}$$

where $h\left(x,t_1,t_2\right)=Q(-x-t_1-t_2)-Q(x+t_1-t_2)$. In the agnostic system, the probability that the destination makes the correct decision is given by:

$$P_s^{\mathrm{A}}(c|x=1,\tilde{x}=j,\theta'=1,\hat{\theta}'=1)=P\left(-S_1'-n_1<n_2+S_2<S_1'+n_1,S_1'+n_1>0\right). \quad (2.98)$$

Conditioned on $\hat{h}_{sd}$ and $\hat{h}_{rd}$, (2.98) can be rewritten as the following:

$$P_s^{\mathrm{A}}(c|\hat{h}_{sd},\hat{h}_{rd},x=1,\tilde{x}=j,\theta'=1,\hat{\theta}'=1)=\int_{-S_1'}^{+\infty}\int_{-\nu_1-S_1'-S_2}^{\nu_1+S_1'-S_2}\frac{e^{-\frac{{\nu_2}^2}{2}}}{\sqrt{2\pi}}\cdot\frac{e^{-\frac{{\nu_1}^2}{2}}}{\sqrt{2\pi}}d\nu_2 d\nu_1$$

$$=\int_{-S_1'}^{+\infty}\frac{e^{-\frac{{\nu_1}^2}{2}}}{\sqrt{2\pi}}\left[Q\left(-\nu_1-S_1'-S_2\right)-Q\left(\nu_1+S_1'-S_2\right)\right]d\nu_1=\int_{-S_1'}^{+\infty}\frac{e^{-\frac{{\nu_1}^2}{2}}}{\sqrt{2\pi}}h\left(\nu_1,S_1',S_2\right)d\nu_1. \quad (2.99)$$

Partial derivatives $\partial h/\partial t_1$ and $\partial h/\partial t_2$ have simple forms as follows:

$$\frac{\partial h}{\partial t_1}(x,t_1,t_2)=\frac{1}{\sqrt{2\pi}}\left[e^{-(x+t_1+t_2)^2}+e^{-(x+t_1-t_2)^2}\right]>0, \quad (2.100)$$

$$\frac{\partial h}{\partial t_2}(x,t_1,t_2)=\frac{1}{\sqrt{2\pi}}\left[e^{-(x+t_1+t_2)^2}-e^{-(x+t_1-t_2)^2}\right]. \quad (2.101)$$

In accordance with (2.101), we have $\frac{\partial h}{\partial t_2}(x,t_1,t_2)\leq 0$, for all $t_2\geq 0$ as long as $x+t_1\geq 0$. From $\sigma_2>\sigma_1$ follows that $S_1>S_1'$, and we also have $S_2\geq 0$. From this and (2.100), (2.101), the following inequality is proved for $\nu_1>-S_1'$:

$$h\left(\nu_1,S_1',S_2\right)\leq h\left(\nu_1,S_1,0\right). \quad (2.102)$$

From (2.97), (2.99) and (2.102) follows that (2.93) holds for $z=j$.

Sub-event $\tilde{x}=-j$: Due to symmetry, (2.93) can be shown to be true for $z=-j$ in the same manner as in the case of sub-event $\tilde{x}=j$.

Sub-event $\tilde{x}=-1$: From (2.47) and (2.85), we have $\mathbf{r}^{\mathrm{A}}=[S^I-S^{\mathrm{Er}}+n_{sd}^I+n_{rd}^I,n_{sd}^Q+n_{rd}^Q]$ and $\mathbf{r}^{\mathrm{Id}}=[S^I+n_{sd}^I,n_{sd}^Q]$. The signal-to-noise ratios in the first components of these I-Q vectors obviously show that (2.93) holds in this case.

Finally, by averaging over all the channel realizations, (2.89) is proven.

2.9 Simulation Results

We assumed that a fixed total power is distributed between the source and the relay such that $\mathcal{P}_1+\mathcal{P}_2=\mathcal{P}$. This power constraint is imposed to guarantee a fair performance

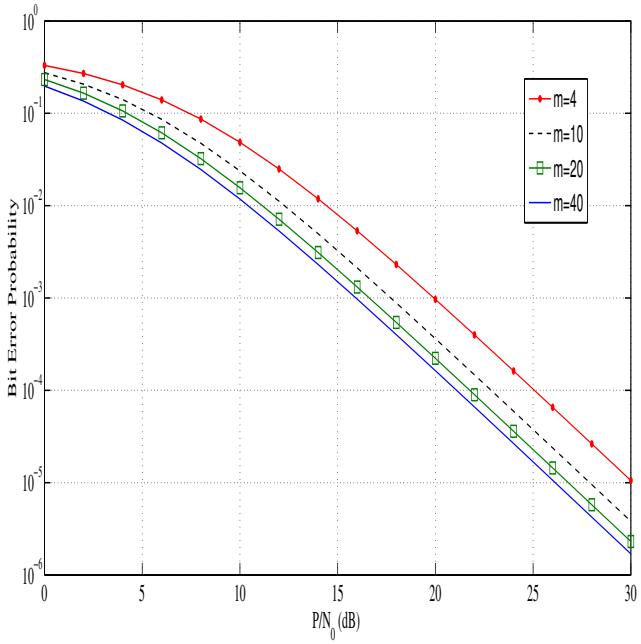

Figure 2.4: BEP against $\mathcal{P}/N_0$ for α=β=0.1, $r = \mathcal{P}_1/\mathcal{P} = 0.61$ and different frame lengths

comparison with the direct transmission scenario [15] [30] [66]. We point out that the BEP expression in (2.29) can be written as a function of α, β, m, r and $\mathcal{P}$ where:

$$P^{\mathrm{Id}}(e) \equiv f\left(\alpha, \beta, m, r, \mathcal{P}\right), \;\; \mathcal{P} = \mathcal{P}_1 + \mathcal{P}_2, \;\; r = \frac{\mathcal{P}_1}{\mathcal{P}}. \tag{2.103}$$

Figure 2.4 shows the lower bound expression (2.29) against P/N_0 for m=4, 10, 20 and 40 where m is the frame length. Parameters α, β and $r = \mathcal{P}_1/P$ are set to 0.10, 0.10 and 0.61 respectively. For this figure, all channels are assumed to have unit variance.

Figure 2.5 shows the lower bound expression (2.29) versus both α and β for m=4, $r = \mathcal{P}_1/\mathcal{P}$=0.61. Figure 2.6 shows the lower bound expression (2.29) versus r for $\alpha = \beta$=0.30 and different frame lengths.

Figure 2.7 shows the BEP of an *Agnostic System* based on the Monte-Carlo simulation in comparison with the lower bound expression (2.29) against P/N_0 for α=β=0.30, r=0.81 and m=40. Matlab was used for Monte-Carlo simulation, and 10^8 transmitted BPSK symbols were generated in order to estimate the BEP. The node-to-node channels are modelled by

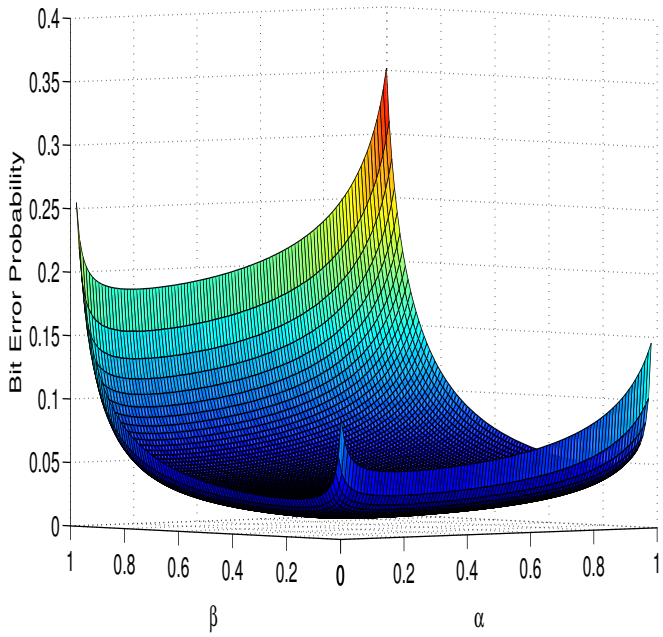

Figure 2.5: BEP against α and β for $r = \mathcal{P}_1/\mathcal{P}$=0.61 and $m = 4$

zero mean independent Gaussian random variables. For this figure, in both *Ideal* and *Agnostic Systems*, variances of source-relay, source-destination and relay-destination channels are set to 1, 1, and 0.05, respectively. As for the forwarding policy in the *Agnostic System*, for this simulation we chose the policy of forwarding all symbols detected by the relay. As for the destination's symbol detection rule, we chose maximum ratio combining (MRC). As this figure shows, the lower bound (2.29) is very tight for this *Agnostic System*. In order to numerically compare the BEP of this *Agnostic System* and the BEP of the *Ideal System* (2.29), we defined error percentage as the ratio $100 \times (\text{BEP}_{Agnostic} - \text{BEP}_{Ideal})/\text{BEP}_{Agnostic}$. The error percentage at P/N_0=5 dB, 10 dB, 15 dB, 20 dB and 25 dB turns out to be 4.11, 2.87, 1.93, 1.44, and 4.26, respectively. These results indicate that there is a slight difference between the values of the BEP of the *Ideal System* and the BEP of the *Agnostic System*.

In Table 2.1, the optimum values for α, β and r for m= 4, 10, 20, 40 and 80 under different SNRs are tabulated. In order to optimally allocate power to training and data transmission phases so that (2.29) is minimized, one can solve the following optimization

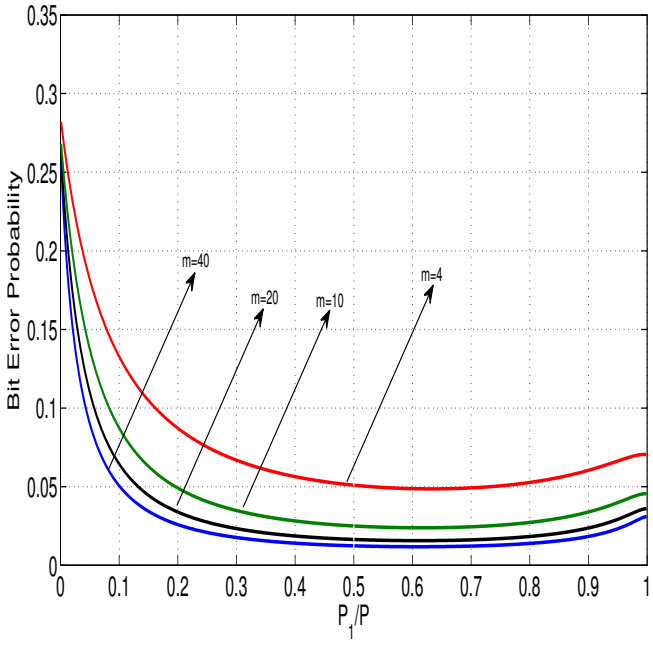

Figure 2.6: BEP against $r = \mathcal{P}_1/\mathcal{P}$ for α=β=0.3 and different frame lengths

problem:

$$(\alpha_{opt}, \beta_{opt}, r_{opt}) = \arg \min_{\alpha,\beta,r} f(\alpha, \beta, m, r, \mathcal{P}),$$
$$\text{subject to} : 0 \leq \alpha \leq 1, \;\; 0 \leq \beta \leq 1, \;\; 0 \leq \text{r} \leq 1. \tag{2.104}$$

We evaluated the lower bound expression (2.29) for sampled values of α, β and r with a sampling interval of 0.01 for each SNR and searched for the values of α, β and r that minimizes the lower bound expression.

2.10 Summary and Discussions

This chapter was motivated by our desire to extend rigorous theoretical analysis of decode-and-forward (DF) cooperative communication systems to the models that consider practical implementability more than we typically find in the literature. We used system models that address imperfect channel gain information at the receivers. Also, in our system modelling,

Table 2.1: Results of optimization for m= 10, 20, 40, and 80 for different values of $\mathcal{P}/N_0$

		m=10	m=20	m= 40	m= 80
$\mathcal{P}/\mathrm{N}_0 = 10\mathrm{dB}$	r_{opt}	0.61	0.61	0.61	0.61
	α_{opt}	0.26	0.20	0.14	0.11
	β_{opt}	0.27	0.20	0.14	0.11
	BEP	1.61×10^{-2}	1.33×10^{-2}	1.13×10^{-2}	9.9×10^{-3}
$\mathcal{P}/\mathrm{N}_0 = 15\mathrm{dB}$	r_{opt}	0.60	0.60	0.60	0.60
	α_{opt}	0.25	0.19	0.14	0.10
	β_{opt}	0.26	0.19	0.14	0.10
	BEP	2.1×10^{-3}	1.7×10^{-3}	1.4×10^{-3}	1.3×10^{-3}
$\mathcal{P}/\mathrm{N}_0 = 20\mathrm{dB}$	r_{opt}	0.59	0.59	0.59	0.59
	α_{opt}	0.25	0.19	0.14	0.10
	β_{opt}	0.25	0.19	0.14	0.10
	BEP	2.3355×10^{-4}	1.8860×10^{-4}	1.5782×10^{-4}	1.3711×10^{-4}
$\mathcal{P}/\mathrm{N}_0 = 25\mathrm{dB}$	r_{opt}	0.59	0.59	0.59	0.59
	α_{opt}	0.25	0.19	0.14	0.10
	β_{opt}	0.25	0.19	0.14	0.10
	BEP	2.4088×10^{-5}	1.9419×10^{-5}	1.6228×10^{-5}	1.4083×10^{-5}
$\mathcal{P}/\mathrm{N}_0 = 30\mathrm{dB}$	r_{opt}	0.59	0.59	0.59	0.59
	α_{opt}	0.25	0.19	0.14	0.10
	β_{opt}	0.25	0.19	0.14	0.10
	BEP	2.4327×10^{-6}	1.9601×10^{-6}	1.6373×10^{-6}	1.4204×10^{-6}

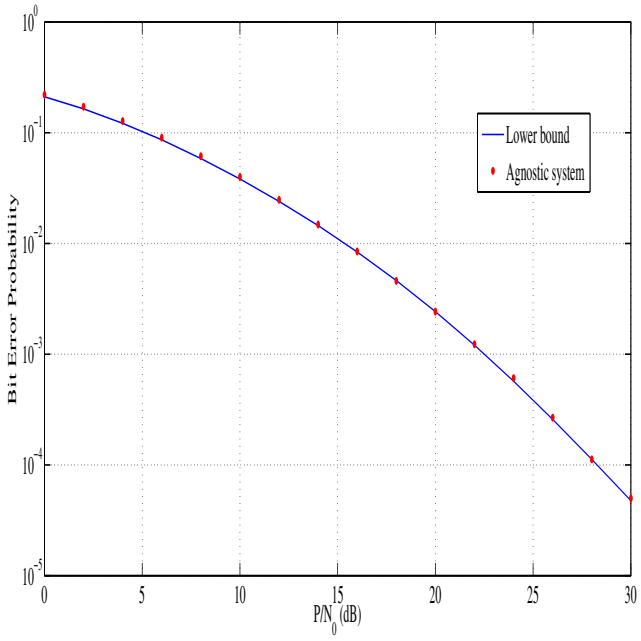

Figure 2.7: BEP against P/N_0 for α=β=0.30, $r = \mathcal{P}_1/P = 0.81$ and $m = 40$

we considered different levels of practical implementability in terms of the relay's and destination's knowledge of detection error and symbol forwarding decisions; we classified single-antenna, three-node, uncoded, fixed-throughput DF cooperative communication systems to i) *Ideal*, ii) *Relay-Agnostic*, and iii) *Agnostic Systems*. Then, we derived a closed-form expression of the BEP for the "*Ideal System*." We proved that this closed-form expression serves as a lower bound on the BEP performance of all systems that are classified as the "*Relay-Agnostic System*" or the "*Agnostic System*." Furthermore, we showed that the BEP performance of the "*Relay-Agnostic System*" is a lower bound on the BEP performance of the "*Agnostic System*."

The quantitative difference between the lower bound (2.29) and the BEP of a system in the class of the "*Relay-Agnostic System*" or the "*Agnostic System*" depends on the destination's detection scheme and also on the relay's forwarding policy employed by the system. We find that the lower bound (2.29) derived in this chapter is a good approximation for a system that employs a reasonably good relaying policy and detection scheme. For example,

we compared bound (2.29) and the BEP of the system introduced in [30], which employs a sub-optimal detection scheme implementable at the destination node. We found that the BEP-vs-SNR curve of this system is very close to that of (2.29).

The "*Ideal System*", which has BEP (2.29), has a modelling assumption that the relay is perfectly capable of diagnosing whether there has been an error in the detection of the binary symbol transmitted by the source. Under this ideal assumption, in the case of the BPSK system one might think of another fictitious system, in which the relay simply corrects the wrongly detected bit by flipping it and always forwards a correct bit to the destination. It can be easily shown that the BEP of this fictitious system is a lower bound on the BEP of the "*Ideal System*" (and thus a lower bound on the BEP of the "*Agnostic System*") discussed in this chapter. We note that the "*Ideal System*" presented in this chapter provides a tighter lower bound on the BEP performance of the "*Agnostic System*."

Chapter 3

Design and Analysis of Symbol Detection Schemes for SDF Networks in the Presence of CEE

3.1 Objective

In chapter 2, we studied three system models for the SDF relay-assisted communication system in the presence of channel estimation error. In the present chapter, we study yet another model, which we term as *Destination Agnostic System*. With this fourth model, we focus on the issue of signal detection at the destination. In particular, we present a novel signal detection scheme in the presence of channel estimation error for the SDF protocol. Simulation results are presented to show that the presented signal detection scheme results in a good performance.

3.2 System model and contribution

In chapter 2, we defined *Ideal*, *Relay-Agnostic*, and *Agnostic Systems*. For the *Ideal System* we assumed that the relay node perfectly knows whether a particular symbol has been detected correctly or not, and the destination node knows whether the relay has forwarded a particular symbol or not. For the *Relay-Agnostic System* we assumed that the relay node does not necessarily know whether the symbol has been detected correctly or not, but the

destination node perfectly knows whether the relay has forwarded the detected symbol or not. For the *Agnostic System* we assumed that the relay node does not necessarily know whether the symbol has been detected correctly or not, and the destination node does not know whether the relay has forwarded the detected symbol or not. In this chapter, we term another system as *Destination Agnostic System*, in which the relay node perfectly knows whether a symbol has been detected correctly or not, but the destination node does not know whether the relay has forwarded a particular symbol or not. We also assume that in the *Destination Agnostic System*, if the relay correctly detects the received symbol, then the relay will forward it to the destination in the second time slot; otherwise, the relay will remain silent. In this chapter, we will discuss the issue of optimally detecting data symbols at the destination in the *Destination Agnostic System*. For simplicity, we assume that all the channel gains have the same variance (i.e., $\sigma^2_{h_{sd}} = \sigma^2_{h_{sr}} = \sigma^2_{h_{rd}} = \sigma^2_h$).

We first analyze the optimal signal detection and its complexity in section 3.3. In Sections 3.4, we introduce our suboptimal symbol detection schemes. Performance evaluation is presented in Section 3.5, followed by conclusion and future work in Section 3.6.

3.3 Optimal Signal Detection and Complexity

3.3.1 Optimal detection of symbols in a block

In this section, for theoretical perspective we study the optimal symbol detection rule in the presence of channel estimation error using MMSE channel estimator. It will become apparent that the optimal symbol detection at the destination node has high computational complexity, and we will present computationally efficient and well-performing suboptimal detection schemes in the next section.

As mentioned in (2.12), the received signals at the destination during two time slots can be written as:

$$\begin{aligned} y^i_{sd} &= \sqrt{\mathcal{P}_s}\hat{h}_{sd}x_i + \sqrt{\mathcal{P}_s}e_{sd}x_i + n^i_{sd}, \\ y^i_{rd} &= \theta_i\sqrt{\mathcal{P}_r}\hat{h}_{rd}x_i + \theta_i\sqrt{\mathcal{P}_r}e_{rd}x_i + n^i_{rd}, \end{aligned} \tag{3.1}$$

where $i = 1, 2, ..., m-1$ and $\theta_i \in \{0, 1\}$. Assuming that the transmitted symbol has equal a priori probability, the maximum a posteriori (MAP) detection is reduced to the maximum likelihood (ML) detection. Signals available at the destination are pilot signals received (y^t_{sd},

y_{rd}^t) and data signal vectors received ($\mathbf{y}_{sd} = \left[y_{sd}^1\, y_{sd}^2 \ldots y_{sd}^{m-1}\right]$, $\mathbf{y}_{rd} = \left[y_{rd}^1\, y_{rd}^2 \ldots y_{rd}^{m-1}\right]$). ML detection of $\mathbf{x} = [x_1\, x_2 \ldots x_{m-1}]$ can be obtained at the receiver as:

$$\begin{aligned}\hat{\mathbf{x}} &= \arg\max_{\mathbf{x}} \left\{ p(y_{sd}^t, y_{rd}^t, \mathbf{y}_{sd}, \mathbf{y}_{rd}|\mathbf{x}) \right\} \\ &= \arg\max_{\mathbf{x}} \left\{ p(y_{sd}^t, y_{rd}^t|\mathbf{x}) \times p(\mathbf{y}_{sd}, \mathbf{y}_{rd}|\mathbf{x}, y_{sd}^t, y_{rd}^t) \right\}, \end{aligned} \tag{3.2}$$

where $\hat{\mathbf{x}} = [\hat{x}_1\, \hat{x}_2 \ldots \hat{x}_{m-1}]$. Since y_{sd}^t and y_{rd}^t are independent from data sequences x_1, x_2, ... , x_{m-1}, 3.2 can be written as:

$$\begin{aligned}\hat{\mathbf{x}} &= \arg\max_{\mathbf{x}} \left\{ p(y_{sd}^t, y_{rd}^t) \times p(\mathbf{y}_{sd}, \mathbf{y}_{rd}|\mathbf{x}, y_{sd}^t, y_{rd}^t) \right\} \\ &= \arg\max_{\mathbf{x}} \left\{ p(\mathbf{y}_{sd}, \mathbf{y}_{rd}|\mathbf{x}, y_{sd}^t, y_{rd}^t) \right\}. \end{aligned} \tag{3.3}$$

As shown in MMSE channel estimator, $\hat{h}_{sd}$ and $\hat{h}_{rd}$ are one-to-one functions of y_{sd}^t and y_{rd}^t, respectively, so in (3.3), y_{sd}^t and y_{rd}^t can be replaced by $\hat{h}_{sd}$ and $\hat{h}_{rd}$ and we can write

$$\hat{\mathbf{x}} = \arg \max_{\mathbf{x}} \left\{ p(\mathbf{y}_{sd}, \mathbf{y}_{rd}|\mathbf{x}, \hat{h}_{sd}, \hat{h}_{rd}) \right\}. \tag{3.4}$$

Probability density function of the received signals from the relay (i.e., $p(\mathbf{y}_{rd})$) depends on θ_i. We can therefore rewrite (3.4) as in the following:

$$\begin{aligned}\hat{\mathbf{x}} &= \arg\max_{\mathbf{x}} \Bigg\{ \sum_{\xi_1=0}^{1} \sum_{\xi_2=0}^{1} \ldots \sum_{\xi_{m-1}=0}^{1} p(\mathbf{y}_{sd}, \mathbf{y}_{rd}|\mathbf{x}, \hat{h}_{sd}, \hat{h}_{rd}, \theta_1 = \xi_1, \theta_2 = \xi_2, ..., \theta_{m-1} = \xi_{m-1}) \\ &\qquad \times P(\theta_1 = \xi_1, \theta_2 = \xi_2, ..., \theta_{m-1} = \xi_{m-1}|\mathbf{x}, \hat{h}_{sd}, \hat{h}_{rd}) \Bigg\} \\ &= \arg\max_{\mathbf{x}} \Bigg\{ \sum_{\xi_1=0}^{1} \sum_{\xi_2=0}^{1} \ldots \sum_{\xi_{m-1}=0}^{1} p(\mathbf{y}_{sd}, \mathbf{y}_{rd}|\mathbf{x}, \hat{h}_{sd}, \hat{h}_{rd}, \theta_1 = \xi_1, \theta_2 = \xi_2, ..., \theta_{m-1} = \xi_{m-1}) \\ &\qquad \times P(\theta_1 = \xi_1, \theta_2 = \xi_2, ..., \theta_{m-1} = \xi_{m-1}) \Bigg\}. \end{aligned} \tag{3.5}$$

where the last equality in (3.5) comes from the fact that the relay node's decision for sending or not sending a particular symbol, does not depend on the estimated channel gains ($\hat{h}_{sd}$, $\hat{h}_{rd}$) and also transmitted data signal vector ($\mathbf{x}$). We note that detection based on (3.5) has unmanageable computational complexity because the number of hypotheses to choose from is 2^{m-1}. In this chapter, we consider a simpler detection, which is discussed in the next subsection.

3.3.2 Symbol-by-symbol detection

We consider a method in which the symbols are detected individually (i.e., in a symbol-by-symbol fashion); the symbol-by-symbol detection requires much less computation than the block detection. Detection rule can be written as in the following:

$$\begin{aligned}\hat{x} &= \arg\max_{x\in\{-1,+1\}} \Big\{ p(y_{sd}, y_{rd}|x, \hat{h}_{sd}, \hat{h}_{rd}, \theta=0)P(\theta=0) \\ &\qquad + p(y_{sd}, y_{rd}|x, \hat{h}_{sd}, \hat{h}_{rd}, \theta=1)P(\theta=1)\Big\}. \end{aligned} \tag{3.6}$$

We denote by P_e^R, the probability that the relay detects the symbol with error and can be obtained as follows [35]:

$$P_e^R = \frac{1}{2}\left(1 - \sqrt{\frac{A_1}{A_1+\lambda_{sr}}}\right), \tag{3.7}$$

where $A_1 = \frac{\mathcal{P}_s}{\mathcal{P}_s\sigma^2_{e_{sr}}+N_0}$ and $\lambda_{sr} = \frac{\alpha\mathcal{P}_1\sigma_h^2+N_0}{\alpha\mathcal{P}_1\sigma_h^4}$. By using (3.1), conditioned on the estimated channel gains ($\hat{h}_{sd}$ and $\hat{h}_{rd}$), transmitted symbol (x) and θ, it can be easily seen that y_{sd} and y_{rd} are two independent complex Gaussian random variables with means $\sqrt{\mathcal{P}_s}\hat{h}_{sd}x$, $\theta\sqrt{\mathcal{P}_r}\hat{h}_{rd}x$ and variances $\mathcal{P}_s\sigma^2_{e_{sd}}+N_0$, $\theta\mathcal{P}_r\sigma^2_{e_{rd}}+N_0$, respectively. The decision rule becomes as follows:

$$\begin{aligned}\hat{x} &= \arg\max_{x\in\{-1,+1\}} \Bigg\{ \frac{1}{\pi(\mathcal{P}_s\sigma^2_{e_{sd}}+N_0)} e^{\frac{-|y_{sd}-\sqrt{\mathcal{P}_s}\hat{h}_{sd}x|^2}{\mathcal{P}_s\sigma^2_{e_{sd}}+N_0}} \cdot \frac{1}{\pi N_0} e^{\frac{-|y_{rd}|^2}{N_0}} \cdot P_e^R \\ &\qquad + \frac{1}{\pi(\mathcal{P}_s\sigma^2_{e_{sd}}+N_0)} e^{\frac{-|y_{sd}-\sqrt{\mathcal{P}_s}\hat{h}_{sd}x|^2}{\mathcal{P}_s\sigma^2_{e_{sd}}+N_0}} \cdot \frac{1}{\pi(\mathcal{P}_r\sigma^2_{e_{rd}}+N_0)} e^{\frac{-|y_{rd}-\sqrt{\mathcal{P}_r}\hat{h}_{rd}x|^2}{\mathcal{P}_r\sigma^2_{e_{rd}}+N_0}} \cdot [1-P_e^R]\Bigg\} \\ &= \arg\max_{x\in\{-1,+1\}} e^{\frac{-|y_{sd}-\sqrt{\mathcal{P}_s}\hat{h}_{sd}x|^2}{\mathcal{P}_s\sigma^2_{e_{sd}}+N_0}} \cdot \left(\frac{1}{N_0} e^{\frac{-|y_{rd}|^2}{N_0}} \cdot P_e^R + \frac{1}{\mathcal{P}_r\sigma^2_{e_{rd}}+N_0} e^{\frac{-|y_{rd}-\sqrt{\mathcal{P}_r}\hat{h}_{rd}x|^2}{\mathcal{P}_r\sigma^2_{e_{rd}}+N_0}} \cdot [1-P_e^R]\right). \end{aligned} \tag{3.8}$$

Signal detection based on (3.8) has high computational complexity. In the next section, we introduce two sub-optimal signal detection schemes which have much less complexity in comparison with the optimal signal detection scheme (Eq. 3.8).

3.4 Computationally Efficient and Well Performing Suboptimal Symbol Detection

In this section, we present computationally efficient suboptimal symbol detection schemes. We will later show that these schemes have BEP performances close to the optimal detection. It will be shown in subsection 3.4.3 that if the destination knew without error whether the relay is sending data or not, (i.e., spectrum sensing), the optimal signal detection at the destination would have much less complexity than in the case in which the destination does not know for sure whether the relay has forwarded the symbol or not. We first discuss in subsections 3.4.1 and 3.4.2 how the destination node guesses whether the relay has forwarded the symbol, and in subsection 3.4.3 we present the symbol detection scheme.

3.4.1 Optimal detection of θ

The destination node has information $y_{sd}, y_{rd}, \hat{h}_{sd}, \hat{h}_{rd}$, and the optimal detection of θ (whether the relay node has forwarded the symbol) is

$$\begin{aligned}\hat{\theta} &= \arg\max_{\theta\in\{0,1\}}\Big\{p(\theta|y_{sd},y_{rd},\hat{h}_{sd},\hat{h}_{rd})\Big\} = \arg\max_{\theta\in\{0,1\}}\Big\{p(y_{sd},y_{rd}|\theta,\hat{h}_{sd},\hat{h}_{rd})p(\theta,\hat{h}_{sd},\hat{h}_{rd})\Big\}\\ &= \arg\max_{\theta\in\{0,1\}}\Big\{p(y_{sd},y_{rd}|\theta,\hat{h}_{sd},\hat{h}_{rd})p(\hat{h}_{sd},\hat{h}_{rd})\times p(\theta|\hat{h}_{sd},\hat{h}_{rd})\Big\}\\ &= \arg\max_{\theta\in\{0,1\}}\Big\{p(y_{sd},y_{rd}|\theta,\hat{h}_{sd},\hat{h}_{rd})p(\theta)\Big\}, \qquad (3.9)\end{aligned}$$

where the last equality is due to the fact that θ is statistically independent from $(\hat{h}_{sd}, \hat{h}_{rd})$ since the relay node's decision to forward the symbol or not depends on y_{sr} in (2.1) and y_{sr}^t in (2.6), and these random variables are independent of $(\hat{h}_{sd}, \hat{h}_{rd})$. From (3.9) follows:

$$\begin{aligned}\hat{\theta} = \arg\max_{\theta\in\{0,1\}}\Big\{&p(y_{sd},y_{rd}|\theta,\hat{h}_{sd},\hat{h}_{rd},x=+1)P(x=+1|\theta,\hat{h}_{sd},\hat{h}_{rd})\\ &+p(y_{sd},y_{rd}|\theta,\hat{h}_{sd},\hat{h}_{rd},x=-1)P(x=-1|\theta,\hat{h}_{sd},\hat{h}_{rd})\Big\}p(\theta). \qquad (3.10)\end{aligned}$$

As for $P(x=+1|\theta,\hat{h}_{sd},\hat{h}_{rd})$ and $P(x=-1|\theta,\hat{h}_{sd},\hat{h}_{rd})$ in (3.10), the source's data symbol x is obviously independent of the channel gains (h_{sd}, h_{rd}) and the channel estimation errors based on the pilot symbols. Also, in view of 2.12, θ is statistically independent of x.

Therefore from (3.10) follows:

$$\hat{\theta} = \arg \max_{\theta \in \{0,1\}} \Big\{ p(y_{sd}, y_{rd}|\theta, \hat{h}_{sd}, \hat{h}_{rd}, x=+1) + p(y_{sd}, y_{rd}|\theta, \hat{h}_{sd}, \hat{h}_{rd}, x=-1) \Big\} p(\theta). \tag{3.11}$$

MAP detection of θ results in

$$\hat{\theta} = \begin{cases} 0 & \text{if } \Lambda_0 > \Lambda_1 \\ 1 & \text{otherwise} \end{cases} \tag{3.12}$$

where Λ_0 and Λ_1 are as follows:

$$\begin{aligned} \Lambda_0 &= \Big[p(y_{sd}, y_{rd}|\theta=0, \hat{h}_{sd}, \hat{h}_{rd}, x=+1) + p(y_{sd}, y_{rd}|\theta=0, \hat{h}_{sd}, \hat{h}_{rd}, x=-1) \Big] \times P(\theta=0) \\ &= \frac{1}{\pi(\mathcal{P}_s \sigma^2_{e_{sd}} + N_0)} \left[e^{\frac{-|y_{sd} - \sqrt{\mathcal{P}_s}\hat{h}_{sd}|^2}{\mathcal{P}_s \sigma^2_{e_{sd}} + N_0}} + e^{\frac{-|y_{sd} + \sqrt{\mathcal{P}_s}\hat{h}_{sd}|^2}{\mathcal{P}_s \sigma^2_{e_{sd}} + N_0}} \right] \times \frac{1}{\pi N_0} e^{\frac{-|y_{rd}|^2}{N_0}} \cdot P_e^R, \end{aligned} \tag{3.13}$$

$$\begin{aligned} \Lambda_1 &= \Big[p(y_{sd}, y_{rd}|\theta=1, \hat{h}_{sd}, \hat{h}_{rd}, x=+1) + p(y_{sd}, y_{rd}|\theta=1, \hat{h}_{sd}, \hat{h}_{rd}, x=-1) \Big] \times P(\theta=1) \\ &= \frac{1}{\pi(\mathcal{P}_s \sigma^2_{e_{sd}} + N_0)} \frac{1}{\pi(\mathcal{P}_r \sigma^2_{e_{rd}} + N_0)} \left[e^{\frac{-|y_{sd} - \sqrt{\mathcal{P}_s}\hat{h}_{sd}|^2}{\mathcal{P}_s \sigma^2_{e_{sd}} + N_0}} \cdot e^{\frac{-|y_{rd} - \sqrt{\mathcal{P}_r}\hat{h}_{rd}|^2}{\mathcal{P}_r \sigma^2_{e_{rd}} + N_0}} \right. \\ &\quad \left. + e^{\frac{-|y_{sd} + \sqrt{\mathcal{P}_s}\hat{h}_{sd}|^2}{\mathcal{P}_s \sigma^2_{e_{sd}} + N_0}} \cdot e^{\frac{-|y_{rd} + \sqrt{\mathcal{P}_r}\hat{h}_{rd}|^2}{\mathcal{P}_r \sigma^2_{e_{rd}} + N_0}} \right] \times \left(1 - P_e^R\right). \end{aligned} \tag{3.14}$$

Optimal spectrum detection based on (3.12) has still high computational complexity. In the next subsection, we present two sub-optimal detection rules for spectrum sensing.

3.4.2 Sub-optimal detection of θ

In the following, we present two sub-optimal schemes, which are computationally less burdensome than optimal scheme (3.12), for detecting θ. The two sub-optimal schemes to be shortly presented do not use the whole information of $(y_{sd}, y_{rd}, \hat{h}_{sd}, \hat{h}_{rd})$. Another basic feature of these two suboptimal schemes is to perform ternary hypothesis test on the values of $x' = \theta x \in \{-1, 0, 1\}$ instead of binary hypothesis test on $\theta \in \{0, 1\}$. By performing the ternary hypothesis test, one can avoid the computation of exponential functions and their addition in (3.13) and (3.14) at the expense of giving up optimality. By denoting $\theta x = x'$, the received signal at the second time slot (y_{rd}) can be rewritten as:

$$y_{rd} = \sqrt{\mathcal{P}_r} x' \hat{h}_{rd} + \sqrt{\mathcal{P}_r} x' e_{rd} + n_{rd}, \tag{3.15}$$

where $x' \in \{-1, 0, +1\}$ performs a ternary signal modulation.

Scheme I: In this scheme, first, a primary detection of the transmitted data symbol, x, is performed at the destination based on the received signal in the first time slot. We first consider the case in which $\hat{\hat{x}} = +1$ where $\hat{\hat{x}}$ is the estimate of x based on y_{sd} in (2.2). We denote by P'_e, the probability that the destination's detection from the signal received at first time slot is in error (i.e., $P'_e = P(\hat{\hat{x}} \neq x)$). By using the results of [35], P'_e can be obtained as in the following:

$$P'_e = \frac{1}{2}\left(1 - \sqrt{\frac{A_2}{A_2 + \lambda_{sd}}}\right), \tag{3.16}$$

where $A_2 = \frac{\mathcal{P}_s}{\mathcal{P}_s \sigma^2_{e_{sd}} + N_0}$ and $\lambda_{sd} = \frac{\alpha \mathcal{P}_1 \sigma_h^2 + N_0}{\alpha \mathcal{P}_1 \sigma_h^4}$. Using y_{rd}, $\hat{h}_{rd}$ and $\hat{\hat{x}} = +1$ as the observations, the MAP detection of x' yields,

$$\begin{aligned} \hat{x'} &= \arg\max_{x'} \left\{ p\left(x' | y_{rd}, \hat{h}_{rd}, \hat{\hat{x}} = +1\right) \right\} \\ &= \arg\max_{x'} \left\{ P\left(\hat{\hat{x}} = +1, y_{rd} | \hat{h}_{rd}, x'\right) \cdot p\left(\hat{h}_{rd}, x'\right) \right\}. \end{aligned} \tag{3.17}$$

Due the fact that x' and $\hat{h}_{rd}$ are independent, we have:

$$\hat{x'} = \arg\max_{x'} \left\{ P\left(\hat{\hat{x}} = +1 | \hat{h}_{rd}, x'\right) \cdot p\left(y_{rd} | \hat{h}_{rd}, \hat{\hat{x}} = +1, x'\right) \times p\left(\hat{h}_{rd}\right) p\left(x'\right) \right\}. \tag{3.18}$$

Since $P\left(\hat{\hat{x}} = +1 | \hat{h}_{rd}, x'\right) = P\left(\hat{\hat{x}} = +1 | x'\right)$, the detection rule can be simplified to

$$\hat{x'} = \arg\max_{x'} \left\{ P\left(\hat{\hat{x}} = +1 | x'\right) \cdot p\left(y_{rd} | \hat{h}_{rd}, \hat{\hat{x}} = +1, x'\right) \cdot p\left(x'\right) \right\}. \tag{3.19}$$

From (3.15), it can be easily seen that given x' and $\hat{h}_{rd}$, the received signal at the second time slot (y_{rd}) and $\hat{\hat{x}} = +1$ are independent. We can therefore simplify (3.19) as:

$$\hat{x'} = \arg\max_{x'} \left\{ p\left(y_{rd} | \hat{h}_{rd}, x'\right) \cdot P\left(\hat{\hat{x}} = +1 | x'\right) \cdot p\left(x'\right) \right\}. \tag{3.20}$$

We define Λ'_i as:

$$\Lambda'_i = p\left(y_{rd} | \hat{h}_{rd}, x' = i\right) \cdot P\left(\hat{\hat{x}} = +1 | x' = i\right) \cdot P\left(x' = i\right), \tag{3.21}$$

where $i \in \{-1, 0, +1\}$. If $\Lambda'_0 > \Lambda'_{-1}$ and $\Lambda'_0 > \Lambda'_{+1}$, $x' = 0$ is chosen. Since $x' = 0$ implies that $\theta = 0$, we formulate detection of θ as in the following:

$$\hat{\theta} = \begin{cases} 0 & \text{if } \Lambda'_0 > \max\{\Lambda'_{-1}, \Lambda'_{+1}\} \\ 1 & \text{otherwise} \end{cases} \tag{3.22}$$

Conditioned on the estimated relay-destination channel gain ($\hat{h}_{rd}$) and transmitted symbol (x'), y_{rd} is a complex Gaussian random variable with mean $\sqrt{\mathcal{P}_r}\hat{h}_{rd}x'$ and variance $\mathcal{P}_r\sigma^2_{e_{rd}}|x'| + N_0$. By using the following equalities (proof in appendix B):

$$P\left(\hat{\hat{x}} = +1|x' = +1\right) P\left(x' = +1\right) = \left(1 - P'_e\right)\left(1 - P^R_e\right)\left(\frac{1}{2}\right), \tag{3.23}$$

$$P\left(\hat{\hat{x}} = +1|x' = 0\right) P\left(x' = 0\right) = \frac{1}{2}P^R_e, \tag{3.24}$$

and,

$$P\left(\hat{\hat{x}} = +1|x' = -1\right) P\left(x' = -1\right) = P'_e\left(1 - P^R_e\right)\left(\frac{1}{2}\right), \tag{3.25}$$

and in accordance with (3.22), $\hat{\theta} = 0$ is chosen at the destination if

$$\underbrace{\frac{1}{2}\frac{P^R_e}{\pi\sigma^2_0}e^{-\frac{|y_{rd}|^2}{\sigma^2_0}}}_{\Lambda'_0} > \underbrace{\frac{1}{2}\frac{\left(1 - P^R_e\right)\left(1 - P'_e\right)}{\pi\sigma^2_1}e^{-\frac{|y_{rd} - \sqrt{\mathcal{P}_r}\hat{h}_{rd}|^2}{\sigma^2_1}}}_{\Lambda'_{+1}}, \tag{3.26}$$

and,

$$\underbrace{\frac{1}{2}\frac{P^R_e}{\pi\sigma^2_0}e^{-\frac{|y_{rd}|^2}{\sigma^2_0}}}_{\Lambda'_0} > \underbrace{\frac{1}{2}\frac{\left(1 - P^R_e\right)P'_e}{\pi\sigma^2_1}e^{-\frac{|y_{rd} + \sqrt{\mathcal{P}_r}\hat{h}_{rd}|^2}{\sigma^2_1}}}_{\Lambda'_{-1}}. \tag{3.27}$$

where $\sigma^2_1 = \mathcal{P}_r\sigma^2_{e_{rd}} + N_0$ and $\sigma^2_0 = N_0$. From (3.26) and (3.27), decision rule (3.22) can be simplified as:

$$\hat{\theta} = \begin{cases} 0 & |2\sqrt{\mathcal{P}_r}\,\mathrm{Re}\{y_{rd}\hat{h}^*_{rd}\} - T_1| < T_2 \\ 1 & \text{otherwise} \end{cases} \tag{3.28}$$

where T_1 and T_2 are as follows:

$$\begin{aligned} T_1 &= \frac{1}{2}\sigma^2_1 \ln\left(\frac{P'_e}{1 - P'_e}\right), \\ T_2 &= \mathcal{P}_r|\hat{h}_{rd}|^2 - \left(\frac{\sigma^2_1 - \sigma^2_0}{\sigma^2_0}\right)|y_{rd}|^2 - \sigma^2_1 \ln\left(\frac{\sigma^2_0\left(1 - P^R_e\right)\sqrt{\left(1 - P'_e\right)P'_e}}{\sigma^2_1 P^R_e}\right). \end{aligned} \tag{3.29}$$

It can be simply shown that if $\hat{\hat{x}} = -1$, the detection of θ based on scheme I becomes

$$\hat{\theta} = \begin{cases} 0 & |2\sqrt{\mathcal{P}_r}\,\mathrm{Re}\{y_{rd}\hat{h}^*_{rd}\} + T_1| < T_2 \\ 1 & \text{otherwise} \end{cases} \tag{3.30}$$

Scheme II: In this scheme, destination detects θ only based on the received signal at the second time slot, (i.e., y_{rd}). As in scheme I, the destination performs MAP detection for x' with the difference that it only considers y_{rd} and $\hat{h}_{rd}$ as the observation. The MAP detection of x' becomes

$$\hat{x'} = \arg\max_{x'} \left\{ p\Big(x'|y_{rd}, \hat{h}_{rd}\Big) \right\} = \arg\max_{x'} \left\{ p\Big(y_{rd}|x', \hat{h}_{rd}\Big)\, p\left(x'\right) \right\}. \tag{3.31}$$

As in scheme I, we define Λ_i'' as:

$$\Lambda_i'' = p\left(y_{rd}|\hat{h}_{rd}, x' = i\right) \cdot P\left(x' = i\right), \tag{3.32}$$

where $i \in \{-1, 0, +1\}$. If $\Lambda_0'' > \Lambda_{-1}''$ and $\Lambda_0'' > \Lambda_{+1}''$, $x' = 0$ is chosen. Since $x' = 0$ implies that $\theta = 0$, we formulate detection of θ as in the following:

$$\hat{\theta} \;=\; \begin{cases} 0 & \text{if } \Lambda_0'' > \max\{\Lambda_{-1}'', \Lambda_{+1}''\} \\ 1 & \text{otherwise} \end{cases} \tag{3.33}$$

We note that the detection based on scheme II, can be obtained by scheme I, by replacing P_e' by $1/2$. In other words, the detection based on scheme II simply becomes

$$\hat{\theta} = \begin{cases} 0 & |2\sqrt{\mathcal{P}_r}\,\mathrm{Re}\{y_{rd}\hat{h}_{rd}^*\}| < T_2' \\ 1 & \text{otherwise} \end{cases} \tag{3.34}$$

where

$$T_2' \;=\; \mathcal{P}_r|\hat{h}_{rd}|^2 - \left(\frac{\sigma_1^2 - \sigma_0^2}{\sigma_0^2}\right)|y_{rd}|^2 - \sigma_1^2 \ln\left(\frac{\sigma_0^2\left(1 - P_e^R\right)}{2\sigma_1^2 P_e^R}\right). \tag{3.35}$$

Using the proposed spectrum sensing schemes in our symbol detection scheme at the destination, for the purpose of detecting the symbol x, first the destination detects θ and then treats the detected value of θ as the true θ. It should be noted as there can be an error in θ detection, BEP performance of the system in which the destination perfectly knows θ differs from that of the system in which the destination treats the detected value of θ as the true value. However, our simulation results indicate that this difference, which is caused by possible detection error, is negligibly small. In the next subsection, we will study the symbol detection based on having the error-free value of θ at the destination. We show that having perfect knowledge of θ at the destination results in a simple signal detection scheme.

3.4.3 Optimal symbol-by-symbol detection conditional on θ

In this section, we assume that destination knows θ perfectly; In other words, at each time slot, destination knows whether the relay is in transmission mode or not. Then, we derive the optimal signal detection rule. We point out that this system model is the same as the "*Ideal System*" introduced in chapter 2. With the destination knowing θ, the optimal detection rule can be written as in the following:

$$\hat{x} = \arg \max_{x\in\{-1,+1\}} \left\{ p(y_{sd}, y_{rd}|x, \hat{h}_{sd}, \hat{h}_{rd}, \theta) \right\}. \tag{3.36}$$

By using (3.1), conditioned on the estimated channel gains ($\hat{h}_{sd}$ and $\hat{h}_{rd}$), transmitted symbol (x) and θ, the decision rule becomes

$$\begin{aligned} \hat{x} &= \arg \max_{x\in\{-1,+1\}} \left(\frac{1}{\pi(\mathcal{P}_s\sigma^2_{e_{sd}} + N_0)} e^{\frac{-|y_{sd}-\sqrt{\mathcal{P}_s}\hat{h}_{sd}x|^2}{\mathcal{P}_s\sigma^2_{e_{sd}}+N_0}} \right. \\ &\times \left. \frac{1}{\pi(\theta\mathcal{P}_r\sigma^2_{e_{rd}} + N_0)} e^{\frac{-|y_{rd}-\theta\sqrt{\mathcal{P}_r}\hat{h}_{rd}x|^2}{\theta\mathcal{P}_r\sigma^2_{e_{rd}}+N_0}} \right). \end{aligned} \tag{3.37}$$

The decision rule can be written as:

$$\begin{aligned} \hat{x} &= \arg \min_{x\in\{-1,+1\}} \left(\frac{|y_{sd} - \sqrt{\mathcal{P}_s}\hat{h}_{sd}x|^2}{\mathcal{P}_s\sigma^2_{e_{sd}} + N_0} + \frac{|y_{rd} - \theta\sqrt{\mathcal{P}_r}\hat{h}_{rd}x|^2}{\theta\mathcal{P}_r\sigma^2_{e_{rd}} + N_0} \right) \\ &= \arg \min_{x\in\{-1,+1\}} \left(\frac{|y_{sd}|^2 + \mathcal{P}_s|\hat{h}_{sd}|^2 - 2\mathrm{Re}\{\sqrt{\mathcal{P}_s}y_{sd}\hat{h}^*_{sd}x\}}{\mathcal{P}_s\sigma^2_{e_{sd}} + N_0} \right. \\ &+ \left. \frac{|y_{rd}|^2 + \theta\mathcal{P}_r|\hat{h}_{rd}|^2 - 2\mathrm{Re}\{\theta\sqrt{\mathcal{P}_r}y_{rd}\hat{h}^*_{rd}x\}}{\theta\mathcal{P}_r\sigma^2_{e_{rd}} + N_0} \right) \\ &= \arg \max_{x\in\{-1,+1\}} \mathrm{Re}\left\{ \left(\frac{\sqrt{\mathcal{P}_s}}{\mathcal{P}_s\sigma^2_{e_{sd}} + N_0}\hat{h}^*_{sd}y_{sd} + \frac{\theta\sqrt{\mathcal{P}_r}}{\mathcal{P}_r\sigma^2_{e_{rd}} + N_0}\hat{h}^*_{rd}y_{rd} \right) x \right\}. \end{aligned} \tag{3.38}$$

In order to implement this decision rule, we can use maximum ratio combining (MRC) which treats the estimated channels as true channels [39]:

$$y^{\mathrm{MRC}} = \frac{\sqrt{\mathcal{P}_s}}{\mathcal{P}_s\sigma^2_{e_{sd}} + N_0}\hat{h}^*_{sd}y_{sd} + \frac{\theta\sqrt{\mathcal{P}_r}}{\mathcal{P}_r\sigma^2_{e_{rd}} + N_0}\hat{h}^*_{rd}y_{rd}. \tag{3.39}$$

3.5 Performance Evaluation

In the following system setup, we present Monte-Carlo simulation results to corroborate the theoretical analysis. The transmitted symbols are drawn from an BPSK constellation. The

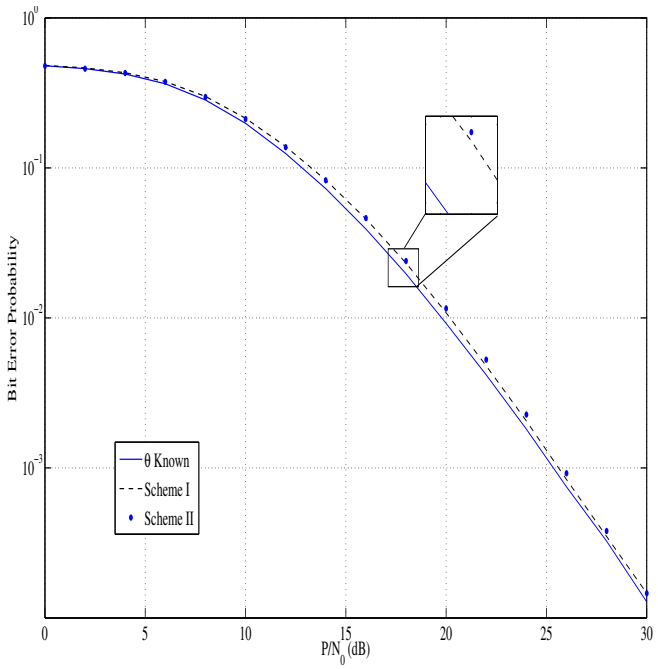

Figure 3.1: BEP against $\mathcal{P}/N_0$ for different spectrum detection scenarios

node-to-node channel is assumed to be zero mean independent Gaussian random variable with unit variance. The variance of noise components is set to $N_0 = 1$. We assume that a fixed total power is distributed between the source and the relay such that $\mathcal{P}_1 + \mathcal{P}_2 = \mathcal{P}$. This power constraint is imposed to guarantee a fair performance comparison with the direct transmission scenario [65] [66].

We considered four different schemes for signal detection: optimal signal detections (i.e., Eq. (3.6)), sub-optimal signal detection (schemes I and II) and the *Ideal System* where destination perfectly knows θ (i.e., Eq. (3.36)). It can be shown that the following inequality holds for the BEP performance of three different detection schemes

$$\mathrm{P_e^{sub-optimal}} \geq \mathrm{P_e^{optimal}} \geq \mathrm{P_e^{ideal}}. \tag{3.40}$$

Since the optimal detection scheme has better performance in comparison with sub-optimal detection scheme, the first inequality can be easily concluded, and the second inequality is proved in Theorem 2.5.1. As simulation results show (Fig. 3.1), performances of sub-optimal scheme and ideal scheme are very close.

Figure 3.1 shows the BEP performances of proposed sub-optimal schemes and the ideal

Table 3.1: BEP against $\mathcal{P}/N_0$ for different spectrum detection schemes

	Scheme I	**Scheme II**	**Ideal system**
$\mathcal{P}/N_0 = 20$ dB	1.027×10^{-2}	1.096×10^{-2}	9.393×10^{-3}
$\mathcal{P}/N_0 = 25$ dB	8.073×10^{-4}	8.301×10^{-4}	7.688×10^{-4}
$\mathcal{P}/N_0 = 30$ dB	1.401×10^{-4}	1.406×10^{-4}	1.347×10^{-4}

system against $\mathcal{P}/N_0$ for m=8, $\mathcal{P}_1/\mathcal{P} = 0.61$ and $\alpha = \beta = 0.30$. It can be observed that the performance of scheme I is better than scheme II. On the other hand, scheme I has higher complexity than scheme II, whereas the enhancement in performance is not significant. This tradeoff between complexity and performance suggests that scheme II is the best candidate for the considered scheme.

In Table 3.1 the BEP performance under SNR = 20 dB, 25 dB and 30 dB for three different schemes are tabulated. In order to compare the performance of schemes I, II, and ideal scheme, we define the ratio d_i as d_i = (BEP of scheme i - BEP of ideal scheme)/BEP of scheme i. For $\mathcal{P}/N_0 = 30$ dB, we have d_1= 0.0387 and $d_2 = 0.0420$ and for $\mathcal{P}/N_0 = 25$ dB, we have d_1= 0.0477 and $d_2 = 0.0738$ which demonstrates a slight difference between performances of the proposed schemes (scheme I, II and ideal scheme).

3.6 Conclusion and Future Work

We have explored the issues related to optimally detecting data symbols in the SDF relay communication system in the presence of CEE. We designed two novel schemes that can be used by the destination for detecting whether the relay has forwarded the symbols in the frame or not. We have shown that our signal detection schemes result in BEP performances very close to the *Ideal System* presented in chapter 2. In this chapter we assumed that the relay node perfectly knows whether in each frame any particular symbol is detected with error or not. We are currently designing the relay's schemes for detecting whether the frame is error free or not. The study of these schemes is left for future research.

Part II

Cross Layer Issues between Physical Layer and Link Layer in Wireless Communication Systems

Chapter 4

Frame Error Probability for Imperfectly Known Fading Channel Gains

4.1 Objective

In this chapter, we study the issue of optimally allocating the transmission energy between a pilot symbol and data symbols for a point-to-point communication system over the slow fading channel. In the system studied, our performance criterion for the optimal energy allocation is the frame error probability (FEP). A pilot symbol-assisted modulation (PSAM) scheme is used along with a channel estimation scheme based on the minimum mean square error (MMSE) criterion. We derive an approximate expression for the FEP in the presence of channel estimation error and use this expression for minimizing the FEP in allocating the transmission energy. Numerical simulation results are presented to show that the derived approximate FEP expression is very close to the actual FEP.

4.2 Related work and contribution

Much work has been presented on the power allocation between training and data sequences for a wireless communication system. For instance, B. Hassibi et al. [61] optimized the training data, power, and duration in multiple-antenna wireless links by maximizing a lower

bound on the channel capacity. K. Ahmed et al. [62] investigated the effect of power allocation between pilot and data symbols on pair-wise error probability in orthogonal frequency-division multiplexing (OFDM) system. M. Wu et al. [63] optimized power allocation between pilot and data by minimizing the instantaneous symbol error probability outage. A. Z. Ghanavati et al. [64] optimized power allocation between pilot and data symbols in a vehicular Ad-Hoc network. In [35], the power allocation problem between pilot and data sequences for cooperative communication system has been studied.

In the present chapter, we consider FEP performance metric and optimally allocate power between pilot and data symbols for minimizing the FEP expression. In section 4.3, we model the general wireless communication system and its frame structure. In section 4.4, we will derive the FEP expression under the assumption of the receiver's imperfect estimation of the channel gain. As the exact FEP takes the form of complicated integrals, we will suggest a new approximate formula for the FEP and use it for optimizing the energy allocation between the pilot and data symbols. In section 4.5, we will present our simulation results and discuss the quality of our approximation.

4.3 System Model and Channel Estimation

We consider a point-to-point communication system which consists of a source and a destination node. We assume binary phase shift keying (BPSK) transmission over flat fading channel and complex baseband system representation is used such that the transmitted signal, is either $\sqrt{\mathcal{P}_x}$ or $-\sqrt{\mathcal{P}_x}$. We represent the channel gain by h, a zero-mean complex Gaussian random variable with variance σ_h^2. Furthermore, the channel is assumed to be constant during the frame transmission where each frame consists of a fixed number of symbols. The transmission frame consists of two phases–training phase and data transmission phase. Over these phases the source is subject to the following power constraint [34]:

$$\|\mathbf{x}_t\|^2 + \mathrm{E}\{\|\mathbf{x}_d\|\}^2 \leq m\mathcal{P}_s. \tag{4.1}$$

where $\mathbf{x}_t$, $\mathbf{x}_d$, m and $\mathcal{P}_s$ are the source training vector, data signal vector, the frame length and average symbol energy, respectively.

4.3.1 Training Phase

We assume that the communication between nodes is through single-input-single-output (SISO) channel. As in section 2.3, we assume that only one pilot symbol is used to estimate the channel coefficient. We assume that the source can allocate power to the pilot and data signals in different proportions. We also assume that in the frame of m symbols, one symbol time is used to send the pilot signal and the rest are used for data transmission (Figure 4.1). At the beginning of the frame, the source sends a pilot symbol, which we denote as x_t, to the destination. The received pilot signal, y_t can be expressed as follows:

$$y_t = hx_t + n_t. \tag{4.2}$$

The noise term n_t is modelled as a zero mean complex Gaussian random variables with variance N_0 ($N_0/2$ per real dimension). Also, $|x_t|^2$, the transmit energy for the training phase is equal to $\alpha\, m\mathcal{P}_s$, where $0 < \alpha < 1$ is the ratio of pilot energy to the total energy of each frame. The communication system considered in the present chapter assumes that the destination estimates the wireless channel gain from the received pilot signal using MMSE channel estimation method. MMSE estimate of the channel at the destination is given by [34]:

$$\hat{h} = \mathrm{E}\{h{y_t}^*\}\left(\mathrm{E}\{y_t{y_t}^*\}\right)^{-1} y_t. \tag{4.3}$$

In accordance with [37], we can write

$$h = \hat{h} + e, \tag{4.4}$$

where e is the channel estimation error modelled as a zero mean complex Gaussian random variable with variance σ_e^2 and we have [37]:

$$\hat{h} \sim \mathcal{CN}\left(0, \frac{\sigma_h^4|x_t|^2}{\sigma_h^2|x_t|^2 + N_0}\right), \quad e \sim \mathcal{CN}\left(0, \frac{\sigma_h^2 N_0}{\sigma_h^2|x_t|^2 + N_0}\right), \tag{4.5}$$

where $\mathcal{CN}(\cdot,\cdot)$ denotes complex Gaussian distribution. It can be easily shown that e and $\hat{h}$ are uncorrelated random variables and since they have jointly Gaussian distribution, they are also independent.

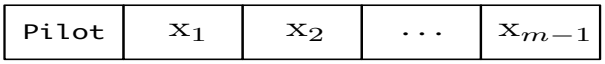

Figure 4.1: Transmission structure in a block of m symbols

4.3.2 Data Transmission Phase

As mentioned in the previous subsection, during a block of m symbols, the first symbol is allocated for channel training. In the remaining duration of $m-1$ symbols, data transmission takes place. Denoting the transmitted data signals by $(m-1)$ dimensional vector $\mathbf{x}_d = [x_1, x_2, ..., x_{m-1}]$, and the received data signals by $(m-1)$ dimensional vector $\mathbf{y}_d = \left[y_d^1, y_d^2, ..., y_d^{m-1}\right]$, we have:

$$\mathbf{y}_d = h\mathbf{x}_d + \mathbf{n}_d, \tag{4.6}$$

where $x_i \in \{\sqrt{\mathcal{P}_x}, -\sqrt{\mathcal{P}_x}\}$. The input vector $\mathbf{x}_d$ is assumed to be composed of independent random variables with equal energy and the corresponding covariance matrix is:

$$\mathrm{E}\{\mathbf{x}_d {\mathbf{x}_d}^{\mathrm{H}}\} = \frac{(1-\alpha)\, m\mathcal{P}_s}{m-1}\mathbf{I} = \mathcal{P}_x\mathbf{I}, \tag{4.7}$$

where I is the $m-1$ dimensional identity matrix. Also the elements of noise vector $\mathbf{n}_d$ are assumed to be zero mean independent complex Gaussian random variables with variance N_0 ($N_0/2$ per real dimension).

4.3.3 Optimal detection of symbols in a block

In this section, for theoretical perspective we study the optimal symbol detection rule in the presence of channel estimation error using MMSE channel estimator. Using (4.4) and (4.6), received signals at the destination can be written as:

$$y_d^i = \hat{h}x_i + ex_i + n_d^i \quad , i = 1, 2, ..., m-1. \tag{4.8}$$

Assuming that the transmitted symbol has equal a priori probability, the maximum a posteriori (MAP) detection is reduced to the maximum likelihood (ML) detection. Signals available at the destination are pilot signal received (y_t) and data signals received ($y_d^1, y_d^2, ...$

and y_d^{m-1}). ML detection of $\mathbf{x}_d \equiv [x_1\ x_2\ ...x_{m-1}]^{\mathrm{T}}$ can be obtained at the receiver as:

$$\begin{aligned}\hat{\mathbf{x}_d} &= \arg\max_{x_1,x_2,...,x_{m-1}} p(y_t, y_d^1, y_d^2, ..., y_d^{m-1}|x_1, x_2, ..., x_{m-1}) \\ &= \arg\max_{x_1,x_2,...,x_{m-1}} p(y_t|x_1, x_2, ..., x_{m-1}) \times p(y_d^1, y_d^2, ..., y_d^{m-1}|x_1, x_2, ..., x_{m-1}, y_t), \quad (4.9)\end{aligned}$$

where $\hat{\mathbf{x}_d} \equiv [\hat{x}_1\ \hat{x}_2\ ...\ \hat{x}_{m-1}]^{\mathrm{T}}$. Since y_t is independent from data sequences x_1, x_2,..., x_{m-1}, (4.9) can be written as:

$$\begin{aligned}\hat{\mathbf{x}_d} &= \arg\max_{x_1,x_2,...,x_{m-1}} p(y_t) \times p(y_d^1, y_d^2, ..., y_d^{m-1}|x_1, x_2, ..., x_{m-1}, y_t) \\ &= \arg\max_{x_1,x_2,...,x_{m-1}} p(y_d^1, y_d^2, ..., y_d^{m-1}|x_1, x_2, ..., x_{m-1}, y_t). \quad (4.10)\end{aligned}$$

As shown in the MMSE channel estimator formula (4.3), $\hat{h}$ and y_t have one-to-one correspondence, so in (4.10), y_t can be replaced by $\hat{h}$ and we can write

$$\hat{\mathbf{x}_d} = \arg\max_{x_1,x_2,...,x_{m-1}} p(y_d^1, y_d^2, ..., y_d^{m-1}|x_1, x_2, ..., x_{m-1}, \hat{h}). \quad (4.11)$$

Let us assume that

$$w_d^i = ex_i + n_d^i \quad , i = 1, 2, ..., m-1. \quad (4.12)$$

We can therefore rewrite (4.8) as:

$$\mathbf{y}_d = \hat{h}\mathbf{x}_d + \mathbf{w}_d, \quad (4.13)$$

where $\mathbf{w}_d = [w_d^1\ w_d^2\ ...\ w_d^{m-1}]^{\mathrm{T}}$. Since $e, n_d^1, n_d^2, ...$ and n_d^{m-1} are zero mean complex jointly Gaussian random variables, it can be easily concluded that conditioned on the transmitted data symbols, w_d^1, w_d^2, ... and w_d^{m-1} are zero mean complex jointly Gaussian random variables. Conditioned on the transmitted data symbols, we define $\Sigma_{\mathbf{w}_d}$ as:

$$\Sigma_{\mathbf{w}_d} = \mathrm{E}\{\mathbf{w}_d\mathbf{w}_d^{\mathrm{H}}\}, \quad (4.14)$$

where $\Sigma_{\mathbf{w}_d}$ is the complex covariance matrix: If $i \neq j$:

$$\Sigma_{\mathbf{w}_d}(i,j) = \mathrm{E}\{(ex_i + n_d^i)(e^*x_j + n_d^{j*})\} = \mathrm{E}\{|e|^2\}x_ix_j = \sigma_e^2 x_i x_j. \quad (4.15)$$

If $i = j$:

$$\Sigma_{\mathbf{w}_d}(i,i) = \mathrm{E}\{(ex_i + n_d^i)(e^*x_i + n_d^{i*})\} = \mathrm{E}\{|e|^2\}|x_i|^2 + \mathrm{E}\{|n_d^i|^2\} = \sigma_e^2\mathcal{P}_x + N_0. \quad (4.16)$$

Conditioned on the estimated channel gain and the transmitted data symbols, y_d^1, y_d^2, ... and y_d^{m-1} are complex jointly Gaussian random variables. We can therefore rewrite (4.11) as:

$$\hat{\mathbf{x}_d} = \arg \max_{x_1,x_2,...,x_{m-1}} \{\frac{1}{\pi^{m-1}\det(\Sigma_{\mathbf{w}_d})} \exp\{-(\mathbf{y}_d - \hat{h}\mathbf{x}_d)^{\mathrm{H}}{\Sigma_{\mathbf{w}_d}}^{-1}(\mathbf{y}_d - \hat{h}\mathbf{x}_d)\}\}. \quad (4.17)$$

We note that detection based on (4.17) has unmanageable computational complexity because the number of hypotheses to choose from is 2^{m-1}. In this chapter, we consider a simpler detection, which is discussed in the next subsection.

4.3.4 Symbol-by-symbol detection

We now consider a method in which symbols are detected individually (i.e., in a symbol-by-symbol fashion); the symbol-by-symbol detection requires much less computation than the block detection. Sub-optimal detection rule can be written as in the following:

$$\hat{x}_i = \arg \max_{x_i} p(y_d^i | x_i, \hat{h}), \;\; i = 1, 2, ..., m-1. \quad (4.18)$$

Conditioned on the transmitted data symbol and estimated channel gain, y_d^i is a complex Gaussian random variable and the decision rule becomes minimum distance rule and after some simple manipulations we can write [67]

$$\hat{x}_i = \arg \max_{x_i} \mathrm{Re}\{y_d^i \, \hat{h}^* x_i\}, \;\; i = 1, 2, ..., m-1. \quad (4.19)$$

4.4 FEP Analysis and Power Allocation

For the purpose of determining the FEP-minimizing power allocation, in this section we discuss the FEP performance of BPSK modulation for the wireless communication system model presented in section 4.3. We will present how the statistical correlation among received signals within the frame complicates the mathematical expression of the FEP. We will suggest an approximate expression and then apply the approximate expression of FEP as the performance metric of the system for determining the power allocation among the pilot and data signals. Due to symmetry, the conditional probability (conditioned on estimated channel gain $\hat{h}$) of frame error can be expressed as:

$$\begin{aligned} P(FE|\hat{h}) &= P(FE|\hat{h}, x_1 = x_2 = \cdots = x_{m-1} = +\sqrt{\mathcal{P}_x}) \\ &= 1 - P(\hat{x}_1 = \hat{x}_2 = \cdots = \hat{x}_{m-1} = +\sqrt{\mathcal{P}_x} \mid \hat{h}, x_1 = x_2 = \cdots = x_{m-1} = +\sqrt{\mathcal{P}_x}). \end{aligned} \quad (4.20)$$

Since $y_d^i = \hat{h}x_i + w_d^i$, conditioned on $x_i = +\sqrt{\mathcal{P}_x}$, we have $y_d^i = \hat{h}\sqrt{\mathcal{P}_x} + w_d^i$ and by using (4.19), the i^{th} symbol is detected correctly if and only if $\text{Re}\{|\hat{h}|^2\sqrt{\mathcal{P}_x} + \hat{h}^* w_d^i\} \geq 0$ for each realization of the estimated channel gain. After some modifications, we can write the conditional frame error probability as in the following:

$$\begin{aligned} P(FE|\hat{h}) &= 1 - P(|\hat{h}|^2\sqrt{\mathcal{P}_x} + \text{Re}\{\hat{h}^* w_d^1\} \geq 0, |\hat{h}|^2\sqrt{\mathcal{P}_x} \\ &+ \text{Re}\{\hat{h}^* w_d^2\} \geq 0, \cdots, |\hat{h}|^2\sqrt{\mathcal{P}_x} + \text{Re}\{\hat{h}^* w_d^{m-1}\} \geq 0). \end{aligned} \tag{4.21}$$

Conditioned on $\hat{h}$ and assuming that all the transmitted symbols are $+\sqrt{\mathcal{P}_x}$, the conditional FEP can be written as:

$$P(FE|\hat{h}) = 1 - \int_{-|\hat{h}|\sqrt{\mathcal{P}_x}}^{\infty} \int_{-|\hat{h}|\sqrt{\mathcal{P}_x}}^{\infty} \cdots \int_{-|\hat{h}|\sqrt{\mathcal{P}_x}}^{\infty} p_{\tilde{\mathbf{w}}_d}(\tilde{\mathbf{w}}_d)\, d\tilde{w}_d^1\, d\tilde{w}_d^2 \cdots d\tilde{w}_d^{m-1}, \tag{4.22}$$

where $\tilde{\mathbf{w}}_d = \text{Re}\{\mathbf{w}_d\}$. We denote $|\hat{h}|^2$ by Z. In accordance with the complex Gaussian channel model, Z is exponentially distributed ; we can write

$$f_Z(z) = \lambda\, e^{-\lambda z},\ z \geq 0, \tag{4.23}$$

where

$$\lambda = \frac{1}{\sigma_{\hat{h}}^2} = \frac{\sigma_h^2 \alpha\, m\mathcal{P}_s + N_0}{\sigma_h^4 \alpha\, m\mathcal{P}_s}. \tag{4.24}$$

The unconditional frame error probability is given by:

$$\begin{aligned} P(FE) = 1 - \int_0^{\infty} \int_{-\sqrt{z\mathcal{P}_x}}^{\infty} \int_{-\sqrt{z\mathcal{P}_x}}^{\infty} \cdots \int_{-\sqrt{z\mathcal{P}_x}}^{\infty} \frac{1}{\sqrt{(2\pi)^{m-1}\det(\Sigma_{\tilde{\mathbf{w}}_d})}} \exp\left(-\frac{1}{2}\tilde{\mathbf{w}}_d^{\text{T}} {\Sigma_{\tilde{\mathbf{w}}_d}}^{-1} \tilde{\mathbf{w}}_d\right) \\ \lambda e^{-\lambda z} d\tilde{w}_d^1\, d\tilde{w}_d^2 \cdots d\tilde{w}_d^{m-1} dz. \end{aligned} \tag{4.25}$$

We could take a linear transformation of $\tilde{\mathbf{w}}_d$ to obtain an statistically independent set of Gaussian random variables. Although such a transform provides a product form of joint probability density function, the lower limits of the integrals in (4.25) would have dependency, which complicates the computation of the FEP. We experiment with ignoring the correlation between the random variables in $\tilde{\mathbf{w}}_d$. In other words, we approximate (4.14) by $(\sigma_e^2\mathcal{P}_x + N_0)\mathbf{I}$, and accordingly we approximate $\Sigma_{\tilde{\mathbf{w}}_d}$ by a diagonal matrix as:

$$\Sigma_{\tilde{\mathbf{w}}_d}(i,j) \approx \begin{cases} \frac{1}{2}(\sigma_e^2\mathcal{P}_x + N_0) & i = j \\ 0 & i \neq j \end{cases} \tag{4.26}$$

By substituting (4.26) in (4.25), we have:

$$\begin{aligned} P(FE) &\approx 1-\int_0^{\infty}\lambda\, e^{-\lambda z}\prod_{i=1}^{m-1}\int_{-\sqrt{z\mathcal{P}_x}}^{\infty}\frac{1}{\sqrt{\pi(\sigma_e^2\mathcal{P}_x+N_0)}}\times e^{-\frac{(\tilde{w}_d^i)^2}{\sigma_e^2\mathcal{P}_x+N_0}}\,d\tilde{w}_d^i\,dz \\ &= 1-\int_0^{\infty}\lambda\, e^{-\lambda z}\left(1-Q\left(\sqrt{\frac{2\mathcal{P}_x\, z}{\sigma_e^2\mathcal{P}_x+N_0}}\right)\right)^{m-1}dz. \end{aligned} \tag{4.27}$$

By using the bionomial expansion, the FEP expression becomes

$$P(FE)\approx 1-\int_0^{\infty}\lambda\, e^{-\lambda z}\sum_{k=0}^{m-1}\binom{m-1}{k}(-1)^k Q^k(\sqrt{2C\cdot z})dz, \tag{4.28}$$

where $C=\frac{\mathcal{P}_x}{\sigma_e^2\mathcal{P}_x+N_0}$. By using the result of [68], we can approximate the Q-function as:

$$Q(x)\approx\frac{1}{\sqrt{2\pi}}\frac{1}{\sqrt{1+x^2}}\,e^{-\frac{x^2}{2}},\quad \text{for } x\gg 1, \tag{4.29}$$

and frame error probability can be approximated as the following:

$$P(FE)\approx 1-\int_0^{\infty}\lambda\, e^{-\lambda z}\sum_{k=0}^{m-1}\binom{m-1}{k}(-1)^k\,(\frac{1}{\sqrt{2\pi}})^k\left(\frac{1}{\sqrt{1+2C\cdot z}}\right)^k e^{-k\,C\cdot z}dz. \tag{4.30}$$

After some simple manipulations, (4.30) can be rewritten as follows:

$$P(FE)\approx 1-\sum_{k=0}^{m-1}\lambda\binom{m-1}{k}(-1)^k\,(\frac{1}{\sqrt{2\pi}})^k\frac{1}{2C}\int_0^{\infty}(1+z)^{-\frac{k}{2}}\,e^{-(\frac{k\,C+\lambda}{2C})z}\,dz. \tag{4.31}$$

By using the result from [73, p. 347], which is

$$\int_0^{\infty}(1+x)^{-v}\,e^{-\mu x}\,dx=\mu^{\frac{v}{2}-1}e^{\frac{\mu}{2}}\,W_{-\frac{v}{2},\frac{1-v}{2}}(\mu), \tag{4.32}$$

where $W_{\lambda,\mu}(z)$ is Whittaker function. The probability of frame error can be expressed as:

$$P(FE)\approx 1-\sum_{k=0}^{m-1}\lambda\binom{m-1}{k}(-1)^k\,(\frac{1}{\sqrt{2\pi}})^k\frac{1}{2C}\,I(k)\equiv g\left(\alpha,\frac{\mathcal{P}_s}{N_0}\right), \tag{4.33}$$

where

$$I(k)=\left(\frac{\lambda+kC}{2C}\right)^{\frac{k}{4}-1}e^{\frac{\lambda+kC}{4C}}W_{-\frac{k}{4},\frac{2-k}{4}}(\frac{\lambda+kC}{2C}). \tag{4.34}$$

To obtain the optimal values of α, an optimization problem is formulated as follows:

$$\begin{aligned} \alpha_{opt} &= \arg\ \min_{\alpha} g\left(\alpha,\frac{\mathcal{P}_s}{N_0}\right) \\ &\text{subject to}: 0\le\alpha\le 1. \end{aligned} \tag{4.35}$$

The results of optimization are tabulated in table 4.1.

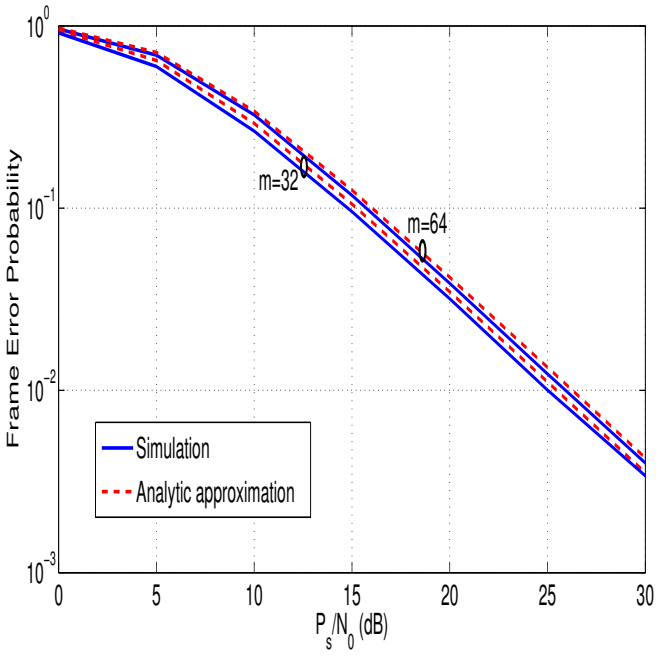

Figure 4.2: FEP against $\mathcal{P}_s/N_0$ for $\alpha = 0.30$

4.5 Simulation Results

In this section, Monte-Carlo simulation results are presented in order to evaluate the accuracy of our approximation in (4.33). Matlab was used for Monte-Carlo simulation, and 10^7 transmitted symbols were drawn from the BPSK constellation in order to estimate the FEP. The node-to-node channel is modelled by zero mean independent Gaussian random variable with unit variance.

Figure 4.2 shows the present chapter's FEP analysis resulting in (4.33) in comparison with the simulation results for $m = 32$ and 64 where m is the frame length. Parameter α is set to 0.30. As the figure shows, all simulation curves and the approximate analytical expression are very close.

In Figure 4.3, the FEP is plotted against α for $\mathcal{P}_s/N_0 = 10$ dB. From the derived FEP expression (4.33), it is apparent that for a fixed total power, the power allocation among pilot and data affects the FEP performance. If we allocate too much power for pilots, channel estimation error will be reduced but detection of the data in noise is more difficult

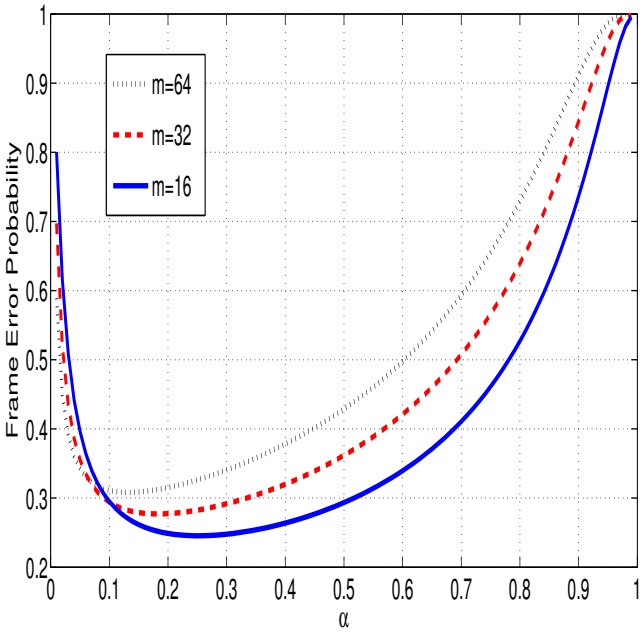

Figure 4.3: FEP against α for $\mathcal{P}_s/N_0 = 10$ dB

because of low data SNR. On the other hand, lower power for pilots results in poor channel estimation and thus in poor detection [64] [35]. The optimum values of α under $\mathcal{P}_s/N_0 = 10$ dB and $m = 16, 32$ and 64 turns out to be at $\alpha = 0.25$, $\alpha = 0.18$ and $\alpha = 0.13$, respectively.

In order to numerically compare the FEP curve obtained by simulation and the FEP curve obtained by analytical expression, for each frame length (m) we define the ratio d_m as $d_m = (\text{FEP}_{\text{analytical expression}} - \text{FEP}_{\text{simulation}})/\text{FEP}_{\text{analytical expression}}$. Figure 4.4 shows the error percentage (i.e., $100d_m$) against α for $\mathcal{P}_s/N_0 = 20$ dB and $m = 32$. As it can be seen from this figure, increasing α decreases the error percentage. This can be explained as the following. By increasing α, more power is allocated to the pilot symbol, which reduces channel estimation error. By decreasing the channel estimation error variance, the correlation between error events entire a frame decreases in accordance with (4.15). Thus, our approximation in (4.26) becomes more accurate, and finally our approximation (4.33) becomes more accurate.

Figure 4.5 shows the FEP expression proposed in this chapter in comparison with the

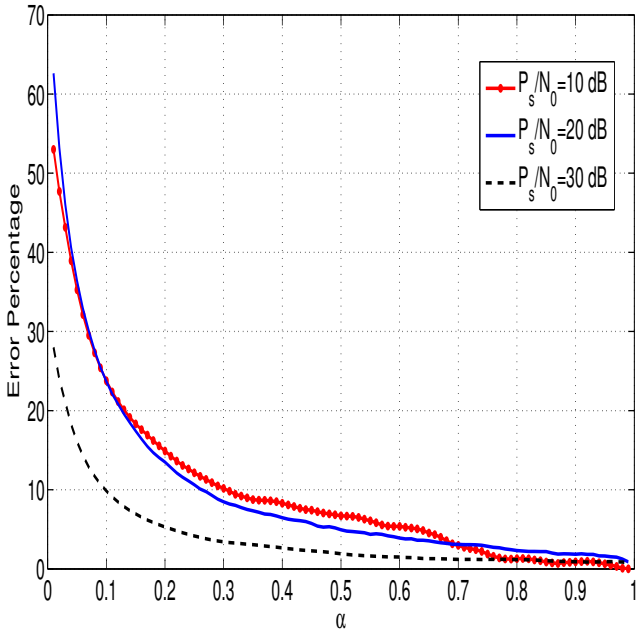

Figure 4.4: Error Percentage against α for $m = 32$

simulation results for $m = 32$ and two different values of $\alpha = 0.10$ and $\alpha = 0.90$. As figure shows, for $\alpha = 0.90$, the difference between simulation curve and our analytic expression (Eq. 4.33) is smaller.

In table 4.1, the optimum values for α for $m = 16, 32$, and 64 are tabulated. These values are obtained by solving the optimization problem in (4.35). It is noteworthy that the optimum values of α are insensitive to per-symbol SNRs. In table 4.2, the values of error difference (d_m) for three different frame lengths are tabulated. These results indicate that there is a slight difference between the values of FEP obtained from simulation and analytical expression. Table 4.3 shows d_m for analytic expression which is obtained by using Chenroff bound for three different frame lengths. These results indicate that there is huge difference between the values of FEP obtained from simulation and analytical expression based on Chernoff bound. By comparing this table with table 4.2, the accuracy of our approximation can be readily observed.

		m= 64	m=32	m=16
$\mathcal{P}_s/N_0 = 30$ dB	α_{opt}	0.13	0.18	0.25
	FEP	0.0037	0.0033	0.0029
$\mathcal{P}_s/N_0 = 25$ dB	α_{opt}	0.13	0.18	0.25
	FEP	0.0118	0.0104	0.0091
$\mathcal{P}_s/N_0 = 20$ dB	α_{opt}	0.13	0.18	0.25
	FEP	0.0367	0.0324	0.0284
$\mathcal{P}_s/N_0 = 15$ dB	α_{opt}	0.13	0.18	0.25
	FEP	0.1110	0.0986	0.0866
$\mathcal{P}_s/N_0 = 10$ dB	α_{opt}	0.13	0.18	0.25
	FEP	0.3081	0.2771	0.2455

Table 4.1: Results of optimization for $m = 16, 32$ and 64

	m= 32	m=64	m=80
$\mathcal{P}_s/N_0 = 5$ dB	0.0740	0.0342	0.0307
$\mathcal{P}_s/N_0 = 10$ dB	0.0913	0.0463	0.0514
$\mathcal{P}_s/N_0 = 15$ dB	0.0937	0.0624	0.0679
$\mathcal{P}_s/N_0 = 20$ dB	0.0830	0.0729	0.0705
$\mathcal{P}_s/N_0 = 25$ dB	0.0689	0.0813	0.0477
$\mathcal{P}_s/N_0 = 30$ dB	0.0393	0.0617	0.0440

Table 4.2: Ratio d_m for $m = 32, 64$ and 80 for $\alpha = 0.30$ based on (4.33)

	m= 32	m=64	m=80
$\mathcal{P}_s/N_0 = 5$ dB	0.2298	0.1615	0.1482
$\mathcal{P}_s/N_0 = 10$ dB	0.3232	0.2516	0.2337
$\mathcal{P}_s/N_0 = 15$ dB	0.3584	0.2982	0.2651
$\mathcal{P}_s/N_0 = 20$ dB	0.3835	0.3283	0.2619
$\mathcal{P}_s/N_0 = 25$ dB	0.3949	0.3403	0.2712
$\mathcal{P}_s/N_0 = 30$ dB	0.4193	0.3139	0.3613

Table 4.3: Ratio d_m for $m = 32, 64$ and 80 for $\alpha = 0.30$ based on Chernoff bound

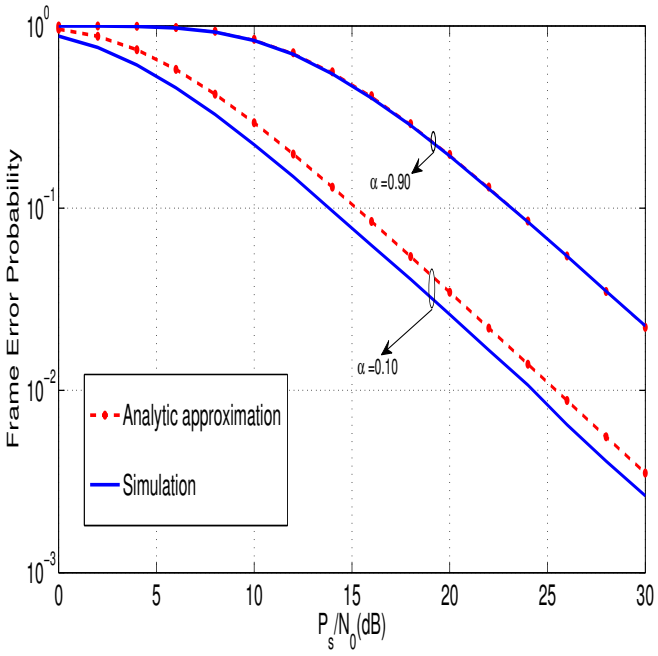

Figure 4.5: FEP against $\mathcal{P}_s/N_0$ for $m = 32$, $\alpha = 0.10$ and $\alpha = 0.90$

4.6 Conclusion

We have explored the issues related to optimally allocating the transmit energy between pilot and data symbols. We have investigated the effect of power allocation between training and data sequences on the FEP performance of a point-to-point communication system over a slow fading channel. We have also derived an approximation for FEP performance of BPSK modulation. We presented simulation results to show the proposed approximate analytical expression is close to the actual FEP. The accuracy of our approximation depends on power allocation between pilot and data symbols and also the frame length. The more power is allocated to the pilot symbol and the larger is the frame length, the more accurate our approximation of the FEP is. It is observed that our analytic approximation is more accurate than the approximations based on the Chenroff bound for all power allocation and frame lengths we tried in our numerical study.

Chapter 5

Optimizing Bit Transmission Power for Link Layer Energy Efficiency

5.1 Objective

In this chapter, we study the issue of optimizing transmission power (energy per symbol) for minimizing the total expected energy, including energy for retransmissions, required to deliver a frame to the destination node in a point-to-point link employing an automatic repeat request (ARQ) scheme over a fading channel. We derive the expected energy as a function of the transmission power and derive a simple optimization algorithm based on the properties of this function.

5.2 Related work and contribution

There has been much work on the link layer performance analysis of wireless networks. However, most of the current work in this area focus on the goodput and delay as the link layer performance metric [42]-[53]. In this chapter, we focus on the transmit energy efficiency under delay constraint in point to point wireless communication systems. We study the issue of optimizing transmission power for minimizing the expected energy required to successfully deliver a frame for wireless communication systems that employ ARQ scheme over a fading channel.

In section 5.3, we will present a simple system model. In section 5.4, we will present a simple derivation of the expected transmission energy for link layer. In section 5.5, which

is the main contribution of this chapter, we will formulate an optimization problem for determining the transmission power. Then, we will present a simple algorithm to determine the optimal transmission power.

5.3 System Model and Symbol Detection

We consider a point-to-point communication system which consists of a source and a destination node. We assume binary phase shift keying (BPSK) transmission over a fast fading channel and the complex baseband system representation is used. The transmitted signal is either $\sqrt{\mathcal{P}_x}$ or $-\sqrt{\mathcal{P}_x}$. Let h represent the channel gain which is assumed to be a zero mean complex Gaussian random variable with variance σ_h^2. For transmission of each frame, source transmits m data symbols as:

$$y_i = h_i x_i + n_i,\ i = 1, 2, ..., m. \tag{5.1}$$

The noise term n_i is modelled as a zero mean complex Gaussian random variables with variance N_0 ($N_0/2$ per real dimension). Since fast fading channel is considered, h_1, h_2,..., h_m form a sequence of i.i.d. (independent and identically distributed) random variables. Assuming that the transmitted symbol is a priori equally likely to be $\sqrt{\mathcal{P}_x}$ or $-\sqrt{\mathcal{P}_x}$, the maximum a posteriori (MAP) detection is reduced to the maximum likelihood (ML) detection. ML detection of $\mathbf{x}_d \equiv [x_1\ x_2\ ...x_m]$ can be obtained at the receiver as:

$$\hat{\mathbf{x}_d} = \arg \max_{x_1, x_2, ..., x_m} p(y_1, y_2, ..., y_m | x_1, x_2, ..., x_m, h_1, h_2, ..., h_m), \tag{5.2}$$

where $\hat{\mathbf{x}_d} \equiv [\hat{x}_1\ \hat{x}_2\ ...\ \hat{x}_m]$. Conditioned on the channel gains and the transmitted data symbols, y_1, y_2, ... and y_m are independent complex Gaussian random variables. We can therefore rewrite (5.2) as:

$$\hat{\mathbf{x}_d} = \arg \max_{x_1, x_2, ..., x_m} \prod_{i=1}^{m} p(y_i | x_i, h_i). \tag{5.3}$$

The optimal decision rule becomes

$$\hat{x}_i = \arg \max_{x_i} p(y_i | x_i, h_i) = \arg \max_{x_i} \mathrm{Re}\{y_i\, h_i^* x_i\},\ \ i = 1, 2, ..., m. \tag{5.4}$$

5.4 Expected Transmission Energy for Reliable Frame Delivery

In this section, we discuss the FEP performance of BPSK modulation for the wireless communication system model presented in section 5.3. We will then discuss the expected frame energy needed for reliable transmission of a single frame. Due to the symmetric nature of a complex-valued proper Gaussian noise model, the frame error probability conditioned on the channel gains can be expressed as:

$$P(FE|h_1, h_2, ..., \ h_m) = P(FE|h_1, h_2, ..., \ h_m, x_1 = x_2 = \cdots = x_m = +\sqrt{\mathcal{P}_x}). \tag{5.5}$$

By using the optimal decision rule (5.4), we can write the conditional frame error probability as in the following:

$$P(FE|h_1, h_2, ..., \ h_m) = 1 - P\Big(|h_1|^2\sqrt{\mathcal{P}_x}+\mathrm{Re}\{h_1^* n_1\} \geq 0, \tag{5.6}$$
$$|h_2|^2\sqrt{\mathcal{P}_x}+\mathrm{Re}\{h_2^* n_2\} \geq 0, \cdots, |h_m|^2\sqrt{\mathcal{P}_x}+\mathrm{Re}\{h_m^* n_m\} \geq 0\Big).$$

Conditioned on h_1, h_2, ..., h_m and assuming that all the transmitted symbols are equal to $+\sqrt{\mathcal{P}_x}$, the FEP can be written as:

$$P(FE|h_1, h_2, ..., h_m) = 1 - \int_{-|h_1|\sqrt{\mathcal{P}_x}}^{\infty} \int_{-|h_2|\sqrt{\mathcal{P}_x}}^{\infty} \cdots \int_{-|h_m|\sqrt{\mathcal{P}_x}}^{\infty} p_{\tilde{\mathbf{n}}}(\tilde{\mathbf{n}}) d\tilde{n}_1 \, d\tilde{n}_2 \cdots d\tilde{n}_m, \tag{5.7}$$

where $\tilde{\mathbf{n}} = \Big[\mathrm{Re}\{\frac{h_1^*}{|h_1|} n_1\} \, \mathrm{Re}\{\frac{h_2^*}{|h_2|} n_2\}\} \ \cdots \ \mathrm{Re}\{\frac{h_m^*}{|h_m|} n_m\}\}\Big]$. Since n_1, n_2, ..., n_m are independent zero mean circular symmetric complex Gaussian random variables with variance N_0, $\mathrm{Re}\{n_1\}$, $\mathrm{Re}\{n_2\}$, ..., and $\mathrm{Re}\{n_m\}$ become independent zero mean real Gaussian random variables with variance $N_0/2$ and conditional FEP becomes

$$\begin{aligned} P(FE|h_1, h_2, ..., h_m) &= 1 - \prod_{i=1}^{m} \int_{-\sqrt{\mathcal{P}_x}|h_i|}^{\infty} \frac{1}{\sqrt{\pi N_0}} \times e^{-\frac{(\tilde{n}_i)^2}{N_0}} \, d\tilde{n}_i \\ &= 1 - \prod_{i=1}^{m} \left(1 - Q\left(\sqrt{\frac{2\mathcal{P}_x \, |h_i|^2}{N_0}}\right)\right). \end{aligned} \tag{5.8}$$

We denote $|h_i|^2$ by Z_i. In accordance with the complex Gaussian channel model, Z_1, Z_2, ..., Z_m are i.i.d and exponentially distributed; we can write

$$f_{Z_i}(z_i) = \lambda \, e^{-\lambda z_i}, \ z_i \geq 0, \ \ \lambda = \frac{1}{\sigma_h^2}. \tag{5.9}$$

Unconditional frame error probability can be written as:

$$\begin{aligned} P(FE) &= 1-\prod_{i=1}^{m}\left(1-\int_0^\infty \lambda e^{-\lambda z_i} Q\left(\sqrt{\frac{2\mathcal{P}_x\, z_i}{N_0}}\right) dz_i\right) \\ &= 1-\left(1-\int_0^\infty \lambda e^{-\lambda z} Q\left(\sqrt{\frac{2\mathcal{P}_x\, z}{N_0}}\right) dz\right)^m = 1-(1-\mathbf{J})^m, \end{aligned} \tag{5.10}$$

where

$$\mathbf{J} = \int_0^\infty \lambda e^{-\lambda z} Q\left(\sqrt{\frac{2\mathcal{P}_x\, z}{N_0}}\right) dz. \tag{5.11}$$

By using the following equality for the Q-function [40]:

$$Q(x) = \frac{1}{\pi}\int_0^{\frac{\pi}{2}} e^{-\frac{x^2}{2\sin^2\theta}} d\theta, \tag{5.12}$$

$\mathbf{J}$ can be written as:

$$\mathbf{J} = \int_0^\infty \lambda e^{-\lambda z}\frac{1}{\pi}\int_0^{\frac{\pi}{2}} e^{-\frac{Az}{\sin^2\theta}} d\theta dz = \frac{1}{\pi}\int_0^{\frac{\pi}{2}}\int_0^\infty \lambda e^{-\left(\lambda+\frac{A}{\sin^2\theta}\right)z} dz d\theta, \tag{5.13}$$

where $A = \frac{\mathcal{P}_x}{N_0}$. After some simple manipulations, $\mathbf{J}$ can be written as in the following:

$$\mathbf{J} = \frac{1}{2} - \frac{A}{\pi}\int_0^{\frac{\pi}{2}} \frac{d\theta}{A+\lambda\sin^2\theta}. \tag{5.14}$$

By using the result from [73, p. 177] which is

$$\int \frac{dx}{a+b\sin^2 x} = \frac{\operatorname{sign} a}{\sqrt{a(a+b)}}\tan^{-1}\left(\sqrt{\frac{a+b}{a}}\tan x\right),$$

FEP becomes

$$P(FE) = 1-\left(\frac{1}{2}\right)^m\left(1+\sqrt{\frac{A}{A+\lambda}}\right)^m. \tag{5.15}$$

Thus, $P(FE)$ is a function of transmission power $\mathcal{P}_x$. Figure 5.1 shows $P(FE)$ in terms of $\mathcal{P}_x/N_0$ for $m = 5$, 10, 20, 40 and 80. In our analysis, we also use a variable $E \equiv m\mathcal{P}_x$, which denotes the energy consumed for transmitting a frame once. Due to the simple relation $E \equiv m\mathcal{P}_x$, a function of $\mathcal{P}_x$ can be expressed as a function of E, and vice versa. Energy for transmitting a frame is simply energy required for transmitting a symbol times frame length (i.e., $E = m\mathcal{P}_x$). From (5.15) follows

$$P(FE) = 1-\left(\frac{1}{2}\right)^m\left(1+\sqrt{\frac{E}{E+\frac{mN_0}{\sigma_h^2}}}\right)^m. \tag{5.16}$$

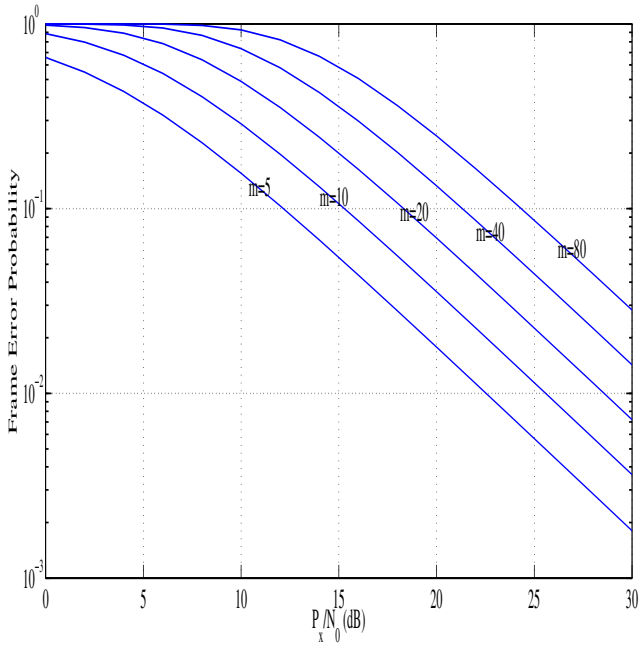

Figure 5.1: FEP per $\mathcal{P}_x/N_0$ for different frame lengths

Since the original transmission and subsequent retransmissions of a frame are independent events, it follows that the number of transmissions needed for successful delivery of a frame is geometrically distributed with parameter $P(FE)$ [54] where $P(FE)$ is the frame error probability. Accordingly, the expected number of transmissions needed for the reliable transfer of one frame is $1/(1-P(FE))$. Since each reliable transfer of a frame needs $1/(1-P(FE))$ attempts on average, the expected consumed energy for such reliable transfer of each frame can be obtained as follows:

$$\nu(E) = \frac{E}{1-P(FE)}, \tag{5.17}$$

where $\nu(E)$ and E are expected energy required for reliable transfer of a frame and the transmit energy of each frame, respectively. $\nu(E)$ can be written as:

$$\nu(E) = \frac{2^m E}{[1+g(E)]^m}, \tag{5.18}$$

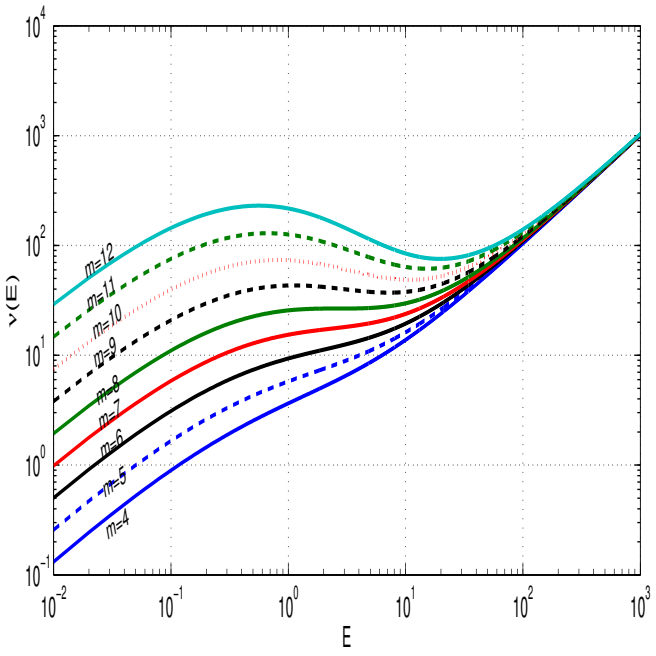

Figure 5.2: $\nu(E)$ per E for different frame lengths and $\sigma_h^2/N_0 = 1$

where

$$g(E) = \sqrt{\frac{E}{E+\beta}},\ \beta = \frac{mN_0}{\sigma_h^2}. \tag{5.19}$$

Note that energy function $\nu(E)$ of E can be expressed as a function, $\nu(m\mathcal{P}_x)$ of $\mathcal{P}_x$. Figure 5.2 shows $\nu(E)$ versus E for different values of m. In the next section, we discuss minimizing these functions. From the derived expression for $\nu(E) = \nu(m\mathcal{P}_x)$, it is clear that the energy required for each frame transmission affects the expected energy required for a reliable frame transmission. We point out that with constraint $E \geq 0$ without an additional constraint, the minimum value of $\nu(E)$ is obtained at $E = 0$. However, at $E = 0$, the expected number of transmission needed for frame delivery may become extremely large. We assume that the system has a constraint on the expected frame delivery time; namely, $s\left(\frac{2^m}{[1+g(E)]^m}\right) \leq d$ where $s(\cdot)$ is a monotonically increasing function, $\frac{2^m}{[1+g(E)]^m}$ is the expected number of trials required to successfully deliver a frame and d represents the delay requirement [55] [56]. This is equivalent to constraint $E \geq E_T$ for some E_T. Thus, in the following, we try to design

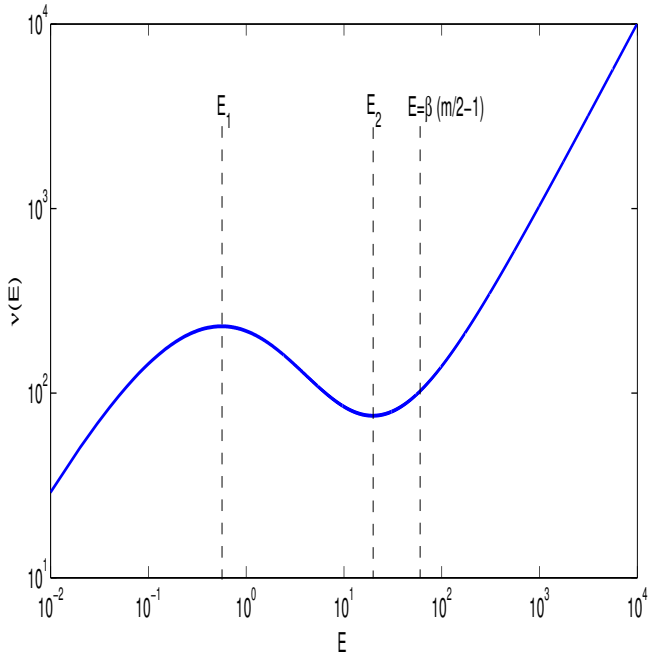

Figure 5.3: $\nu(E)$ per E for m=12 and $\sigma_h^2/N_0 = 1$

an algorithm for minimizing $\nu(E)$ in terms of E under the delay-constrained condition.

5.5 Optimization of Transmission Power (Symbol Energy)

To obtain the optimum value of E, an optimization problem is formulated as follows:

$$\begin{aligned} E_{\text{opt}} &= \arg \min_{E} \nu(E) \\ &\text{subject to} : E \geq E_T. \end{aligned} \tag{5.20}$$

We point out that since the transmitted energy required for transmission of a single symbol is $\mathcal{P}_x = E/m$, we do our analysis based on the frame energy (E) and the optimal value of symbol energy can be simply obtained as $P_{x,\text{opt}} = E_{\text{opt}}/m$. We start solving the optimization problem with taking the derivative of $\nu(E)$ with respect to E as in the following:

$$\frac{\partial \nu(E)}{\partial E} = \frac{2^m}{[1+g(E)]^{m+1}} \left(1 + g(E) - mEg'(E)\right). \tag{5.21}$$

By taking the derivative of $g(E)$ with respect to E, we have

$$g'(E) = \frac{\beta g^3(E)}{2E^2}. \tag{5.22}$$

we can therefore write (5.21) as:

$$\frac{\partial \nu(E)}{\partial E} = \frac{2^m}{[1+g(E)]^{m+1}}\left(1+g(E) - \frac{m\beta g^3(E)}{2E}\right). \tag{5.23}$$

Eqn. (5.23) is equivalent to

$$\frac{\partial \nu(E)}{\partial E} = \frac{2^m}{[1+g(E)]^{m+1}}\left(1+g(E)\underbrace{\left[1-\frac{m\beta}{2\left(E+\beta\right)}\right]}_{h(E)}\right). \tag{5.24}$$

It can be readily shown that for each value of $E \geq \beta(\frac{m}{2}-1)$, we have $h(E) \geq 0$, and thus we have $\frac{\partial \nu(E)}{\partial E} > 0$ for $E \geq \beta(\frac{m}{2}-1)$. That is, function $\nu(E)$ is monotonically increasing in interval $[\beta(\frac{m}{2}-1), \infty)$. For $E < \beta(\frac{m}{2}-1)$, we now examine if there is a local maximum or minimum. To this end we find the roots of $\frac{\partial \nu(E)}{\partial E}$ in interval $\left[0, \beta(\frac{m}{2}-1)\right)$. From (5.24) it follows that $\frac{\partial \nu(E)}{\partial E}$ is zero if

$$1+g(E)\left[1-\frac{m\beta}{2\left(E+\beta\right)}\right] = 0, \tag{5.25}$$

or equivalently

$$g(E) = \frac{2\left(E+\beta\right)}{\left(m-2\right)\beta - 2E}. \tag{5.26}$$

For $E < \beta(\frac{m}{2}-1)$, the right-hand side of (5.26) is positive; by substituting (5.19) into (5.26), squaring both sides of the equation, and some simple modifications, we can show that (5.26) is equivalent to

$$\left(m+1\right)E^2 + \beta\left(-\frac{m^2}{4}+m+2\right)E + \beta^2 = 0. \tag{5.27}$$

We denote $\left(-\frac{m^2}{4}+m+2\right)^2 - 4\left(m+1\right)$ by Δ_m. It can be easily shown that if $\Delta_m > 0$, Eq. (5.27) has two positive roots:

$$\begin{aligned} E_1 &= \frac{\beta}{2\left(m+1\right)}\left[\frac{m^2}{4}-m-2-\sqrt{\Delta_m}\right], \\ E_2 &= \frac{\beta}{2\left(m+1\right)}\left[\frac{m^2}{4}-m-2+\sqrt{\Delta_m}\right], \end{aligned} \tag{5.28}$$

and we have $E_1 < E_2$. It can be shown that for $m < 8$ we have $\Delta_m < 0$; for $m = 8$ we have $\Delta_m = 0$; for $m > 8$ we have $\Delta_m > 0$. Also, we note that $\frac{\partial \nu(E)}{\partial E}$ is a continuous function and $\lim_{E\to 0+} \frac{\partial \nu(E)}{\partial E} = 2^m > 0$. For $m < 8$ we have $\Delta_m < 0$ and therefore Eq. (5.27) does not have any root, which implies function $\nu(E)$ being monotonically increasing. For $m = 8$ we have $\Delta_m = 0$, which implies function $\nu(E)$ being monotonically nondecreasing due to the fact that (5.27) has only one root and $\frac{\partial \nu(E)}{\partial E}$ is positive in the positive neighbourhood of 0. For $m > 8$ we can conclude that (5.27) has two different roots E_1 and E_2 in the interval $\left[0, \beta(\frac{m}{2} - 1)\right)$, as Appendix C shows $E_2 < \beta(\frac{m}{2} - 1)$. In this case, $\nu(E)$ is monotonically increasing in $(0, E_1)$ and (E_2, ∞) and decreasing in (E_1, E_2). Figure 5.3 shows $\nu(E)$ against E for m =12 under $N_0/\sigma_h^2 = 1$. As it can be seen from this figure, for $E < E_1$ and $E > E_2$, $\nu(E)$ increases as E increases. Also when $E_1 < E < E_2$, $\nu(E)$ decreases as E increases. Based on the previous analysis, we suggest an algorithm for solving the optimization problem defined in (5.20) as in the following:

For $m \leq 8$, since $\nu(E)$ is monotonically nondecreasing function of E, we can easily conclude that $E_{\text{opt}} = E_T$. If the frame length is larger than 8, first, the value of E_T is compared with $\beta\left(\frac{m}{2} - 1\right)$. If $E_T \geq \beta\left(\frac{m}{2} - 1\right)$, we conclude that $E_{\text{opt}} = E_T$; otherwise, E_1 and E_2 are calculated as in (5.28) and compared with E_T. If $E_T > E_2$, then $E_{\text{opt}} = E_T$. If $E_1 < E_T < E_2$, then based on the figure 5.3 it is obvious that $E_{\text{opt}} = E_2$. Finally, if $E_T < E_1$, $\nu(E_T)$ is compared with $\nu(E_2)$; if $\nu(E_T) > \nu(E_2)$, we conclude that $E_{\text{opt}} = E_2$, otherwise $E_{\text{opt}} = E_T$.

5.6 Discussions

In this chapter, we discussed optimizing the transmission power (bit transmission energy) for minimizing the expected transmission energy for successful delivery of the link layer frame. The expected transmission energy has nice properties, which we exploited for the optimization. The nice property of the expected energy function is somewhat attributed to our simple model. For obtaining simple insight, we used very simple models for wireless channels and ARQ schemes. In the physical layer, we assumed that the random channel gains for different symbols are statistically independent. Thus, this model is suitable for fast fading channels [57] or a for the system in which bit interleaving is employed. We assumed that the transmitter does not know the channel gain and thus there is no adaptation at the transmitter side. We limited the scope of our ARQ schemes to the ones in which a packet

Algorithm 1

if $m \leq 8$ **then**
  $E_{\text{opt}} = E_T$
else
  if $E_T \geq \beta\left(\frac{m}{2} - 1\right)$ **then**
    $E_{\text{opt}} = E_T$
  else
    Calculate E_1 and E_2
    if $E_T > E_2$ **then**
      $E_{\text{opt}} = E_T$
    else
      if $E_1 \leq E_T < E_2$ **then**
        $E_{\text{opt}} = E_2$
      else
        Compare $\nu(\mathrm{E_T})$ with $\nu(\mathrm{E_2})$
        if $\nu(E_T) > \nu(E_2)$ **then**
          $E_{\text{opt}} = E_2$
        else
          $E_{\text{opt}} = E_T$
        end if
      end if
    end if
  end if
end if

that is considered error-free by the receiver's link layer entity will never be retransmitted by the transmitting side. Thus, Go-Back-N ARQ will be excluded by our model, for example. Also, we implicitly assumed that the frame is successfully delivered to the destination only if there is no bit error at all, while in a real ARQ scheme the frame can be delivered even though it contains some bit errors [58]. However, the probability that a bit error is undetected in most error detection codes used by an ARQ scheme is very low. We study the optimization problem under more complex model in the next chapter.

Because this chapter focuses on the expected transmission energy rather than throughput, the findings of this chapter are more relevant to wireless networks in which energy efficiency is more important that data throughput.

Chapter 6

Optimizing Bit Transmission Power for Link Layer Energy Efficiency under Channel Estimation Error

6.1 Objective

In chapter 5 we studied the issue of optimizing the transmission power (energy per symbol) for minimizing the expected energy required to reliably deliver a frame to the destination node through ARQ, assuming perfect channel estimation at the receiver. In this chapter, we relax the assumption of perfect channel estimation and study the issue of optimizing the transmission power for a bit-interleaved system. A pilot symbol-assisted modulation (PSAM) scheme is used along with a channel estimation scheme based on the minimum mean square error (MMSE) criterion. We derive a closed-form expression for the frame error probability (FEP) in the presence of channel estimation error and use this expression for minimizing the FEP in allocating the transmission energy. We also derive the expected energy as a function of the transmission power and design an optimization algorithm based on the properties of this function.

6.2 Related work and contribution

Most of the existing work in the link-layer analysis assumes perfect channel information at the receiver side and the communication system is designed for a known channel [42]-[53]. In this chapter, we analyze link-layer performance in a point-to-point wireless communication system in which channel estimation error exists. In particular, we study the issue of transmit energy efficiency under an expected delay constraint for a bit-interleaved wireless communication system. Furthermore, we consider the FEP performance metric and allocate power optimally between pilot and data symbols for minimizing the FEP expression.

In section 6.3, we will derive the FEP expression under the assumption of the receiver's imperfect estimation of the channel gain. Section 6.4 is the main contribution of this chapter, we will formulate an optimization problems for determining the transmission power and show a special property the cost (the expected packet transmission energy for successful delivery). Then, we will present an algorithm to determine the optimal transmission power. In section 6.5, we will present our simulation results, followed by discussion in section 6.6.

6.3 FEP Analysis and Power Allocation

In this section, we discuss the FEP performance of BPSK modulation for the wireless communication system model presented in section 4.3. We will apply the expression of FEP as the performance metric of the system for determining the power allocation among the pilot and data signals. We will then discuss the expected frame energy needed for reliable transmission of a single frame. For the purpose of security and privacy, we assume bit interleaving at the transmitter. After bit interleaving, since the transmitted symbols entire each frame experience different channel gains, by using (4.4) and (4.6), received signals at the destination can be written as:

$$y_d^i = \hat{h}_i x_i + e_i x_i + n_d^i = \hat{h}_i x_i + w_d^i \quad , i = 1, 2, ..., m-1, \tag{6.1}$$

where $w_d^i = e_i x_i + n_d^i$. Due to the symmetric nature of a complex-valued proper Gaussian noise model, the frame error probability conditioned on the estimated channel gains can be expressed as [60]:

$$P(FE|\hat{h}_1, \hat{h}_2, \cdots, \hat{h}_{m-1}) = P(FE|\hat{h}_1, \hat{h}_2, \cdots, \hat{h}_{m-1}, x_1 = x_2 = \cdots = x_{m-1} = +\sqrt{\mathcal{P}_x}). \tag{6.2}$$

In this chapter, we just focus on receiver that does symbol-by-symbol detection for each frame [1]. Maximum likelihood (ML) detection rule applied to an individual symbol is

$$\hat{x}_i = \arg \max_{x_i \in \{\sqrt{\mathcal{P}_x}, -\sqrt{\mathcal{P}_x}\}} p(y_d^i | x_i, \hat{h}_i) = \arg \max_{x_i} \mathrm{Re}\{y_d^i \, \hat{h}_i^* x_i\}, i = 1, 2, ..., m-1. \tag{6.3}$$

For the optimal decision rule (6.3), in accordance with (6.2), we can write the conditional frame error probability as:

$$\begin{aligned} P(FE|\hat{h}_1, \hat{h}_2, ..., \hat{h}_{m-1}) &= 1 - P\Big(\sqrt{\mathcal{P}_x}|\hat{h}_1|^2 + \mathrm{Re}\{\hat{h}_1^* w_d^1\} \geq 0, \\ &\qquad \sqrt{\mathcal{P}_x}|\hat{h}_2|^2 + \mathrm{Re}\{\hat{h}_2^* w_d^2\} \geq 0, \cdots, \sqrt{\mathcal{P}_x}|\hat{h}_{m-1}|^2 + \mathrm{Re}\{\hat{h}_{m-1}^* w_d^{m-1}\} \geq 0\Big) \\ &= 1 - \int_{-\sqrt{\mathcal{P}_x}|\hat{h}_1|}^{\infty} \int_{-\sqrt{\mathcal{P}_x}|\hat{h}_2|}^{\infty} \cdots \int_{-\sqrt{\mathcal{P}_x}|\hat{h}_{m-1}|}^{\infty} p_{\tilde{\mathbf{w}}_d}(\tilde{\mathbf{w}}_d) \, d\tilde{w}_d^1 \, d\tilde{w}_d^2 \cdots d\tilde{w}_d^{m-1}, \end{aligned} \tag{6.4}$$

where $\tilde{\mathbf{w}}_d = \big[\mathrm{Re}\{w_d^1\} \; \mathrm{Re}\{w_d^2\} \; \cdots \; \mathrm{Re}\{w_d^{m-1}\}\big]$. It can be easily shown that $\mathrm{Re}\{w_d^1\}$, $\mathrm{Re}\{w_d^2\}$, ..., and $\mathrm{Re}\{w_d^{m-1}\}$ are independent zero-mean real Gaussian random variables with variance $(\mathcal{P}_x \sigma_e^2 + N_0)/2$. From (6.4) follows:

$$\begin{aligned} P(FE|\hat{h}_1, \hat{h}_2, ..., \hat{h}_{m-1}) &= 1 - \prod_{i=1}^{m-1} \int_{-\sqrt{\mathcal{P}_x}|\hat{h}_i|}^{\infty} \frac{1}{\sqrt{\pi(\sigma_e^2 \mathcal{P}_x + N_0)}} \times e^{-\frac{(\tilde{w}_d^i)^2}{\sigma_e^2 \mathcal{P}_x + N_0}} \, d\tilde{w}_d^i \\ &= 1 - \prod_{i=1}^{m-1} \left(1 - Q\left(\sqrt{\frac{2\mathcal{P}_x \, |\hat{h}_i|^2}{\sigma_e^2 \mathcal{P}_x + N_0}}\right)\right). \end{aligned} \tag{6.5}$$

We denote $|\hat{h}_i|^2$ by Z_i. In accordance with the complex Gaussian channel model, Z_1, Z_2, ..., Z_{m-1} are i.i.d and exponentially distributed ; we can write

$$f_{Z_i}(z_i) = \lambda \, e^{-\lambda z_i}, \; z_i \geq 0, \tag{6.6}$$

where

$$\lambda = \frac{1}{\sigma_{\hat{h}}^2} = \frac{\sigma_h^2 \alpha \, m \mathcal{P}_s + N_0}{\sigma_h^4 \alpha \, m \mathcal{P}_s}. \tag{6.7}$$

[1] Due to the correlation among the received symbols in different frames, we can improve the performance by applying ML detection to the whole received frames instead of individual symbols in each frame; however, the result has unmanageable computational complexity.

Unconditional frame error probability can be written as:

$$P(FE) = 1 - \prod_{i=1}^{m-1} \left(1 - \int_0^\infty \lambda e^{-\lambda z_i} Q\left(\sqrt{\frac{2\mathcal{P}_x\, z_i}{\sigma_e^2 \mathcal{P}_x + N_0}}\right) dz_i\right)$$
$$= 1 - \left(1 - \int_0^\infty \lambda e^{-\lambda z} Q\left(\sqrt{\frac{2\mathcal{P}_x\, z}{\sigma_e^2 \mathcal{P}_x + N_0}}\right) dz\right)^{m-1} = 1 - (1 - \mathbf{J})^{m-1}, \quad (6.8)$$

where

$$\mathbf{J} = \int_0^\infty \lambda e^{-\lambda z} Q\left(\sqrt{\frac{2\mathcal{P}_x\, z}{\sigma_e^2 \mathcal{P}_x + N_0}}\right) dz. \quad (6.9)$$

By using $Q(x) = \frac{1}{\pi}\int_0^{\frac{\pi}{2}} \exp\left(-\frac{x^2}{2\sin^2\theta}\right) d\theta$ [40], $\mathbf{J}$ can be written as:

$$\mathbf{J} = \int_0^\infty \lambda e^{-\lambda z} \frac{1}{\pi} \int_0^{\frac{\pi}{2}} \exp\left(-\frac{Az}{\sin^2\theta}\right) d\theta dz = \frac{1}{\pi}\int_0^{\frac{\pi}{2}} M_Z\left(-\frac{A}{\sin^2\theta}\right) d\theta$$
$$= \frac{1}{\pi}\int_0^{\frac{\pi}{2}} \frac{\sin^2\theta}{\sin^2\theta + A/\lambda} d\theta, \quad (6.10)$$

where $M_Z()$ denotes the moment generating function of Z, and

$$Z_i = |\hat{h}_i|^2,\ A = \frac{\mathcal{P}_x}{\sigma_e^2 \mathcal{P}_x + N_0}. \quad (6.11)$$

Then, using (5A.9) of [40], we obtain

$$\mathbf{J} = \frac{1}{2}\left(1 - \sqrt{\frac{A}{A+\lambda}}\right). \quad (6.12)$$

From (6.8) and (6.12), we have the following FEP expression:

$$P(FE) = 1 - \left(\frac{1}{2}\right)^{m-1} \left(1 + \sqrt{\frac{A}{A+\lambda}}\right)^{m-1}. \quad (6.13)$$

For the purpose of determining the FEP-minimizing power allocation, we derive the FEP expression in terms of α. Based on (4.5) and (4.7) we have:

$$\mathcal{P}_x = \frac{(1-\alpha)m\mathcal{P}_s}{m-1},\ \sigma_e^2 = \frac{\sigma_h^2 N_0}{\alpha\sigma_h^2 m\mathcal{P}_s + N_0}. \quad (6.14)$$

By using (6.14) and (6.13), we can write FEP as the following:

$$P(FE) = 1 - \left(\frac{1}{2} + \frac{1}{2}\sqrt{\frac{\alpha(1-\alpha)\sigma_h^4 m^2 \mathcal{P}_s^2}{\alpha(1-\alpha)\sigma_h^4 m^2\mathcal{P}_s^2 + [1-\alpha+\alpha(m-1)]\,\sigma_h^2 N_0 m\mathcal{P}_s + (m-1)N_0^2}}\right)^{m-1}$$
$$\equiv f(\alpha, m, \bar{\gamma}). \quad (6.15)$$

We point out that FEP in (6.15) is a function of α, m and $\bar{\gamma}$ where

$$\bar{\gamma} = \mathcal{P}_s \sigma_h^2 / N_0. \tag{6.16}$$

To obtain the optimal values of α, for a given frame length and $\bar{\gamma}$, an optimization problem is formulated as follows:

$$\begin{aligned} \alpha_{opt} &= \arg \min_{\alpha} f(\alpha, m, \bar{\gamma}), \\ &\text{subject to} : 0 \leq \alpha \leq 1. \end{aligned} \tag{6.17}$$

where $f(\alpha, m, \bar{\gamma})$ is defined in (6.15). The optimal value of α can be obtained as:

$$\frac{\partial f(\alpha, m, \bar{\gamma})}{\partial \alpha}|_{\alpha=\alpha_{opt}} = 0. \tag{6.18}$$

From (6.18) follows:

$$(2-m)\alpha^2 - 2\left(1 + \frac{m-1}{m\bar{\gamma}}\right)\alpha + 1 + \frac{m-1}{m\bar{\gamma}} = 0. \tag{6.19}$$

The optimal value of α is given by

$$\alpha_{\text{opt}} = \frac{\sqrt{(m\bar{\gamma}+m-1)(m-1)(m\bar{\gamma}+1)} - m\bar{\gamma} - m + 1}{m\bar{\gamma}(m-2)}. \tag{6.20}$$

The results of optimization for the unitary channel variance (i.e., $\sigma_h^2 = 1$) are tabulated in table 6.1. We point out that when $\bar{\gamma}$ is sufficiently large (i.e., $\bar{\gamma} \gg 1$), α_{opt} can be closely approximated as:

$$\alpha_{\text{opt}} \approx \frac{\sqrt{m-1} - 1}{m-2}. \tag{6.21}$$

6.4 Energy Consumption for Frame Delivery and Optimization of Transmission Power (Symbol Energy)

In the previous section, we derived the frame error probability (FEP) expression (6.15). We have shown that for a given symbol transmission power $\mathcal{P}_s$ (average transmission energy per both pilot and data symbols), the FEP depends on the energy allocation α and we have taken an interest in optimizing the value of α. In the present section, we consider a system that exercises an Automatic Repeat Request (ARQ) and focus on the expected

total transmission energy consumed to deliver a frame of source information to the receiver for an arbitrary α. Then, we discuss tuning transmission power $\mathcal{P}_s$ to minimize the total expected transmission energy for a successful delivery of a frame of information. Because $\mathcal{P}_s$ and the energy, E, for one transmission of a frame are simply related by $E = m\mathcal{P}_s$ for a fixed frame size m, we will use E instead of $m\mathcal{P}_s$ as a variable to optimize for simplicity of mathematical expressions.

Since the original transmission and subsequent retransmissions of a frame are independent events, it follows that the number of transmissions needed for successful delivery of a frame is geometrically distributed with parameter $P(FE)$ [54] where $P(FE)$ is the frame error probability. Accordingly, the expected number of transmissions needed for the reliable transfer of one frame is $1/(1 - P(FE))$. Since each reliable transfer of a frame needs $1/(1-P(FE))$ attempts on average, the total expected transmission energy, $\nu(E)$, consumed for reliable transfer of each frame can be obtained as follows:

$$\nu(E) = \frac{E}{1 - P(FE)}. \tag{6.22}$$

We point out that $P(FE)$ in (6.15) can be written as a function of α, m and $\bar{\gamma}$ where $\bar{\gamma} = \sigma_h^2 \mathcal{P}_s / N_0$ and for the simplicity of notations, we assume that $\sigma_h^2/N_0 = 1$. By using (6.15) and (6.22), $\nu(E)$ can be written as:

$$\nu(E) = \frac{2^{m-1}E}{[1 + g(E)]^{m-1}}, \tag{6.23}$$

where

$$g(E) = \sqrt{\frac{\alpha(1-\alpha)E^2}{\alpha(1-\alpha)E^2 + [1-\alpha+\alpha(m-1)]E + (m-1)}}. \tag{6.24}$$

We focus on finding the value of E that minimizes $\nu(E)$.

It is noteworthy that for any practical value of frame size (for any value of $m \geq 2$), we have:

$$\lim_{E \to 0} \nu(E) \quad = \quad 0. \tag{6.25}$$

That is, in the absence of an energy constraint other than the obvious positivity constraint, (6.25) leads to the conclusion that infinitesimally small transmission energy E for single frame transmission ends up with infinitesimally small total expected energy $\nu(E)$. However, we note that at very small value of E, the expected number of transmission needed for

successful frame delivery may become extremely large, which results in extremely long frame delivery time. We assume that the system has a constraint on the expected frame delivery time; namely, $s\left(\frac{2^{m-1}}{[1+g(E)]^{m-1}}\right) \leq d$ where $s(\cdot)$ is a monotonically increasing function, $\frac{2^{m-1}}{[1+g(E)]^{m-1}}$ is the expected number of trials required to successfully deliver a frame and d represents the delay requirement [55] [56]. This is equivalent to constraint $E \geq E_T$ for some E_T. Thus, in the following, we try to design an algorithm to determine the value of E for minimizing $\nu(E)$ under the delay-constrained condition. That is, our optimization problem is formulated as follows:

$$\begin{aligned} E_{\text{opt}} &= \arg \min_{E} \nu(E), \\ &\text{subject to} : E \geq E_T. \end{aligned} \tag{6.26}$$

Although (6.26) seems to be a simple optimization of a single variable, we try to design a very time efficient algorithm for solving (6.26). We will show that the function $\nu(E)$ has nice properties, which we exploit for the optimization. In this section, we will explore the shape of the curve $\nu(E)$ and establish some results about the shape that can be exploited to simply obtains the solution to (6.26). We will later show that $\nu(E)$ is either monotonically non-decreasing or has an up-down-up shape, as is illustrated in Figure 6.3. Since the derivative of a function gives a good perspective about the shape of the function, we start this section with taking the derivative of $\nu(E)$ with respect to E.

For the simplicity of notations, we define $a = \alpha(1-\alpha)$, $b = 1-\alpha+\alpha(m-1)$ and $c = m-1$. We can then write $g(E)$ in (6.24) as:

$$g(E) = \sqrt{\frac{aE^2}{aE^2+bE+c}}. \tag{6.27}$$

The derivative of $\nu(E)$ with respect to E is given by

$$\frac{\partial \nu(E)}{\partial E} = \frac{2^c}{[1+g(E)]^{c+1}}\left(1+g(E)-cEg'(E)\right). \tag{6.28}$$

Taking the derivative of $g(E)$ with respect to E, we have:

$$g'(E) = \frac{(bE+2c)\,g^3(E)}{2aE^3}, \tag{6.29}$$

so we can write (6.28) as:

$$\frac{\partial \nu(E)}{\partial E} = \frac{2^c}{[1+g(E)]^{c+1}}\left(1+g(E)-\frac{c\,(bE+2c)\,g^3(E)}{2aE^2}\right). \tag{6.30}$$

From (6.27) and (6.30) follows that:

$$\frac{\partial \nu(E)}{\partial E} = \frac{2^c}{[1+g(E)]^{c+1}} \left(1 + g(E) \underbrace{\left[1 - \frac{c\,(bE+2c)}{2\,(aE^2+bE+c)} \right]}_{h(E)} \right). \tag{6.31}$$

We are interested in the intervals in which $\nu(E)$ is increasing (i.e., derivative $\nu'(E)$ is positive). Since $g(E) \geq 0$, it can be concluded that we have $\nu'(E) > 0$ if:

$$h(E) \triangleq 1 - \frac{c\,(bE+2c)}{2\,(aE^2+bE+c)} \geq 0. \tag{6.32}$$

$h(E) \geq 0$ if and only if:

$$2aE^2 + b(2-c)E + 2c(1-c) \geq 0. \tag{6.33}$$

Since $E \geq 0$, the inequality in (6.33) holds if and only if:

$$E \geq \frac{\sqrt{b^2\,(c-2)^2 + 16ac\,(c-1)} + b\,(c-2)}{4a} \equiv \eta > 0. \tag{6.34}$$

Thus, the following Lemma is proved:

Lemma 6.4.1. *$\nu'(E) > 0$ in $[\delta_T, +\infty)$; that is, $\nu(E)$ is monotonically increasing in $[\delta_T, +\infty)$.*

Lemma 6.4.2 (monotonic increase)**.** *There exists a positive number $\epsilon < \delta_T$, such that $\nu'(E) > 0$ in $(0, \epsilon]$.*

Proof. From (6.31), it is clear that if $E \to 0^+$, then $\nu'(E) \to 2^c > 0$. By using the continuity of $\nu'(E)$, we conclude that there exists a positive number $\epsilon < \delta_T$ such that $\nu'(E) > 0$ in $(0, \epsilon]$. □

6.4.1 Roots of $\nu'(E)$

Theorem 6.4.1. *For any frame length $m \geq 2$, there exist no more than two distinct positive values of E at which $\nu'(E) = 0$ for any allocation $0 < \alpha < 1$.*

Proof. In accordance with (6.31), $\nu'(E) = 0$ implies $1 + g(E)h(E) = 0$ or equivalently:

$$g(E) = -\frac{2\left(aE^2 + bE + c\right)}{2aE^2 + b(2-c)E + 2c(1-c)}. \tag{6.35}$$

Equality (6.35) implies the following, which is obtained by squaring both sides of (6.35):

$$P(E) = \mu_5 E^5 + \mu_4 E^4 + \mu_3 E^3 + \mu_2 E^2 + \mu_1 E + \mu_0 = 0. \tag{6.36}$$

where

$$\begin{aligned}
\mu_5 &= 4a^2bc + 4a^2b > 0, \\
\mu_4 &= 8a^2c^2 + 4a^2c - ab^2c^2 + 4ab^2c + 8ab^2, \\
\mu_3 &= -4abc^3 + 12abc^2 + 16abc + 4b^3, \\
\mu_2 &= -4ac^4 + 8ac^3 + 8ac^2 + 12b^2c, \\
\mu_1 &= 12bc^2 > 0, \\
\mu_0 &= 4c^3 > 0.
\end{aligned} \tag{6.37}$$

Thus, the number of distinct roots of $\nu'(E)$ can not be more than the number of distinct positive roots of the polynomial $P(E)$. Invoking the Descartes' rule of signs [69], we will prove Theorem 6.4.1 by showing that $P(E)$ does not have more than two positive roots (the polynomial's multiple roots of the same value being separately counted.)

The Descartes' rule of signs states, "If a single-variable polynomial is written from highest to lowest power exponent, then the number of positive real roots of the polynomial is the same or less than by an even numbers as the number of changes in the sign of the coefficients. Multiple roots of the same value are counted separately [69]."

It can be obviously seen from (6.37) that μ_5, μ_1 and μ_0 are positive. Also, each coefficient of μ_4, μ_3 and μ_2 can be zero, positive or negative, so we consider 27 different sign combinations of μ_4, μ_3 and μ_2 (considering zero as a different sign from positive and negative signs). If $\mu_4 < 0$, $\mu_3 > 0$ and $\mu_2 < 0$, in accordance with Descartes' rule of signs, $P(E)$ has at most 4 positive roots. For all other cobinations, $P(E)$ has no more than 2 positive roots. Therefore, Theorem 6.4.1 is proven if we show that $\mu_4 < 0$, $\mu_3 > 0$ and $\mu_2 < 0$ is an impossible combination.

We can write μ_2 and μ_3 in (6.37) as $\mu_2 = 4c \cdot \tilde{\mu}_2$ and $\mu_3 = 4b \cdot \tilde{\mu}_3$ where

$$\begin{aligned}
\tilde{\mu}_3 &= -ac^3 + 3ac^2 + 4ac + b^2, \\
\tilde{\mu}_2 &= -ac^3 + 2ac^2 + 2ac + 3b^2.
\end{aligned} \tag{6.38}$$

Since $b > 0$ and $c > 0$, we have : sign(μ_2)=sign($\tilde{\mu}_2$) and also sign(μ_3)=sign($\tilde{\mu}_3$). In order to prove Theorem 6.4.1, we just need to show that $\tilde{\mu}_3 > 0$ and $\tilde{\mu}_2 < 0$ is an impossible combination.

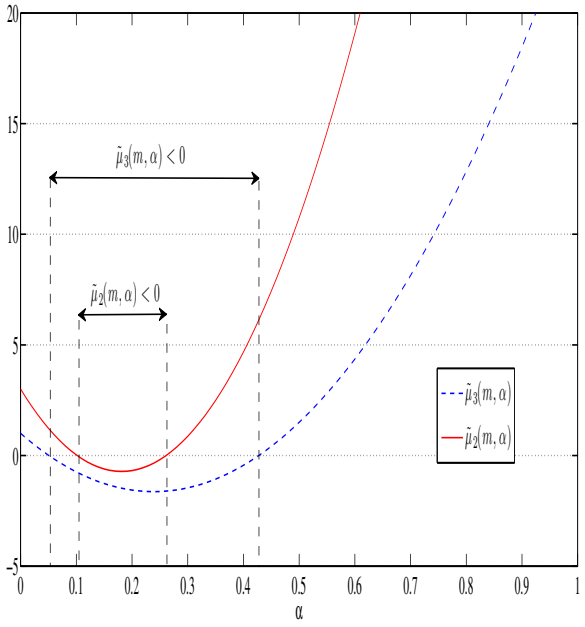

Figure 6.1: $\tilde{\mu}_2(m,\alpha)$ and $\tilde{\mu}_3(m,\alpha)$ against α for $m = 6$

By substituting $a = (1-\alpha)\,\alpha$, $b = 1-\alpha+(m-1)\,\alpha$ and $c = m-1$, we can write $\tilde{\mu}_2$ and $\tilde{\mu}_3$ in terms of α and m as:

$$\begin{aligned}\tilde{\mu}_3 &= \left(m^3-5m^2+m+4\right)\alpha^2+\left(-m^3+6m^2-3m-4\right)\alpha+1 \triangleq a_3(m)\alpha^2+b_3(m)\alpha+1,\\ \tilde{\mu}_2 &= \left(m^3-2m^2-7m+11\right)\alpha^2+\left(-m^3+5m^2+m-11\right)\alpha+3 \triangleq a_2(m)\alpha^2+b_2(m)\alpha+3,\end{aligned} \quad (6.39)$$

where

$$\begin{aligned} a_3(m) &= m^3-5m^2+m+4, \qquad b_3(m) = -m^3+6m^2-3m-4,\\ a_2(m) &= m^3-2m^2-7m+11, \quad b_2(m) = -m^3+5m^2+m-11. \end{aligned} \quad (6.40)$$

For $m \geq 6$, both $\tilde{\mu}_3$ and $\tilde{\mu}_2$ are quadratic functions of α with positive coefficients of quadratic terms. The key idea of the proof of Theorem 6.4.1 from the cases of $m \geq 6$ is to show that the roots of $\tilde{\mu}_2(m,\alpha) = 0$ are surrounded by the roots of $\tilde{\mu}_3(m,\alpha) = 0$, as illustrated in Figure 6.1 and elaborated later. For each value of m between 2 and 5, inclusive, $\tilde{\mu}_2$ in (6.39) as a quadratic function of α has coefficients that make $\tilde{\mu}_2$ non-negative for each value of α between 0 and 1. Thus, Theorem 6.4.1 is proved for the cases of $2 \leq m \leq 5$.

For the rest of the proof, we consider the case of $m \geq 6$ and we will show that $\mu_2 < 0$ and $\mu_3 < 0$ are an impossible combination.

We denote by $\alpha_1^{(2)}(m)$ and $\alpha_2^{(2)}(m)$, the roots of $\tilde{\mu}_2(m,\alpha) = 0$ and $\alpha_1^{(3)}(m)$ and $\alpha_2^{(3)}(m)$, the roots of $\tilde{\mu}_3 = 0(m,\alpha)$:

$$\begin{aligned} \alpha_1^{(2)}(m) &= \frac{-b_2(m) - \sqrt{\Delta_2(m)}}{2a_2(m)},\ \alpha_2^{(2)}(m) = \frac{-b_2(m) + \sqrt{\Delta_2(m)}}{2a_2(m)}, \\ \alpha_1^{(3)}(m) &= \frac{-b_3(m) - \sqrt{\Delta_3(m)}}{2a_3(m)},\ \alpha_2^{(3)}(m) = \frac{-b_3(m) + \sqrt{\Delta_3(m)}}{2a_3(m)}, \end{aligned} \tag{6.41}$$

where

$$\begin{aligned} \Delta_3(m) &= {b_3}^2(m) - 4a_3(m) = m^6 - 12m^5 + 42m^4 - 32m^3 - 19m^2 + 20m, \\ \Delta_2(m) &= {b_2}^2(m) - 12a_2(m) = m^6 - 10m^5 + 23m^4 + 20m^3 - 85m^2 + 62m - 11. \end{aligned} \tag{6.42}$$

For $m \geq 6$ we have:

$$a_2(m) > 0,\ a_3(m) > 0,\ b_2(m) < 0,\ b_3(m) < 0,\ \Delta_2(m) > 0,\ \Delta_3(m) > 0. \tag{6.43}$$

It turns out that the following inequality holds (Proof in the next subsection):

$$\alpha_1^{(3)}(m) < \alpha_1^{(2)}(m) < \alpha_2^{(2)}(m) < \alpha_2^{(3)}(m). \tag{6.44}$$

For each frame length ($m \geq 6$) we have: $\tilde{\mu}_2(m,\alpha) < 0$ if and only if α is in set $\{\alpha | \alpha_1^{(2)}(m) < \alpha < \alpha_2^{(2)}(m)\}$, and $\tilde{\mu}_3(m,\alpha) > 0$ if and only if α is in set $\{\alpha | \alpha < \alpha_1^{(3)}(m)$ or $\alpha > \alpha_2^{(3)}(m)\}$ (Figure 6.1). In accordance with (6.44), these two sets are non-overlapping, so for any value of α, $\mu_2 < 0$ and $\mu_3 > 0$ are an impossible combination. □

6.4.2 Proof of (6.44)

In this subsection, we prove (6.44). The key idea of the proof is to first find a lower bound on $\alpha_1^{(2)}(m)$. We then show that this lower bound, is an upper bound on the $\alpha_1^{(3)}(m)$ which results in the first inequality in (6.44). It turns out that the following inequality holds (proof in the following two Lemmas):

$$\alpha_1^{(2)}(m) > \alpha_1'(m) > \alpha_1^{(3)}(m), \tag{6.45}$$

where

$$\alpha_1'(m) = \frac{-b_2(m) - \sqrt{b_2^2(m) - 12a_3(m)}}{2a_3(m)}. \tag{6.46}$$

We point out that $b_2^2(m) - 12a_3(m) > 0$ because from (6.43) we have: $\Delta_2(m) = b_2^2(m) - 12a_2(m) > 0$. On the other hand, we have $a_2(m) > a_3(m)$ (proof in Appendix D, D.4), which follows that $b_2^2(m) - 12a_3(m) > 0$.

Lemma 6.4.3. *For $m \geq 6$ we have: $\alpha_1^{(2)}(m) > \alpha_1'(m)$.*

proof: See Appendix D.

Lemma 6.4.4. *For $m \geq 6$ we have: $\alpha_1'(m) > \alpha_1^{(3)}(m)$.*

proof: See Appendix E.

By using Lemma 6.4.3 and Lemma 6.4.4, we can therefore conclude that $\alpha_1^{(3)}(m) < \alpha_1^{(2)}(m)$ and first inequality in (6.44) is proved.

Lemma 6.4.5. *For $m \geq 6$ we have: $\alpha_2^{(2)}(m) < \alpha_2^{(3)}(m)$.*

proof: See Appendix F.

By using the Lemma 6.4.5, the last inequality in (6.44) is proved.

6.4.3 Shape of $\nu(E)$

Theorem 6.4.2. *The function $\nu(E)$ is either monotonically non-decreasing in the interval $(0, +\infty)$, or there exist two positive numbers $\xi_1 < \xi_2$ such that $\nu(E)$ is monotonically non-decreasing over $(0, \xi_1]$, monotonically non-increasing over (ξ_1, ξ_2), and monotonically non-decreasing over $[\xi_2, +\infty)$.*

Proof. In accordance with Lemma 6.4.1 and Lemma 6.4.2, there exist positive numbers $\epsilon < \eta$ such that $\nu'(E) > 0$ in $[\eta, +\infty)$ and $(0, \epsilon]$. If $\nu'(E) \geq 0$ in (ϵ, η), then we have $\nu'(E) \geq 0$ in $(0, \infty)$, so $\nu(E)$ is monotonically nondecreasing in $(0, \infty)$. Now we consider the case in which there exists a value $E^* \in (\epsilon, \eta)$ such that $\nu'(E^*)$ is negative. Then there exists $\xi_1 \in (\epsilon, E^*)$ such that $\nu'(\xi_1) = 0$ and there exists $\xi_2 \in (E^*, \eta)$ such that $\nu'(\xi_2) = 0$ because $\nu'(E)$ is a continuous function on $(0, \infty)$ (the intermediate value theorem [70]). In accordance with Theorem 6.4.1, there are no other positive roots of $\nu'(E)$ than ξ_1 and ξ_2. This together with the continuity of $\nu'(E)$ implies that $\nu'(E) \geq 0$ in $[\epsilon, \xi_1]$ and $\nu'(E) \leq 0$ in $[\xi_1, \xi_2]$ and $\nu'(E) \geq 0$ in $[\xi_2, \eta]$. □

6.4.4 Exploiting the shape of $\nu(E)$ for optimization

In the previous subsection, we discussed the different possible shapes of $\nu(E)$ and we showed that $\nu(E)$ is either monotonically non-decreasing in $(0, \infty)$ or has an "up-down-up" shape. In this subsection, we use this property of $\nu(E)$ and suggest an algorithm for solving the optimization problem defined in (6.26).

Whichever kind of shape $\nu(E)$ has, it is clear that if $E_T > \eta$, E_T is optimal because $\nu(E)$ in $[\eta, +\infty)$ is monotonically increasing (Lemma 6.4.1).

For the case in which $\nu(E)$ is monotonically non-decreasing function of E in $(0, \infty)$, we can easily conclude that E_T is optimal because $\nu(E)$ is monotonically non-decreasing function of E in $[E_T, \infty)$.

For the case in which $\nu(E)$ has an "up-down-up" shape, $\nu(E)$ is monotonically non-decreasing over $(0, E_1]$ and $[E_2, +\infty)$, and monotonically non-increasing over $[E_1, E_2]$ (Theorem 6.4.2) where E_1 and E_2 are two roots of $\nu'(E) = 0$. If $E_T > E_2$, then E_T is optimal because $\nu(E)$ is monotonically non-decreasing in $[E_T, +\infty)$. If $E_1 < E_T < E_2$, then it can be seen that $E_{\text{opt}} = E_2$ as illustrated in Figure 6.2.

Finally, if $E_T < E_1$, $\nu(E_T)$ is compared with $\nu(E_2)$; if $\nu(E_T) > \nu(E_2)$, we conclude that $E_{\text{opt}} = E_2$, otherwise $E_{\text{opt}} = E_T$.

We have shown that for solving (6.26), the value of E_2 is needed. It was also shown in subsection 6.4.1 that if $E < \eta$, then the roots of $\nu'(E)$ and the roots of $P(E) = 0$ in (6.36) are equal. In the following, we present a method for finding E_2. From (6.35) and (6.36) follows that E_2 is the largest root of $P(E) = 0$. We can therefore use $P(E)$ for finding E_2. By using Sturm's theorem [72], we can find N_P, the number of roots of $P(E) = 0$. If $N_P < 2$, it means that $\nu(E)$ has at most one root and therefore it is monotonically non-increasing and we have $E_{\text{opt}} = E_T$. If $N_P = 2$, we first find the largest root (E_2). Since $\nu(E)$ in $[\eta, +\infty)$ is monotonically increasing (Lemma 6.4.1), it can be readily concluded that if $E_2 > \eta$, E_2 can not be a root of $\nu'(E) = 0$. In this case, $\nu'(E)$ has at most one root. In other words, if $E_2 > \eta$, $\nu(E)$ is monotonically non-decreasing and E_T is optimal.

We point out that one of the methods that can be used to find E_2, is Newton's algorithm [71]. It can be shown that $P(E)$ is convex in $[E_2, +\infty)$. If we set a proper point as the initial point of Newton's algorithm, the algorithm converges to E_2. Our suggestion is to use Cauchy's upper bound [72] on the largest root as the initial point.

Algorithm 2

Find N_P, the number of roots of $P(E) = 0$
if $N_P < 2$ **then**
    $E_{\text{opt}} = E_T$
else
Find E_2, the largest root of $P(E) = 0$
    if $E_2 \geq \delta_T$ **then**
        $E_{\text{opt}} = E_T$
    else
        if $E_2 < E_T$ **then**
            $E_{\text{opt}} = E_T$
        else
            Compare $\nu(\mathrm{E_T})$ with $\nu(\mathrm{E_2})$
            if $\nu(E_T) > \nu(E_2)$ **then**
                $E_{\text{opt}} = E_2$
            else
                $E_{\text{opt}} = E_T$
            end if
        end if
    end if
end if

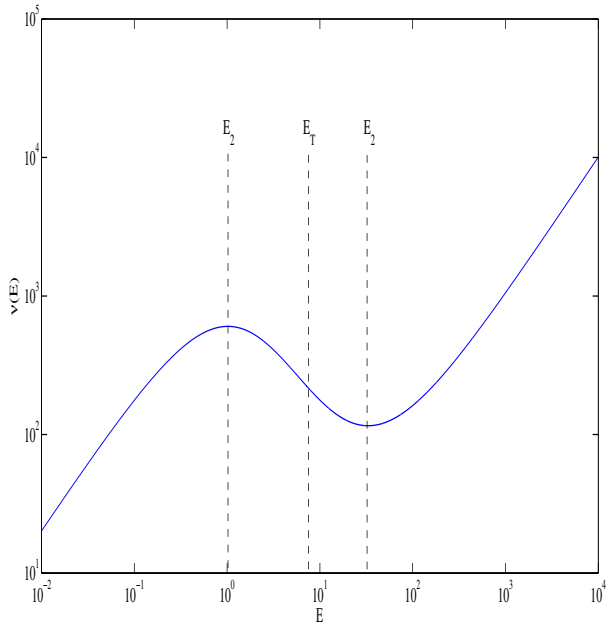

Figure 6.2: $\nu(E)$ against E, α=0.30, m=12

6.5 SIMULATION RESULTS

In the following system setup, we present Monte-Carlo simulation results to corroborate the theoretical analysis. Matlab was used for Monte-Carlo simulation, and 10^7 transmitted symbols were drawn from the BPSK constellation in order to estimate the FEP. The node-to-node channel is modelled by zero mean independent Gaussian random variable with unit variance. The variance of noise components is set to N_0=1.

Figure 6.3 shows the $\nu(E)$ against frame energy (E) for m=5, 10, 15 and 20 and α=0.30. As the figure shows, in the case of m=5, expected frame energy required for a reliable transmission of a frame ($\nu(E)$) is monotonically increasing with respect to E. Figure 6.4 shows the present chapter's FEP analysis resulting in (6.15) in comparison with the simulation results for m=5, 10, 20, 40 and 80 where m is the frame length. Parameter α is set to 0.30.

In Figure 6.5, the FEP is plotted against α for $\mathcal{P}_s/N_0$=15 dB. From the derived FEP expression (6.15), it is apparent that for a fixed total power, the power allocation among pilot and data affects the FEP performance. If we allocate too much power for pilots,

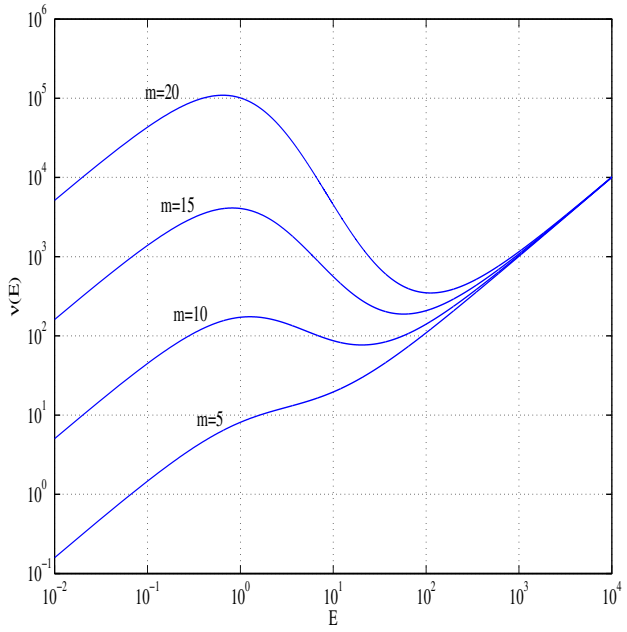

Figure 6.3: $\nu(E)$ against E, α=0.30

channel estimation error will be reduced but detection of the data in noise is more difficult because of low data SNR. On the other hand, lower power for pilots results in poor channel estimation and thus in poor detection [64] [35]. The optimum value of α under $\mathcal{P}_s/N_0$=15 dB and m=10, 20, 40 and 80 turns out to be at $\alpha = 0.25$, $\alpha = 0.19$, $\alpha = 0.14$ and $\alpha = 0.10$, respectively.

Figure 6.6 shows the $\nu(E)$ against α for m=10, 15 and 20 under $\mathcal{P}_s/N_0$=10 dB. In table 6.1, the optimum values for α for m= 16, 32, and 64 are tabulated. These values are obtained by using (6.20). It is noteworthy that the optimum values of α are insensitive to per-symbol SNRs.

6.6 Discussions

In this chapter, we discussed optimizing the transmission power (bit transmission energy) for minimizing the expected transmission energy for successful delivery of the link-layer

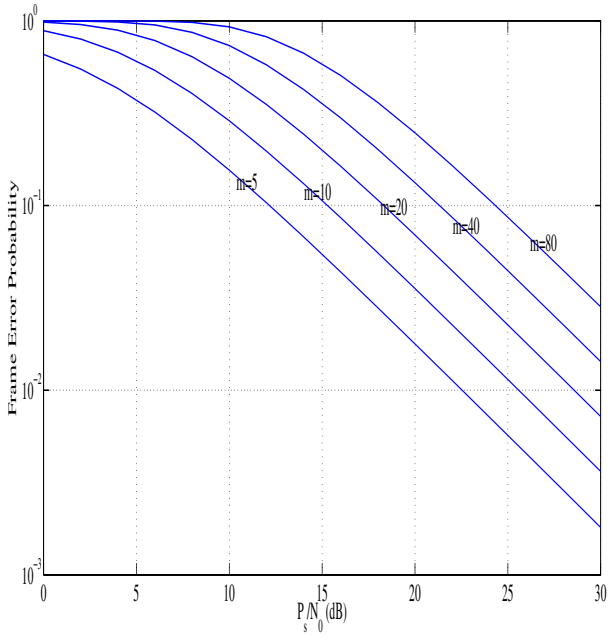

Figure 6.4: FEP against $\mathcal{P}_s/N_0$ for α =0.30

frame under imperfect channel estimation. The expected transmission energy, as a function of energy of each frame, has nice properties, and we exploited them for the optimization. We presented an efficient algorithm for minimizing the transmit energy under delay constraint in a bit-interleaved point-to-point wireless system.

We have derived a closed-form expression for the FEP performance for a point-to-point wireless communication system in which BPSK modulation and bit interleaving are employed. We have also investigated the issue of optimally allocating the transmit energy between pilot and data symbols to minimize the derived FEP expression.

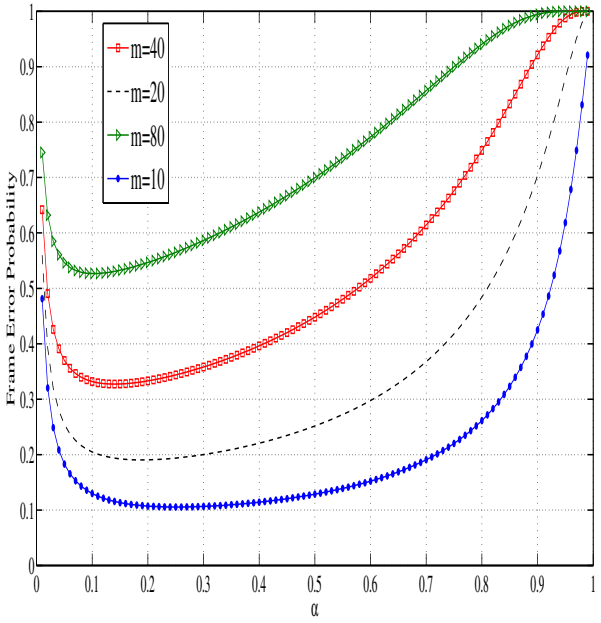

Figure 6.5: FEP against α, $\mathcal{P}_s/N_0$=15 dB

		m= 64	m=32	m=16
$\frac{\mathcal{P}_s}{N_0} = 30$dB	α_{opt}	0.11	0.15	0.21
	FEP	0.0196	0.0104	0.0055
$\frac{\mathcal{P}_s}{N_0} = 25$dB	α_{opt}	0.11	0.15	0.21
	FEP	0.0601	0.0324	0.0174
$\frac{\mathcal{P}_s}{N_0} = 20$dB	α_{opt}	0.11	0.15	0.21
	FEP	0.1774	0.0986	0.0538
$\frac{\mathcal{P}_s}{N_0} = 15$dB	α_{opt}	0.11	0.15	0.21
	FEP	0.4561	0.2764	0.1583
$\frac{\mathcal{P}_s}{N_0} = 10$dB	α_{opt}	0.12	0.16	0.21
	FEP	0.8421	0.6246	0.4062

Table 6.1: Results of optimization for m=16, 32 and 64

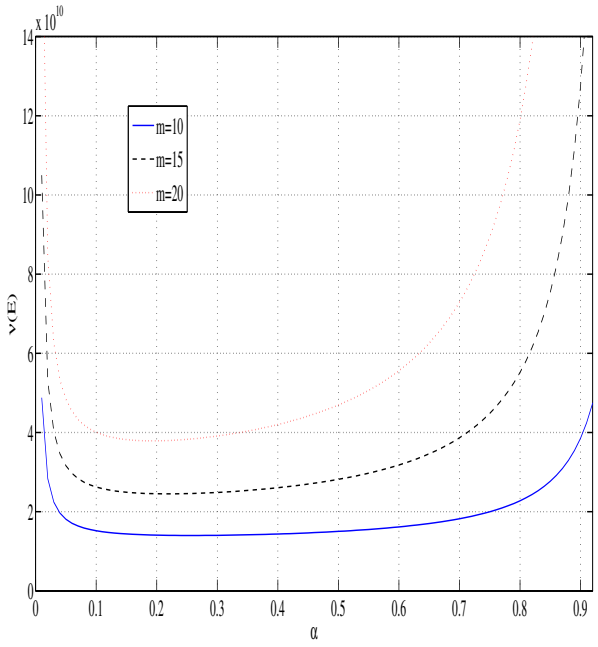

Figure 6.6: $\nu(E)$ against α, $\mathcal{P}_s/N_0$=10 dB

Bibliography

[1] J. N. Laneman, D. N. C. Tse, and G. W. Wornell, "Cooperative diversity in Wireless Networks: Efficient Protocols and Outage Behavior," *IEEE Trans. Inf. Theory*, vol. 50, no. 12, pp. 3062-3080, Dec. 2004.

[2] R. U. Nabar, H. Bolcskei, and F. W. Kneubuhler, "Fading relay channels: performance limits and space-time signal design," *IEEE Journ. Sel. Areas in Commun.*, vol. 22, no. 6, pp. 1099-1109, Aug. 2004.

[3] J. N. Laneman, and G. W. Wornell, "Energy-Efficient Antenna Sharing and Relaying for Wireless Networks," in *Proc. IEEE Wireless Commun. Net. Conf.*, Sep. 2000, pp. 7-12.

[4] A. Ribeiro, X. Cai, and G. B. Giannakis, "Symbol Error Probabilities for General Cooperative Links," *IEEE Trans. Wireless Commun.*, vol. 4, no. 3, pp. 1264-1273, Mar. 2005.

[5] M. Seyfi, "Advanced relay selection techniques for cooperative communications," Ph.D. dissertation, Dept. Eng. Sci., Simon Fraser Univ., Burnaby, British Columbia, 2013.

[6] A. Host-Madsen and J. Zhang, "Capacity Bounds and Power Allocation for Wireless Relay Channels," *IEEE Trans. Inf. Theory*, vol. 51, no. 6, pp. 2020-2040, Jun. 2005.

[7] Q. Li, *et al.* "Cooperative communications for wireless networks: Techniques and applications in LTE-advanced systems, *IEEE Wireless Commun.*, vol. 19, no. 2, pp. 22-29, Apr. 2012.

[8] J. Zhang and Q. Zhang, "Cooperative Routing in Multi-Source Multi-Destination Multi-hop Wireless Networks," in *Proc. IEEE INFOCOM 2008*, Apr. 2008.

[9] X. Tao, X. Xu, and Q. Cui, "An overview of cooperative communications," *IEEE Commun. Mag.*, vol. 50, no. 6, pp. 65-71, Jun. 2012.

[10] A. Nosratinia, T. E. Hunter, and A. Hedayat, "Cooperative communication in wireless networks," *IEEE Commun. Mag.*, vol. 42, no.10, pp. 74-80, Oct. 2004.

[11] C. Gomez, J. Oller, and J. Paradells, "Overview and Evaluation of Bluetooth Low Energy: An Emerging Low-Power Wireless Technology," *Sensors* 2012,*12*, 11734-11753.

[12] T. Wang *et al.*, "High-Performance Cooperative Demodulation with Decode-and-Forward Relays," *IEEE Trans. Commun.*, vol. 55, no. 6, pp. 830-841, Apr. 2007.

[13] J. Adeane , M. R. D. Rodrigues and I. J. Wassell "Characterization of the performance of cooperative networks in Ricean fading channels," *12th Int. Conf. Telecommun.*, 2005.

[14] W. Su *et al.*, "Cooperative Communication Protocols in Wireless Networks: Performance Analysis and Optimum Power Allocation," *Wireless Pers. Commun.*, vol. 44, no. 2, pp. 181-217, Jan. 2008.

[15] A. S. Ibrahim *et al.*, "Cooperative Communications with Relay-Selection: When to Cooperate and whom to Cooperate with?," *IEEE Trans. Wireless Commun.*, vol. 7, no. 7, pp. 2814-2827, Jul. 2008.

[16] A. S. Ibrahim and K. J. R. Liu, "Mitigating channel estimation error with timing synchronization tradeoff in cooperative communications," *IEEE Trans. Signal Process*, vol. 58, pp. 337-348, Jan. 2010.

[17] F. A. Onat *et al.*, "Asymptotic BER Analysis of Threshold Digital Relaying Schemes in Cooperative Wireless Systems," *IEEE Trans. Wireless Commun.*, vol. 7, no. 12, pp. 4938-4947, Dec. 2008.

[18] Y. Lee, and H. W. Shieh, "Detection With Erasure in Relay for Decode-and-Forward Cooperative Communications," *IEEE Trans. Veh. Technol.*, vol. 62, no. 2, pp. 908-913, Feb. 2013.

[19] F. A. Onat *et al.*, "Threshold Selection for SNR-Based Selective Digital Relaying in Cooperative Wireless Networks," *IEEE Trans. Wireless Commun.*, vol. 7, pp. 4226 - 4237, Nov. 2008.

[20] A. H. Bastami, and A. Olfat, "Optimal SNR-Based Selection Relaying Scheme with M-PSK Modulation in Cooperative Wireless Systems," in *Proc. 7th Int. Conf. Inf., Commun. and Signal Process. (ICICS)*, Dec. 2009, pp. 1-6.

[21] G. Al-Habian *et al.*, "Threshold-based relaying in coded cooperative networks, *IEEE Trans. Veh. Technol.*, vol. 60, no. 1, pp. 123-135, Jan. 2011.

[22] T. Hunter and A. Nosratinia, "Diversity through coded cooperation," *IEEE Trans. Wireless Commun.*, vol. 5, no. 2, pp. 283-289, Feb. 2006.

[23] M. Elfituri *et al.*, "A convolutional-based distributed coded cooperation scheme for relay channels, *IEEE Trans. Veh. Technol.*, vol. 58, no. 2, pp. 655-669, Feb. 2009.

[24] J. K. Cavers, "An analysis of pilot symbol assisted modulation for Rayleigh fading channels," *IEEE Trans. Veh. Technol.*, vol. 40, no. 4, pp. 686-693, Nov. 1991.

[25] I. Abou-Faycal *et al.*, "Binary adaptive coded pilot symbol assisted modulation over Rayleigh fading channels without feedback," *IEEE Trans. Commun.*, vol. 53, no. 6, pp. 1036-1046, Jun. 2005.

[26] M. O. Hasna and M. S. Alouini, "A performance study of dual-hop transmissions with fixed gain relays," *IEEE Trans. Wireless Commun.*, vol. 3, no. 6, pp. 1963-1968, Nov. 2004.

[27] P. A. Anghel and M. Kaveh, "Exact symbol error probability of a cooperative network in a Rayleigh-fading environment," *IEEE Trans. Wireless Commun.*, vol. 3, no. 5, pp. 1416-1421, Sep. 2004.

[28] Y. Li and S. Kishore, "Asymptotic analysis of amplify-and-forward relaying in Nakagami-fading environments," *IEEE Trans. Wireless Commun.*, vol. 6, no. 12, pp. 4256-4262, Dec. 2007.

[29] Y. Wu and M. Patzold, "Performance analysis of amplify-and-forward cooperative systems with channel estimation errors," in *Proc. IEEE Int. Conf. Commun. ICC '09*, 2009, pp. 1-6.

[30] A. Zarei Ghanavati, and D. C. Lee, "Design and Analysis of Symbol Detection Schemes with Imperfect CSI for SDF-Relay Networks," in *Proc. 28th IEEE Int. Conf. on Adv. Inf. Net. and Applicat. (AINA)*, May 2014, pp. 884-891.

[31] D. Cabric *et al.*, "Implementation issues in spectrum sensing for cognitive radios," in *Proc. 38th Asilomar Conf. Signals, Systems, and Computers (ASILOMAR '04)*, vol. 1, Nov. 2004, pp. 772-776.

[32] S. Atapattu, C. Tellambura and H. Jiang, "Relay based cooperative spectrum sensing in cognitive radio networks," in *Proc. IEEE Global Telecommun. Conf. (GLOBECOM)*, 2009.

[33] A. Bletsas *et al.*, "A simple cooperative diversity method based on network path selection," *IEEE Journ. Sel. Areas in Commun.*, vol. 24, pp. 659-672, Mar. 2006.

[34] J. Zhang, and M. C. Gursoy, "Achievable Rates and Resource Allocation Strategies for Imperfectly Known Fading Relay Channels," *EURASIP J. on Wireless Commun. and Net.*, 2009.

[35] A. Zarei Ghanavati, and D. C. Lee, "On the Performance of Selective Decode-and-Forward Relaying over Imperfectly Known Fading Relay Channels," in *Proc. Int. Conf. on Wireless and Mobile Commun. (ICWMC)*, Jul. 2013, pp. 173-178.

[36] S. Bhashyam *et al.*, "Feedback gain in multiple antenna systems," *IEEE Trans. Commun.*, vol. 50, no. 5, pp. 785-798, May 2002.

[37] M. C. Gursoy, "An energy efficiency perspective on training for fading channels," in *Proc. IEEE Int. Symp. Inf. Theory (ISIT '07)*, Jun. 2007, pp. 1206-1210.

[38] A. Zarei Ghanavati and D. C. Lee, "Optimal Energy Allocation between Pilot and Data Symbols for Minimizing Frame Error Probability under Imperfect Fading Channel Information," *IEEE Wireless Commun. Net. Conf. (WCNC)*, Apr. 2014, pp. 1990-1995.

[39] R. You, H. Li, and Y. Bar-Ness, "Diversity Combining with Imperfect Channel Estimation," *IEEE Trans. Commun.*, Vol. 53, No. 10, pp. 1655-1662, Oct. 2005.

[40] M. K. Simon and M. S. Alouini, *Digital communication over fading channels*, 2nd ed., New York, John Wiley & Sons, 2004.

[41] A. Paoulis and S.U. Pialli, *Probability, Random Variables and Stochastic Processes,* 4th ed., McGraw-Hill, 2002.

[42] D. Qiao, S. Choi, and K. G. Shin, "Goodput Analysis and Link Adaptation for IEEE 802.11a Wireless LANs," *IEEE Trans. Mobile Computing*, vol. 1, pp. 278-291, Dec. 2002.

[43] J. Yun and M. Kavehrad, "Markov Error structure for Throughput Analysis of Adaptive Modulation Systems Combined with ARQ over Correlated Fading Channels," *IEEE Trans. Veh. Technol.*, vol. 54, no. 1, pp. 235-245, Jan. 2005.

[44] Y. Zhou and J. Wang, "Optimum sub-packet transmission for hybrid ARQ systems," *IEEE Trans. Commun.,* vol. 54, no. 5, pp. 934-942, May 2006.

[45] J. F. T. Cheng, "Coding Performance of Hybrid ARQ Schemes," *IEEE Trans. Commun.,* vol. 54, no. 6, pp. 1017-1029, Jun. 2006.

[46] H.-C. Yang and S. Sasankan, "Analysis of Channel-Adaptive Packet Transmission Over Fading Channels With Transmit Buffer Management," *IEEE Trans. Veh. Technol.*, vol. 57, no. 1, pp. 404-413, Jan. 2008.

[47] A. Steiner and S. S. (Shitz), "Multi-Layer Broadcasting Hybrid-ARQ Strategies for Block Fading Channels," *IEEE Trans. Wireless Commun.*, vol. 7, no. 7, pp. 2640-2650, Jul. 2008.

[48] C. Pimentel and R. L. Siqueira, "Analysis of the Go-Back-N Protocol on Finite-State Markov Rician Fading Channels," *IEEE Trans. Wireless Commun.*, vol. 57, no. 4, 2008.

[49] L. Cao, P. Kam, and M. Tao, "Impact of Imperfect Channel State Information on ARQ Schemes over Rayleigh Fading Channels," in *Proc. IEEE Int. Conf. Commun. (ICC '09)*, Jun. 2009, pp. 1-5.

[50] L. Cao and P. Kam, "On the Performance of Packet ARQ Schemes in Rayleigh Fading: The Role of Receiver Channel State Information and Its Accuracy," *IEEE Trans. Veh. Technol.*, vol. 60, no. 2, pp. 704-709, Feb. 2011.

[51] M. Wu and P. Kam, "ARQ with Channel Gain Monitoring," *IEEE Trans. Commun.*, vol. 60, no.11, pp. 3342-3352, Nov. 2012.

[52] F. Chen and Q. Tuo, "The Improvement of ARQ Acknowledge Algorithm in LTE System," in *Proc. Int. Conf. Comput. Sci., Service Syst. (CSSS),* Aug. 2012, pp.1729-1732.

[53] T. Villa *et al.*, "Adaptive modulation and coding with hybrid-ARQ for latency-constrained networks," in *Proc. 18th European Wireless Conf.*, Apr. 2012, pp. 1-8.

[54] S. Banerjee and A. Misra, "Adapting transmission power for optimal energy reliable multi-hop wireless communication," *Wireless Optimization Workshop (WiOpt 03),* Mar. 2003.

[55] D. C. Lee and W. S. Baek, "Expected file delivery time of Deferred NAK ARQ in CCSDS File Delivery Protocol, *IEEE Trans. Commun.*, vol. 52, no. 8, pp. 1408-1416, Aug. 2004.

[56] W. S. Baek and D. C. Lee, "Analysis of CCSDS File Delivery Protocol: Immediate NAK mode, *IEEE Trans. Aerosp. Electron. Syst.*, vol. 41, no. 2, Apr. 2005.

[57] D. Tse and P. Viswanath, *Fundamentals of wireless communication,* Cambridge: Cambridge University Press., 2005.

[58] S. Lin and D. J. Costello, *Error Control Coding,* 2nd ed., NJ: Prentice-Hall, 2004.

[59] D. Bertsekas and R. Gallager, *Data Networks,* 2nd ed., Englewood Cliffs, NJ: Prentice-Hall, 1992.

[60] A. Zarei Ghanavati, and D. C. Lee, "Optimizing Bit Transmission Power for Link Layer Energy Efficiency," in *Proc. 28th IEEE Int. Conf. Adv. Inf. Net. and Applicat. Workshops (WAINA)*, May 2014, pp. 714-718.

[61] B. Hassibi and B. M. Hochwald, "How much training is needed in multiple-antenna wireless links?," *IEEE Trans. Inf. Theory*, vol 49, no. 4, pp. 951-963, Apr. 2003.

[62] K. Ahmed, C. Tepedelenhoglu, and A. Spanias, "Effect of channel estimation on pair-wise error probability in OFDM," in *Proc. IEEE Conf. Acoust., Speech, Signal Process.*, vol. 4, May 2004, pp. 745-748.

[63] M. Wu and P. Kam, "Instantaneous Symbol Error Outage Probability over Fading Channels with Imperfect Channel State Information," in *Proc. IEEE Veh. Technol. Conf. (VTC 2010 Spring)*, May 2010, pp.1-5.

[64] A. Z. Ghanavati *et al.*, "On the Performance of Imperfect Channel Estimation for Vehicular Ad-Hoc Network," in *Proc. 72nd IEEE Veh. Technol. Conf. (VTC 2010 Fall)*, Sep. 2010, pp. 1-5.

[65] A. S. Ibrahim, A. K. Sadek, W. Su, and K. J. R. Liu, "Cooperative communications with relay-selection: when to cooperate and whom to cooperate with?," *IEEE Trans. Wireless Commun.*, vol. 7, pp. 2814-2827, Jul. 2008.

[66] I. Maric and R. D. Yates, "Bandwidth and power allocation for cooperative strategies in Gaussian relay networks," *IEEE Trans. Inf. Theory*, vol. 56, no. 4, pp. 1880-1889, Apr. 2010.

[67] J. G. Proakis and M. Salehi, *Digital Communications*, 5th ed., McGraw-Hill Higher Education, 2008.

[68] P. O. Borjesson and C. E. Sundberg, "Simple Approximations of the Error Function Q(x) for Communications Applications," *IEEE Trans. Commun.*, vol. 27, no. 3, pp. 639-643, Mar. 1979.

[69] B. E. Meserve, *Fundamental Concepts of Algebra*, New York, Dover Publications, 1982.

[70] H. Anton, *Calculus with Analytic Geometry*, 2nd ed. New York: Wiley, 1984.

[71] R. L. Burden and J. D. Faires, *Numerical Analysis*, 9th ed., Brooks-Cole, 2010.

[72] Q. I. Rahman and G. Schmeisser, *Analytic theory of polynomials*, London Mathematical Society Monographs, Oxford, 2002.

[73] I. S. Gradshteyn and I. M. Ryzhik, *Table of integrals, series and products*, 5th ed., Academic Press Inc., 1980.

Appendix A

Proof of 2.72

From (2.62) follows that:

$$X = \exp\left(\frac{-4\mathcal{P}_r|\hat{h}_{rd}|^2 + 4\sqrt{\mathcal{P}_r}\mathrm{Re}\{\hat{h}_{rd}^*\tilde{n}_{rd}\}}{\sigma_2^2}\right), Y = \exp\left(\frac{-4\mathcal{P}_s|\hat{h}_{sd}|^2 - 4\sqrt{\mathcal{P}_s}\mathrm{Re}\{\hat{h}_{sd}^*\tilde{n}_{sd}\}}{\sigma_1^2}\right) \tag{A.1}$$

We define random variable W as:

$$W = \frac{-4\mathcal{P}_r|\hat{h}_{rd}|^2 + 4\sqrt{\mathcal{P}_r}\mathrm{Re}\{\hat{h}_{rd}^*\tilde{n}_{rd}\}}{\sigma_2^2}. \tag{A.2}$$

Since $\tilde{n}_{rd}$ is a zero mean complex Gaussian random variable with variance σ_2^2, conditioned on $\hat{h}_{rd}$, $\mathrm{Re}\{\hat{h}_{rd}^*\tilde{n}_{rd}\}$ is a zero mean real Gaussian random variable with variance $|\hat{h}_{rd}|^2\sigma_2^2/2$; accordingly W is a real Gaussian random variable as follows:

$$W|\hat{h}_{rd} \sim \mathcal{N}\left(-\frac{4\mathcal{P}_r|\hat{h}_{rd}|^2}{\sigma_2^2}, \frac{8\mathcal{P}_r|\hat{h}_{rd}|^2}{\sigma_2^2}\right). \tag{A.3}$$

The conditional PDF of W is given by:

$$f_{W|\hat{h}_{rd}}(w|\hat{h}_{rd}) = \frac{1}{\sqrt{2\pi\sigma^2_{W|\hat{h}_{rd}}}} \exp\left[-\frac{\left(w - \mu_{W|\hat{h}_{rd}}\right)^2}{2\sigma^2_{W|\hat{h}_{rd}}}\right], \tag{A.4}$$

where

$$\mu_{W|\hat{h}_{rd}} = -\frac{4\mathcal{P}_r|\hat{h}_{rd}|^2}{\sigma_2^2}, \ \sigma^2_{W|\hat{h}_{rd}} = \frac{8\mathcal{P}_r|\hat{h}_{rd}|^2}{\sigma_2^2}. \tag{A.5}$$

We denote $|\hat{h}_{rd}|^2$ and $\angle\hat{h}_{rd}$ by Z_2 and Φ_2, respectively. Conditional PDF of W can be also written as:

$$f_{W|\hat{h}_{rd}}(w|\hat{h}_{rd}) = f_{W|Z_2,\Phi_2}(w|z_2,\phi_2). \tag{A.6}$$

We can derive $f_{W|Z_2}(w|z_2)$ as in the following:

$$\begin{aligned} f_{W|Z_2}(w|z_2) &= \mathrm{E}_{\Phi_2}\left\{f_{W|Z_2,\Phi_2}(w|z_2,\phi_2)\right\} = \mathrm{E}_{\Phi_2}\left\{f_{W|\hat{h}_{rd}}(w|\hat{h}_{rd})\right\} \\ &= \frac{1}{2\pi}\int_0^{2\pi} \frac{\exp\left[-\frac{\left(w-\mu_{W|\hat{h}_{rd}}\right)^2}{2\sigma^2_{W|\hat{h}_{rd}}}\right]}{\sqrt{2\pi\sigma^2_{W|\hat{h}_{rd}}}} d\phi_2 = \frac{\exp\left[-\frac{\left(w-\mu_{W|\hat{h}_{rd}}\right)^2}{2\sigma^2_{W|\hat{h}_{rd}}}\right]}{\sqrt{2\pi\sigma^2_{W|\hat{h}_{rd}}}}. \end{aligned} \tag{A.7}$$

In accordance with (A.1) and (A.2) we have $X = \exp(W)$. The conditional PDF of X can be obtained using [41]:

$$f_{X|Z_2}(x|z_2) = \frac{f_{W|Z_2}(\ln x|z_2)}{x}. \tag{A.8}$$

We also have:

$$\frac{f_{X|Z_2}(x|z_2)}{f_{X|Z_2}\left(\frac{1}{x}\middle|z_2\right)} = \frac{f_{W|Z_2}(\ln x|z_2)}{x^2 f_{W|Z_2}\left(\ln\frac{1}{x}\middle|z_2\right)} = \frac{f_{W|Z_2}(\ln x|z_2)}{x^2 f_{W|Z_2}(-\ln x|z_2)}. \tag{A.9}$$

From (A.7) and (A.9) follows that:

$$\begin{aligned}\frac{f_{X|Z_2}(x|z_2)}{f_{X|Z_2}\left(\frac{1}{x}\middle|z_2\right)} &= \frac{1}{x^2}\exp\left[\frac{\left(-\ln x-\mu_{W|\hat{h}_{rd}}\right)^2}{2\sigma^2_{W|\hat{h}_{rd}}} - \frac{\left(\ln x-\mu_{W|\hat{h}_{rd}}\right)^2}{2\sigma^2_{W|\hat{h}_{rd}}}\right] \\ &= \frac{1}{x^2}\exp\left[\frac{2\mu_{W|\hat{h}_{rd}}\ln x}{\sigma^2_{W|\hat{h}_{rd}}}\right].\end{aligned} \tag{A.10}$$

Finally, after substituting $\mu_{W|\hat{h}_{rd}}$ and $\sigma^2_{W|\hat{h}_{rd}}$ in (A.10), we obtain:

$$f_{X|Z_2}\left(\frac{1}{x}\middle|z_2\right) = x^3 f_{X|Z_2}(x|z_2). \tag{A.11}$$

In the same manner, it can be shown that $f_{Y|Z_1}\left(\frac{1}{y}\middle|z_1\right) = y^3 f_{Y|Z_1}(y|z_1)$.

Appendix B

Proof of 6.2, 3.24 and 3.25

$$P\left(\hat{\hat{x}}=+1|x'=+1\right)P\left(x'=+1\right)=P\left(\hat{\hat{x}}=+1|\theta x=+1\right)P\left(\theta x=+1\right)$$
$$=P\left(\hat{\hat{x}}=+1|x=+1\right)P\left(\theta=1\right)P\left(x=+1\right)=\left(1-P_e'\right)\left(1-P_e^R\right)\left(\frac{1}{2}\right), \tag{B.1}$$

where the third equality in (B.1) is due to the fact that $x'=1$ implies that $\theta=1$ and $x=1$. Also given that the transmitted symbol is $x=+1$, probability that $\hat{\hat{x}}=+1$ and $\theta=1$ are independent. In other words, $P\left(\hat{\hat{x}}=+1|\theta=1,x=+1\right)=P\left(\hat{\hat{x}}=+1|x=+1\right)$. Since the transmitted signal and θ are independent, we also have $P\left(\theta=1,x=+1\right)=P\left(\theta=1\right)P\left(x=+1\right)$. As in (B.1), we obtain

$$P\left(\hat{\hat{x}}=+1|x'=0\right)P\left(x'=0\right)=P\left(\hat{\hat{x}}=+1|\theta x=0\right)P\left(\theta x=0\right)$$
$$=P\left(\hat{\hat{x}}=+1|\theta=0\right)P\left(\theta=0\right)=\frac{1}{2}P_e^R, \tag{B.2}$$

and,

$$P\left(\hat{\hat{x}}=+1|x'=-1\right)P\left(x'=-1\right)=P\left(\hat{\hat{x}}=+1|\theta x=-1\right)P\left(\theta x=-1\right)$$
$$=P\left(\hat{\hat{x}}=+1|x=-1\right)P\left(\theta=1\right)P\left(x=-1\right)=P_e'\left(1-P_e^R\right)\left(\frac{1}{2}\right). \tag{B.3}$$

Appendix C

Proof of $E_2 < \beta(\frac{m}{2} - 1)$

Based on (5.28), $E_2 < \beta\left(\frac{m}{2} - 1\right)$ if and only if:

$$\frac{\beta}{2\,(m+1)}\left[\frac{m^2}{4} - m - 2 + \sqrt{\Delta_m}\right] < \beta\left(\frac{m}{2} - 1\right). \tag{C.1}$$

Multiplying both sides of (C.1) by $2(m+1)/\beta$, we see that (C.1) holds if and only if:

$$\frac{m^2}{4} - m - 2 + \sqrt{\Delta_m} < 2\,(m+1)\left(\frac{m}{2} - 1\right). \tag{C.2}$$

Eq. (C.2) holds if and only if:

$$\frac{m^2}{4} - m - 2 + \sqrt{\Delta_m} < m^2 - m - 2. \tag{C.3}$$

Eq. (C.3) holds if and only if $4\sqrt{\Delta_m} < 3m^2$, or equivalently $16\Delta_m < 9m^4$. By using the following inequalities for $m > 8$:

$$\underbrace{\left(\frac{m^2}{4} - m - 2\right)^2 - 4\,(m+1)}_{\Delta_m} < \left(\frac{m^2}{4} - m - 2\right)^2 < \left(\frac{m^2}{4}\right)^2 = \frac{m^4}{16}, \tag{C.4}$$

we have $16\Delta_m < m^4 < 9m^4$ which results in $E_2 < \beta\left(\frac{m}{2} - 1\right)$.

Appendix D

Proof of Lemma 6.4.3

$\alpha_1^{(2)}(m) > \alpha_1'(m)$ if and only if:

$$\frac{-b_2(m) - \sqrt{b_2^2(m) - 12a_2(m)}}{2a_2(m)} > \frac{-b_2(m) - \sqrt{b_2^2(m) - 12a_3(m)}}{2a_3(m)}. \tag{D.1}$$

Eq. (D.1) holds if and only if:

$$\frac{b_2(m) + \sqrt{b_2^2(m) - 12a_3(m)}}{2a_3(m)} > \frac{b_2(m) + \sqrt{b_2^2(m) - 12a_2(m)}}{2a_2(m)}. \tag{D.2}$$

Eq. (D.2) holds if and only if:

$$a_2(m)\sqrt{b_2^2(m) - 12a_3(m)} - a_3(m)\sqrt{b_2^2(m) - 12a_2(m)} > [a_3(m) - a_2(m)]\, b_2(m). \tag{D.3}$$

From (6.40) we have:

$$a_2(m) - a_3(m) = 3m^2 - 8m + 7 = 3\left[\left(m - \frac{4}{3}\right)^2 + \frac{5}{9}\right] > 0. \tag{D.4}$$

From (D.4) and the fact that $b_2(m) < 0$, we can assume that both sides of inequality in (D.3) are positive, and (D.3) is equivalent to:

$$2b_2^2(m) - 12a_2(m) - 12a_3(m) - 2\sqrt{b_2^2(m) - 12a_2(m)}\sqrt{b_2^2(m) - 12a_3(m)} > 0, \tag{D.5}$$

which results from squaring both sides of (D.3). Inequality (D.5) holds since

$$\left(\sqrt{b_2^2(m) - 12a_2(m)} - \sqrt{b_2^2(m) - 12a_3(m)}\right)^2 > 0. \tag{D.6}$$

Appendix E

Proof of Lemma 6.4.4

For $m \geq 6$, $\alpha_1'(m) > \alpha_1^{(3)}(m)$ if and only if:

$$\frac{-b_2(m) - \sqrt{{b_2}^2(m) - 12a_3(m)}}{2a_3(m)} > \frac{-b_3(m) - \sqrt{{b_3}^2(m) - 4a_3(m)}}{2a_3(m)}. \tag{E.1}$$

Eq. (E.1) holds if and only if:

$$b_3(m) - b_2(m) > \sqrt{{b_2}^2(m) - 12a_3(m)} - \sqrt{{b_3}^2(m) - 4a_3(m)}. \tag{E.2}$$

From (6.40) we have

$$b_3(m) - b_2(m) = m^2 - 4m + 7 = (m-2)^2 + 3 > 0. \tag{E.3}$$

From (E.3) follows that the left hand side (LHS) of (E.2) is positive; therefore, if the right hand side (RHS) of (E.2) is non positive, then inequality in (E.2) obviously holds. If RHS of (E.2) is non negative, (E.2) holds if and only if:

$$[b_3(m) - b_2(m)]^2 > \left(\sqrt{{b_2}^2(m) - 12a_3(m)} - \sqrt{{b_3}^2(m) - 4a_3(m)}\right)^2, \tag{E.4}$$

which is equivalent to:

$$\sqrt{{b_2}^2(m) - 12a_3(m)} \cdot \sqrt{{b_3}^2(m) - 4a_3(m)} > b_2(m)b_3(m) - 8a_3(m). \tag{E.5}$$

If the RHS of (E.5) is non positive, then inequality in (E.5) obviously holds. For the values of m for which the RHS of (E.5) is positive, (E.5) is equivalent to:

$$4b_2(m)b_3(m) - {b_2}^2(m) - 3{b_3}^2(m) - 4a_3(m) > 0, \tag{E.6}$$

which results from squaring both sides of (E.5). From (6.40) follows that (E.6) is equivalent to:

$$2m^5 - 21m^4 + 72m^3 - 110m^2 + 62m - 9 > 0. \tag{E.7}$$

Thus, it remains to be shown that (E.7) holds for each values of $m \geq 6$ for which the RHS of (E.5) is non negative. It turns out that for $m \geq 6$ (E.7) holds. For $6 \leq m \leq 10$ the inequality holds and for $m \geq 11$, (E.7) can be written as

$$(2m - 21)m^4 + (72m - 110)m^2 + 62m - 9 > 0. \tag{E.8}$$

Since $2m - 21$, $72m - 110$ and $62m - 9$ are positive for $m \geq 11$, we proved that for $m \geq 6$ the inequality (E.1) holds.

Appendix F

Proof of Lemma 6.4.5

For $m \geq 6$, $\alpha_2^{(2)}(m) < \alpha_2^{(3)}(m)$ if and only if:

$$\frac{-b_2(m) + \sqrt{{b_2}^2(m) - 12a_2(m)}}{2a_2(m)} < \frac{-b_3(m) + \sqrt{{b_3}^2(m) - 4a_3(m)}}{2a_3(m)}. \tag{F.1}$$

From Lemma 6.4.3 and Lemma 6.4.4, we have proven that $\alpha_1^{(3)}(m) < \alpha_1^{(2)}(m)$; therefore we can write:

$$\frac{-b_3(m) - \sqrt{{b_3}^2(m) - 4a_3(m)}}{2a_3(m)} < \frac{-b_2(m) - \sqrt{{b_2}^2(m) - 12a_2(m)}}{2a_2(m)}. \tag{F.2}$$

From (F.2) follows that

$$\frac{b_2(m) + \sqrt{{b_2}^2(m) - 12a_2(m)}}{2a_2(m)} < \frac{b_3(m) + \sqrt{{b_3}^2(m) - 4a_3(m)}}{2a_3(m)}. \tag{F.3}$$

We define $L(m)$ as:

$$L(m) = a_3(m)b_2(m) - a_2(m)b_3(m) = 2m^5 - 17m^4 + 36m^3 - 19m^2 - 2m. \tag{F.4}$$

It can be easily seen that $L(6) = 600$, $L(7) = 4200$ and $L(8) = 13104$ are positive. Also for $m \geq 9$ we have:

$$\begin{aligned} L(m) &= 2m^5 - 17m^4 + 36m^3 - 19m^2 - 2m > 2m^5 - 17m^4 + 36m^3 - 21m^2 \\ &= (2m - 17)m^4 + (36m - 21)m^2 > 0. \end{aligned} \tag{F.5}$$

Since $L(m)$ for $m \geq 6$ is positive, we have $L(m)/a_2(m)a_3(m) > 0$ and we can therefore write:

$$\frac{b_2(m)}{a_2(m)} > \frac{b_3(m)}{a_3(m)}, \tag{F.6}$$

or equivalently:

$$-\frac{b_2(m)}{a_2(m)} < -\frac{b_3(m)}{a_3(m)}. \tag{F.7}$$

Thus, from (F.3) and (F.7) follows that the addition of left (right) hand sides of (F.3) and (F.7) is the left (right) hand sides of (F.1).